ASSESSMENT OF HOLE DRILLING PROCEDURES ON RESULTING FATIGUE LIVES

A Thesis
Presented to
The Academic Faculty

by

William Carter Ralph

In Partial Fulfillment
Of the Requirements for the Degree
Master of Science in Mechanical Engineering

Georgia Institute of Technology
November 2003

ASSESSMENT OF HOLE DRILLING PROCEDURES ON RESULTING FATIGUE LIVES

Approved by:

Dr. W. Steven Johnson, Chairman

Dr. Richard W. Neu

Dr. Andrew Makeev

Date Approved 24 NOV 03

Dedicated to

Jesus Christ
the Author of my faith

and

Kami Smith
my beautiful bride

ACKNOWLEDGEMENTS

My greatest thanks go to God, the Founder of science. He gave me strong mind and provided me with this opportunity to expand my knowledge and sharpen my thinking. As I learn more about the nature of things, I catch glimpses of His majesty.

My family deserves many thanks, especially in these last months. My parents, William and Mary Ralph, have given me their complete support in all my endeavors, and also funded my excellent undergraduate education—the foundation of my graduate efforts. My fiancée, Kami Smith, has given up many beautiful fall days together without a single complaint, and has always expressed her pride and confidence in me.

I would like to thank my research advisor, Dr. Steven Johnson, for the honor and privilege of working with him. He has taught me to foster my intuition, while requiring me to provide hard evidence for my ideas. He is a world-class researcher who has helped me to become a scientist as well as an engineer.

I want to thank John Bakuckas and the Federal Aviation Administration's William J. Hughes Technical Center for their sponsorship. They funded not only my research, but also my advanced education at a top-notch institution. I earnestly hope that the findings here will further their understanding of aircraft structures, and that we will never know of the lives saved by their aging aircraft work.

In addition, I have had the pleasure of working with the engineers and mechanics at Lockheed Martin Aerospace Corporation in Marietta, Georgia, and Delta Airlines in Atlanta, Georgia, who have generously donated their time and money to this project. In particular, I would like to thank Lockheed Martin's Ed Ingram for his support, Paul

Toivonen for his limitless interest and ideas, Joseph Leonard and Surendra Shah for their organization of the tests, and Ed Bottoms for his masterful drilling. At Delta, I would like to thank Aubrey Carter for his participation and Andrew Makeev for his statistical prowess and technical advice. I hope their investments are rewarded.

Georgia Tech's laboratory technicians, Rick Brown and Robert Cooper, always deserve appreciation for their training, advice, patience, and discipline in the testing facilities. Mr. Brown, in particular, deserves thanks for his clever idea for making the crack detection gages feasible.

I also am obliged to the three who made the x-ray diffraction work possible. Dr. Hamid Garmestani provided me with the necessary theory, and helped me find the testing facilities. Dr. Allan Doolittle generously opened up his machine for my use without obligation. And Walter Henderson taught me how best to put the theory and equipment to use.

As always, Team Johnson deserves thanks. I am fortunate to work with a group of both smart and fun-loving individuals who are always willing to help in any way when asked. Don Rhymer gave me solid advice in practical research, in marriage, and in dealing with some of the quirky people around campus, not to mention giving me a little Homestar Runner just when I needed it. Amanda Wilson was always willing to put aside her own thesis to help me think through even the most trivial questions, and donated several dollars worth of pennies to my education. And whenever I had a truly tricky question, Shelby Highsmith always fielded it with ease. I also greatly appreciate the work of two undergraduates, Morgan Mager and Adam Hadidi for their help in conducting some painfully boring tests.

And to the reader, without you these pages are wasted. Thank you for bearing with my many shortcomings as a scientist and a writer.

TABLE OF CONTENTS

LIST OF TABLES

LIST OF FIGURES

LIST OF SYMBOLS AND ABBREVIATIONS

AGARD	Advisory Group for Aerospace Research and Development
ANOVA	Analysis of Variance, as statistical technique
E	Elastic Modulus
EDM	Electronic Discharge Machining
ksi	Stress in thousands of pounds per square inch
K_f	Fatigue stress concentration factor, material dependent
K_t	Stress intensity factor = σ_{max} / S
m	Length in meters
MPa	Stress in MegaPascals10^6 Pascals, or 10^6 N/m^2
N	Force in Newtons
NASA	National Aeronautics and Space Administration
N_f	Cycles to failure
N_i	Cycles to crack initiation
N_{i1}	Cycles to initiation of first crack
N_{i2}	Cycles to initiation of a crack on the side of the hole opposite that of N_{i1}
R	Stress intensity ratio = S_{min}/S_{max}
S	Remote stress
S_{max}	Maximum stress
S_{min}	Minimum stress
SEM	Scanning Electron Microscope

Cu-kα	X-rays emitted from the k-alpha shell of copper
θ	Theta, the angle between the x-ray emitter and detector
με	Microstrain
μm	Length in micrometers
Ψ	Psi, the x-ray diffraction tilt angle
Ω	Omega, the x-ray incident beam angle

SUMMARY

A study is conducted on the effects of the drilling of fastener holes in 2024-T3 aircraft quality aluminum. The effects are researched using three techniques: a comparison of four hole surface quality metrics, x-ray diffraction, and fatigue at three stress intensities. Six production-line factor variables are considered: the experience of the operator, the use of a pilot hole, the length of the bit, the condition of the bit, the axial pressure or feed rate, and the rotational speed of the bit upon withdrawal from the hole. The four hole quality metrics employed are surface roughness, conicality, the number of large gouge marks, and the angle of those marks. The pilot hole was found to produce the greatest overall effect on hole quality, improving hole quality with its use. X-ray diffraction was used to attempt to measure the relative residual hoop stresses induced by the six drilling factors. Tests found that samples could not be compared using this method due to problems resulting from the combination of the specimen geometry, hole surface quality, and the properties of the aluminum alloy. Fatigue tests are conducted at 25, 21, and 17.5 ksi on both as-drilled and chemically polished specimens. These tests suggest that, although residual stresses do appear to have an effect, hole quality is the predominant factor affecting fatigue life.

CHAPTER I: INTRODUCTION

The structural integrity of an aircraft depends upon a host of complex factors. One such factor is the joining together of the various components, whether by welding, mechanical fastening, or adhesive bonding. In particular, the joining of the fuselage skin panels to each other and to the frame provides a large portion of the structural strength for the entire aircraft. This thin layer of external material ties together and protects the fuselage, and is subjected to some of the harshest conditions and highest stresses of the entire airframe. The most popular material for this application is aluminum, which is typically fastened together with rivets. These rivet holes produce regions of concentrated stress where cracks can form and grow, often hidden beneath the upper layer of the joint or by the head of the rivet.

The infamous Aloha Airlines Flight 243 in 1988 vividly demonstrates the importance of aircraft fastener hole fatigue. While in flight, an 18 foot long section of the fuselage was ripped from the aircraft at 24,000 feet, killing a flight attendant and injuring 65 passengers. The incident was attributed to cracking along a row of rivets in the fuselage skin, caused by a combination of fatigue cracking and corrosion. The cracks from multiple rivet holes linked up, resulting in catastrophic failure.

The overall track record of modern commercial aviation, however, has been very positive. Flying is one of the safest forms of transportation due to high standards of both design and maintenance. In fact, many aircraft greatly outperform their designed life expectations. As an airframe ages, however, costs due to increased maintenance and inspection mount, reducing its profitability.

The aging of the world's commercial aircraft fleet has prompted the Federal Aviation Administration to establish an ongoing effort to study and monitor long-term damage effects such as fatigue cracking. The results allow the agency to provide the industry with a list of maintenance and inspection concerns, and to occasionally mandate procedures to ensure continued safety.

This study is a part of that effort, and seeks to increase the understanding of the present condition of in-service aircraft and to improve future design through better fatigue models. It is primarily concerned with the effects of production-line drilling procedures on fatigue life, and in particular on the formation of residual stresses and machining marks in fastener holes due to the drilling process. It examines the interrelated effects of the beneficial compressive residual hoop stress and the deleterious surface machining marks, and will show that the hole surface quality effects outweigh the subsurface stresses. Three methods of investigation are employed: hole surface quality comparisons, x-ray diffraction, and fatigue testing.

Chapter 2 gives an overview of the concepts related to fatigue life and of research related to this study. Chapter 3 details the properties of the material tested. Chapters 4-6 explain the designs and procedures of the tests of hole surface quality, x-ray diffraction, and fatigue life. Chapter 7 gives the significant results of these tests, and interprets their meanings. Chapter 8 lists the conclusions made, and Chapter 9 recommends future work to answer new questions raised by this study.

CHAPTER II: BACKGROUND

Although drilling may appear to be a simple process, perhaps due to the fact that it is so common, it is in fact deceptively complex. The drill bit has a geometrically complex helical shape and is relatively flexible along its axis. It has two cutting edges working simultaneously inside the workpiece itself. Chips must be removed upwards through the bore, interfering with lubrication and cooling[1]. Since fuselage skins are fractions of an inch thick, these issues are greatly reduced, but other drilling factors become important. Some of the primary factors are the material and geometry of the bit, sharpness of the bit, the workpiece material, and human factors such as steadiness of hand, strength, experience, and even the time of day and the day of the week.

The effects of drilling on the workpiece may be as complex as the drilling process itself. Although primarily a material removal process, the mechanical action of the drill also deforms the area around surface of the hole. The bit leaves scratches and gouges in its path, which may become stress concentrations. The surface is also strained, causing strain hardening and inducing either compressive or tensile residual stresses, which extend radially outward some distance from the bore of the hole. Some amount of heat is generated by the process, which may, upon cooling, induce additional residual stresses, or even cause phase transformations.

Therefore, since drilling is both a common and complex machining process, much research is needed to fully understand the interactions of all of these factors. This understanding will bring improvements to the process and enable optimization of the

factors for each application. Many studies have already been conducted, and have yielded valuable clues to the effects of drilling on the workpiece.

2.1 AGARD R-732

One such study on the effects of drilling, conducted by the North Atlantic Treaty Organization's Advisory Group for Aerospace Research and Development (AGARD) in 1988, found that there were significant differences in the fatigue lives of two sets of fastener holes drilled by independent parties[2]. Both parties drilled the holes using the same batch of material provided by the National Aeronautics and Space Administration (NASA), which were then chemically polished using the same one-minute chemical polishing procedure to "smooth machining marks on the notch surface and to debur the edges of the notch." The holes were then tested under constant amplitude loading at R = 0 and R = -1. These tests found a large difference in the fatigue life between the sets of holes tested at R = 0, as shown in Figure 2-1. In this figure, the squares, marked L-1, represent the specimens from one provider, and the x's, marked WP-1, represent the specimens from the other provider, all polished for one minute. These results show that the holes both lasted much longer than predicted and had a large amount of variability.

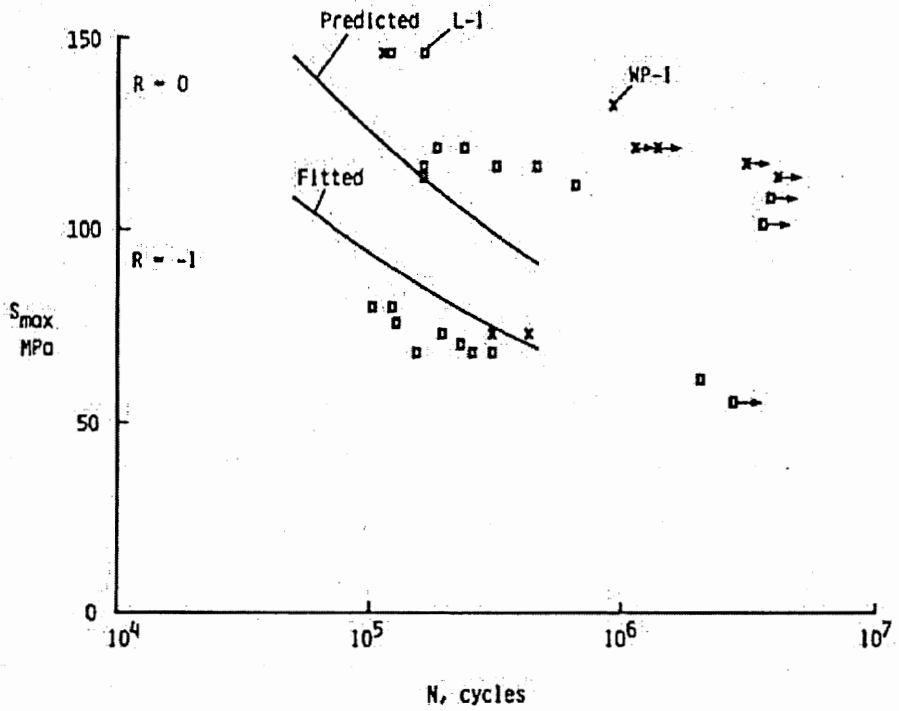

Figure 2-1 Cycles To Failure For Specimens Polished For One Minute[2]

The investigators suspected that machining residual stresses were the cause of these discrepancies, and sought to eliminate the effect for the purpose of the study. A sample mounted with strain gages indicated that the samples from the different providers had compressive residual stresses of 15 MPa (2.2 ksi) for the "L" specimens and 70-95 MPa (10.2-13.8 ksi) for the "WP" specimens, which was consistent with the results from the fatigue tests.

Additional specimens from both providers were polished for either three or five minutes and tested at both R = 0 and R = -1. A baseline set of samples was prepared using a cyclic preload-shakedown procedure, which plastically yielded the notch root in decreasing intensities. As shown in Figure 2-2, the specimen polished for five minutes (WP-5) and the preload-shakedown sample (WP-P) closely matched the prediction in the

fatigue tests, while the specimens polished for one and three minutes (L-1, WP-1, and WP-3) lasted longer in fatigue than predicted.

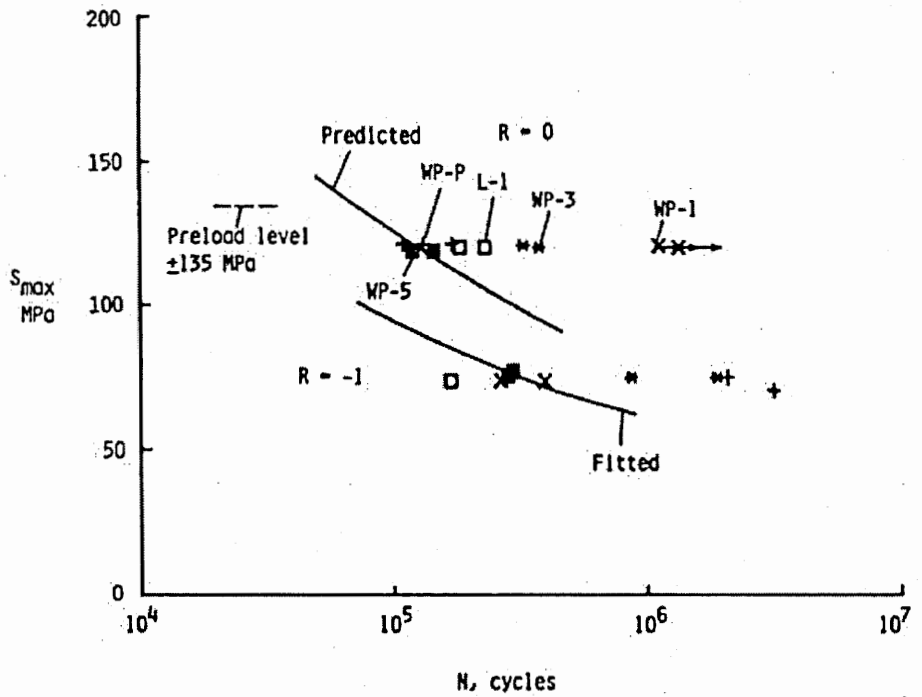

Figure 2-2 Polished and Preload-Shakedown Tests from AGARD R-732[2]

This part of the study concluded that a five-minute polishing procedure was required to remove any machining residual stresses from the fastener holes, in addition to the removal of machining marks and burrs. This amount of polishing removed approximately 0.0008 inches of material from all surfaces. Considering that an effect was still seen with three-minute polishing, the residual stresses should be assumed to extend to about 0.0008 inches, or about 20 microns.

2.2 Residual Stresses

There are many ways that fatigue life can be shortened, but only a few ways that it can be lengthened. The common methods for increasing life are plating processes such as chrome and nickel plating, thermal processes such as carburizing and nitriding, and mechanical cold working processes such as cold rolling and shot peening. In all three of these methods, the benefit is primarily due to residual stresses[3].

2.2.1 Causes and Effects of Residual Stresses

The cause of residual stresses is strain in a component to the point of localized plastic yielding. Upon removal of the stress, the volume around the yielded region attempts to return to its original position, which is resisted by the yielded region. A state of equilibrium is reached with regions of remaining tensile and compressive stresses. When the deformed region is yielded in tension, a compressive residual stress forms in that region, while the surrounding region is left in tension. Likewise, a region yielded in compression results in a tensile residual stress. The exact intensity of the residual stress depends on both the applied stress and the geometry of the region.

This process is easy to imagine with mechanical loads and, in fact, mechanically induced residual stresses are frequently induced on purpose. One common method is radial cold expansion, by which a sleeve is inserted into the hole and a tapered mandrel, slightly larger than the hole, is forced through the sleeve[4]. This results in a compressive hoop stress, which surrounds the hole in a tangential direction—the best orientation to improve fatigue life.

Residual stresses can also be thermally induced. Local heating may expand a region enough that it causes plastic deformation and, upon cooling, residual stresses form. Although this is usually an unwanted byproduct of another process, parts are sometimes carburized and nitrided to induce beneficial residual stresses, and these processes have the added benefit of increasing the strength of the surface material[3].

Heating may also change the crystallographic structure of metals, a process called phase transformation. This is a particular concern in steels, which easily transform between the austenitic and martensitic phases, causing a 4% change in volume. This change is resisted by the surrounding untransformed material, inducing considerable residual stresses[1, 5].

In fatigue, it is the tensile loading that is of primary concern, rather than compressive loading. The remote tension is effectively reduced or increased locally by the magnitude of the residual stress, depending on whether the residual stress is compressive or tensile. This is especially important at the surface of the component, since fatigue damage typically initiates at free surfaces. Therefore, compressive residual stresses are beneficial to the fatigue life of components, while tensile compressive stresses are detrimental[3].

2.2.2 Machining Variables

In the majority of machining operations, plastic deformation of the workpiece by the cutting piece is responsible for most of the residual stresses. As the tool moves along the workpiece it plastically deforms the surrounding volume of material. When the machined surface relaxes, the underlying material creates residual stresses near the surface. One study found that, in turning processes, the magnitude of the resultant

residual stresses is largely a function of cutting speed, depth of cut, feed rate, and tool sharpness[6]. Hoop (tangential) stresses, shown in Figure 2-3, were the largest stresses generated, and tool sharpness was the predominant factor, with stresses decreasing with sharpness. Residual stresses for this process were largely tensile, and linearly increased with cutting speed, linearly decreased with depth of cut, and peaked at a certain feed rate, as shown in Figure 2-4. M'Saoubi et al.[7] also found that an increase in rake angle, the angle of the cutting piece to the workpiece, led to a slight variation in the magnitude and depth of residual stresses. These variables would generally apply to drilling, although the hoop stresses would be reversed.

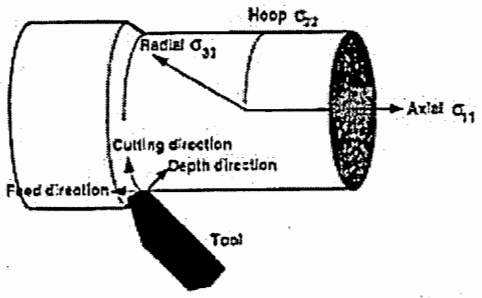

Figure 2-3 Cutting Parameters and Stress Directions for Turning[6]

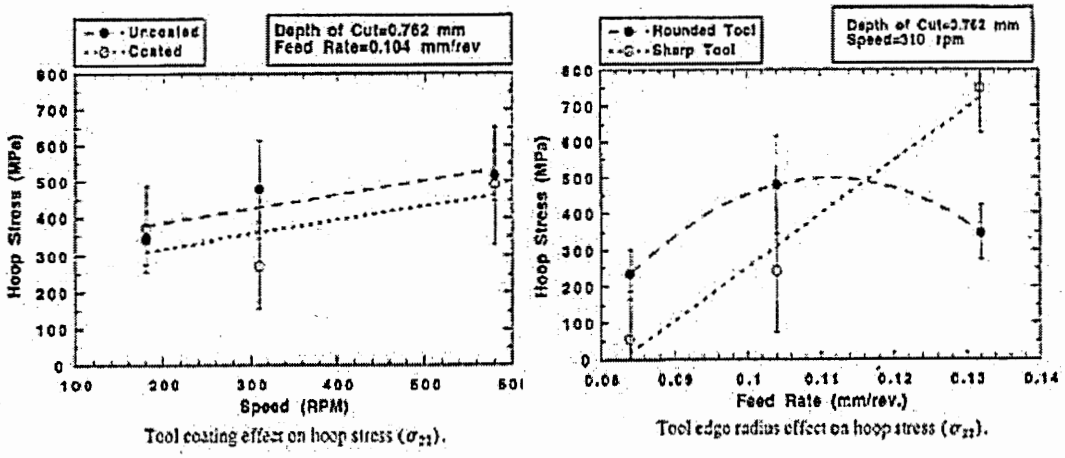

Figure 2-4 Hoop Stresses as Functions of RPM and Feed Rate[6]

Thermal expansion in machining may contribute to the formation of significant residual stresses. While this may be a factor in any machining process, it is of major importance to grinding, which generates a large temperature gradiant. The heat produced by friction creates a zone of thermal expansion, which is resisted by the cooler material around it, as shown in Figure 2-5. When the stress of the expanded material exceeds the yield limit of the material, plastic deformation takes place. Cooling of the surfaces during machining can greatly reduce this effect, but a complete prediction of the residual stress field resulting from any machining process must always take into account the thermal loading effects[8, 9].

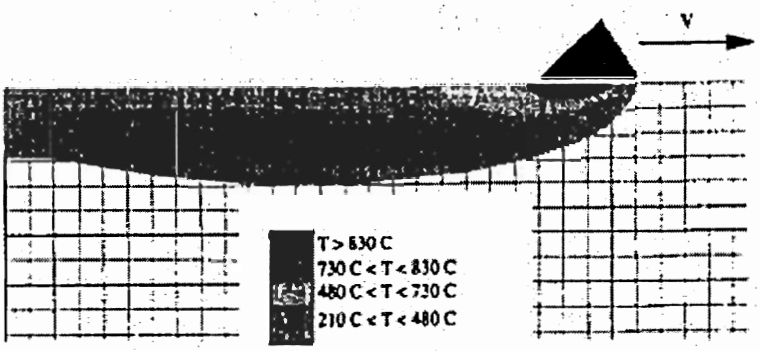

Figure 2-5 Approximated Temperature Gradient of Grinding[8]

These studies clearly show that the interactions between machining tools and the workpiece result in residual stresses. Plastic deformation and temperature gradients are the primary causes of the plastic deformations that produce these effects. Machining processes are more complex than they appear, and their effect cannot yet be accurately predicted.

2.2.3 Geometric and Material Considerations

The exact formation of residual stresses depends upon both the geometry of the component and its constituent materials. Notches, such as fastener holes, can produce stress concentrations, which alter the effects of the remote stress. Different materials may react in very different ways, especially when it comes to temperature changes. These concerns must be taken into account in order to predict the residual stresses to any degree of accuracy.

As mentioned previously, residual stresses are caused by a gradient in the stress-strain field of a component. An example of this would be a beam subjected a bending

moment. In this case, one outer surface will experience the maximum compressive stress, while the opposite surface will experience the maximum tensile stress. Yielding will occur first at the outer surfaces, and the elastic rebounding of the deeper material will induce the residual stresses. A common stress gradient occurs at the base of a notch, called a notch root. The notch causes a stress concentration at the root, causing the root to yield first and subsequently experience the greatest local residual stresses when the surrounding material rebounds, as shown in Figure 2-6.

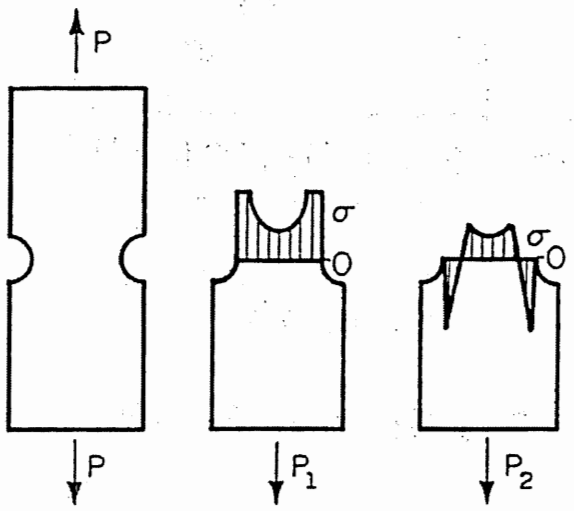

Figure 2-6 Compressive Residual Stress Formation at a Notch Root[3]

In addition to the global effects of machining listed in the previous section, local effects of the machining processes must be considered. A widely recognized local effect is that of the difference between entry and exit faces in radial cold expansion, described above. Despite the expandable sleeve, which serves to protect the bore of the hole from axial deformation as the mandrel is pulled through, there is still a significant difference in

residual stresses between the entry and exit sides of the fastener hole (where the entry side is the one which the mandrel enters). The entry side retains lower compressive residual hoop stresses compared with the exit side. As a result, fatigue cracks usually initiate on the corners of the hole, as shown in Figure 2-7. Lacarac et al. observed that cracks less than about 1 mm in samples with cold expanded holes grew only slightly more slowly than cracks of the same size in as-drilled samples. However, cracks on the order of 2mm showed a much slower growth rate in cold expanded samples[4]. They attributed this effect to the delayed contribution of residual stresses, which only become effective as the crack penetrates through to the highly stressed exit face.

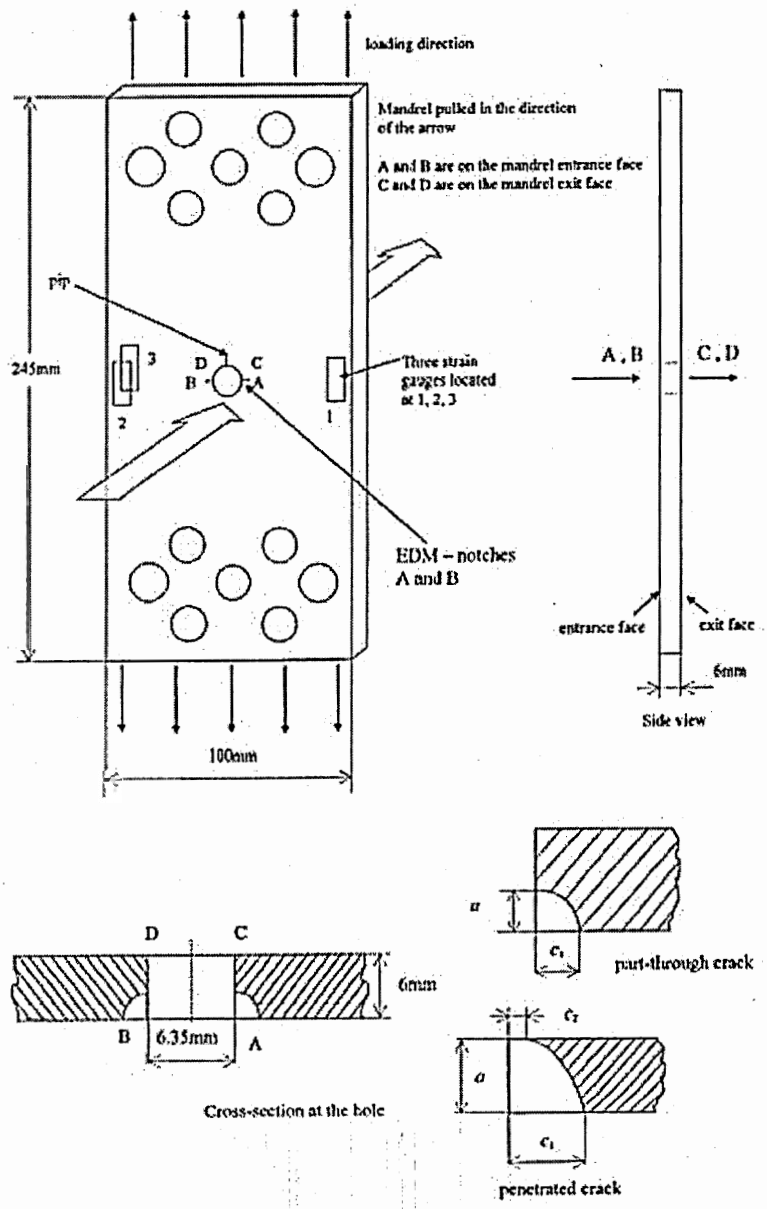

Figure 2-7 Arrangement of Cold Expansion on an Open Hole, and Typical Crack Growth Geometry[4]

An interesting finite element analysis investigated the effect of cold expansion on two adjacent holes. Two models were formed based on the sequence of expansion. In one model, both holes were expanded simultaneously, while in the other the holes were expanded separately[10]. They found that the interaction between the holes led to increased tensile residual stresses in the region between the two holes. Additionally, there was a significant increase and shift in the formation of tensile residual stresses after sequential expansion. Representative stress fields for both of these models are shown in Figures 2-8 and 2-9.

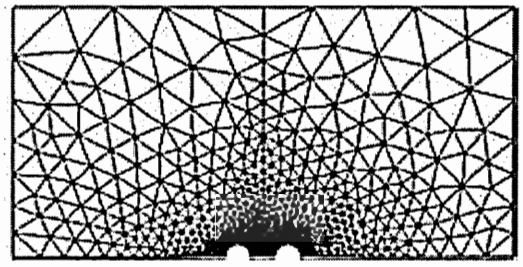

Figure 2-8 Finite Element Mesh Used For Sequential Expansion of Two Holes[10]

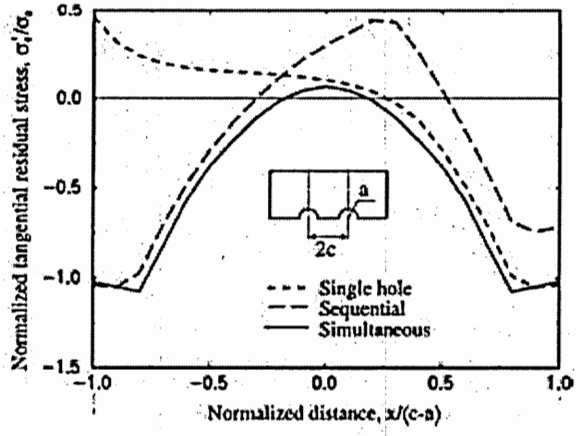

Figure 2-9 Variation of Normalized Tangential Residual Stress for Sequential and Simultaneous Expansion[10]

There may also be important variations in the formation of residual stresses among material types. For example, a recent study was conducted on residual stresses resulting from abrasive waterjet machining on five different alloys, which found that one material achieved its maximum compressive stress below the surface, while all the others were maximized at the surface. However, the other results in the study were analogous among all materials tested[11].

As mentioned above, phase transformations may induce residual stresses in some materials. This is particularly true in certain steels. The transition from the austenite to martensite phase results in approximately 4% volume expansion. The austenite to pearlite transformation also produces a volume expansion[1]. Phase transformations are highly temperature and material dependant, and are very difficult to predict.

Thus, the design and manufacturing of a component can be responsible for producing residual stresses. The exact formation of the stresses is geometry and material dependent, and may be difficult to predict.

2.2.4 Modifying Factors

Before a component is ever loaded, conditions may be applied to reduce or eliminate residual stresses. Loading conditions and high temperatures are two common means that can alter the residual stress fields. Another phenomenon called creep relaxation may also reduce the residual stresses.

Exposure to high temperature is one means of altering residual stresses. When exposed to temperatures sufficiently close to the melting temperature, excitement of the atomic bonds allows the structure to become more compliant, relaxing the residual

stresses partially or fully. This occurs at approximately 250° F for aluminum and 500° F for steel[3].

Additional loading may also alter the stress conditions. One study found that the application of a compressive load could significantly relax the residual stresses, and the combination of a compressive load and high temperature exposure produced an even greater relaxation effect than the sum of these conditions separately applied. Interestingly, the application of a tensile stress during high temperature exposure preserved the residual stresses, and high temperature exposure during cyclic tensile loading yielded no significant increase in crack growth rate[12]. The AGARD study discussed in Section 2.1 used a preload-shakedown procedure to virtually eliminate residual stresses in two samples. The procedure consisted of 30 fully reversed (R = -1) cycles starting well above the yield stress at the notch root and reduced by one percent after each cycle so that the final cycles were below the elastic limit. This procedure created an alternating, continually decreasing residual stress condition at the fatigue-critical location in the samples[2].

Even apart from high temperature exposure, creep relaxation of residual stresses can occur. Creep relaxation is not complete, however, and significant benefit can still be gained from residual stresses even after creep has occurred. In fact, an applied mechanical load can help retain most of the benefits of compressive residual stresses[13].

The magnitude of the load is also a factor. If a tensile load is small, it may never overcome the compressive residual stresses, and a crack may never be able to form[14]. However, if the tensile load is sufficiently large, it can almost completely relax the residual stresses, even within a few cycles and below the yield stress. As a rule of thumb,

longer fatigue lives are obtained when the maximum applied stress is less than 0.5 of the yield strength[4].

The influence of the crack itself must be taken into account. As a crack grows, it forms an area of concentrated stress at its tip, shifting the stress intensity field. During cyclic loading, the crack face expands and contracts, making stress intensity calculations extremely complex. Simply using superposition to calculate the stress intensity becomes insufficient[4, 15, 16]. A stress intensity factor must be determined, which turns out to be the primary factor determining crack growth. This stress intensity factor is, however, modified by the residual stress field.

Thus the formation of residual stresses is a very complex process dependent on a number of factors. These factors include the machining process or processes, the geometry and loading history of the component, the material makeup of the component, and the temperature history. These factors may react with each other to produce residual stress fields different than the sum of the individual effects. A better understanding of these effects is necessary in order to more accurately predict the conditions in the component, which can either extend or reduce its fatigue life.

2.3 Crack Initiation Factors

Fatigue cracks initiate at discrete locations of relative weakness or high stress. These locations may be the result of designed geometry, material imperfections, or surface irregularities. The bulk of the fatigue life of a component is spent initiating a crack at one of these locations, and failure usually occurs relatively quickly afterwards. Residual stresses can retard the initiation and growth of the crack, but once one initiates,

it is typically just a matter of time before the component fails. Therefore, for a given design, the quality of the surface can have a great bearing on the total life of the component, and should be carefully considered.

2.3.1 Hole Quality

Even small irregularities in the surface can magnify the stress and increase the chances of crack initiation. All machining processes produce these irregularities to some degree, and drilling is no exception. Quality can be reduced in drilling by a number of factors, including marks on the bit, imperfections in the drilling angle, vibration, movement of the operator's hand, or chip removal.

Machining processes always produce some amount of surface roughness. In the case of drilling, the end of the flexible drill bit penetrates the workpiece and is followed up by a cutting edge almost perpendicular to the tip. This geometry results in a sharp edge at the point that is most displaced by any axial deflection, which may cause scoring. If the bit is not perfectly orthogonal to the workpiece, or if the axis of drilling is tilted, the edges of the drill bit flutes may also result in scoring. Any marks on the flutes will scratch the surface of the bore of the hole as the bit spirals down through the workpiece.

The bit may also move as a whole during drilling either through vibration or by movement of the operator's hand. This causes the bit to approach the workpiece at different angles, which may cause the sharp edge of the bit to cut into the bore of the hole. Vibrations may also cause the flutes to cut into the edge, resulting in a roughened bore surface.

Chip removal can be problematic in drilling since the chips must be removed back through the hole in the direction opposite of the drilling. These chips can become lodged

between the flutes and the workpiece, resulting in rifling marks. Rifling marks are scoring marks that spiral through the hole bore.

Fastener holes can be mechanically or chemically polished to improve the surface roughness, but this is expensive and not normally done in production, even in the case of fuselage fastener holes. Fasteners may flatten out some of the roughness and perhaps induce a compressive residual stress (or a tensile load), but larger scoring and rifling is likely to remain, especially if the material is strain hardened in their creation.

All of these issues increase the surface roughness of the final hole. Each mark becomes a stress concentration when the component is subjected to fatigue, and becomes a possible site for crack initiation. Larger marks create higher stress concentrations, which are more likely to initiate a crack.

2.3.2 Burrs

As the drill bit penetrates the exit face of the workpiece, and also as it is removed from the workpiece, material is often deformed outward from the bore of the hole. This material, called a burr, is work-hardened and relatively brittle, as well as highly irregular in shape. These burrs may provide additional crack initiation sites.

The removal of burrs is an added machining expense, and the reduction of burr formation has been the subject of a number of investigations. Several studies have attempted to classify types of burrs on the basis of their shape and to explain their creation. One such study identified three types of exit burr shapes, and attributed their creation to three similar mechanisms involving the deformation of the small volume of material at the exit face of the hole which is shown in Figure 2-10[17]. However, this study made no mention of burrs on the entry side of the hole, and the burr formation model

suggests that an entry burr is not possible. Another study by one of the same authors identified the same geometries of burrs, but also recognized the importance of the entry burr. The report stated that high feed rate, cutting speed, and tool wear increase the burr size, and that smoothness of chip flow through the hole decreased burr size, indicating that burr formation is more than just a small, localized, exit phenomenon[18]. Yet another study developed a different burr type classification, which was related to the presence of a burr cap—a thin remnant of material pushed aside by the drill tip. This study attributed burr formation to material properties and drill geometry, as well as cutting conditions[19]. A finite element analysis of burr formation was conducted by another author, but assumed only local deformation of the exit material[20].

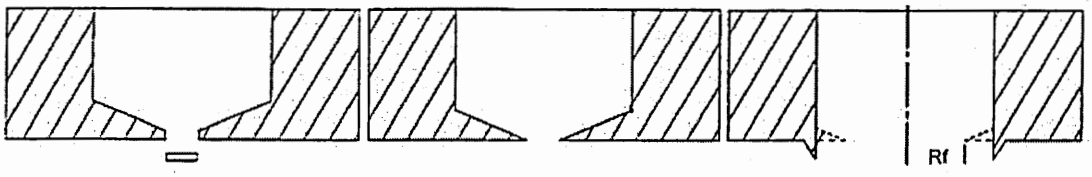

Figure 2-10 Saunders' Model of Burr Formation at the Exit Face[20]

No studies could be found that explained the formation of entry burrs or that asserted that larger-scale plasticity of the hole bore along the drilling axis contributed to burr formation. If burr formation is indeed linked to mechanisms operating deeper in the workpiece, then the shape of the burr may yield important clues to quality of the hole. Since the burr is external, it might then provide an easy method of characterizing hole quality, and perhaps estimating fatigue life.

In aircraft assembly, fastener holes are typically not deburred since the exit faces of the holes are usually in restrictive locations or butt up against the frame. The burr is likely crushed by riveting or fastening, but this may not remove the possibility that it remains a factor in crack initiation.

Thus, it is possible that burrs may have an effect on fatigue life, since they can serve as crack initiation sites. Several differing models for burr formation have been proposed, but none that explained the formation of an entry burr. It is likely that a correct model of burr formation will take machining variables into account, and consider plastic deformation that occurs throughout the drilling process, rather than just at the very end.

Overall, hole quality depends on a large variety of factors, mainly grouped into machining variables and deformation processes. Hole quality is likely to have a large effect on fatigue life due to the stress concentrations that are formed by imperfections in the surface. However, hole quality is a somewhat nebulous term that could be difficult to quantify.

2.4 Finite Element Analysis

Perhaps the greatest boon for fracture mechanics and fatigue has been the exponential improvements in computing. Numerical modeling is now a fundamental tool for complex designs, especially in the realm of aircraft design. Desktop computers are able to solve complex problems in only minutes, efficient algorithms can generate accurate solutions from fairly coarse meshes, and user friendly software has made the technology available to any engineer[21]. These finite element programs are based on the same fundamentals of numerical methods, although they may take different approaches to

fracture mechanics. In particular, the FASTRAN code works well for many fatigue crack growth problems. All of these programs, however, have their limitations.

2.4.1 The Finite Element Method Concept

The finite element method, a popular numerical method, approaches the modeling problem by subdividing the component. These subdivisions, called elements, may have a number of different shapes, and are all connected at nodes. These nodes maintain the continuous structure of the component, and are given properties to estimate the behavior of the material.

The nodes are the key to the finite element method. Each node is given an initial location in space, and boundary conditions are specified at particular nodal points to constrain the body. Stresses are then applied to the body, and the resultant strain, and therefore displacement, for each node is calculated by interpolating over each element. This allows the distribution of stress and strain to be inferred from the displacements of the nodes and the constitutive law[21].

The element geometry and size must be selected according to the component and the degree of accuracy. Of course, a finer mesh of elements requires more nodes, and therefore more calculations and longer computing time. The boundary conditions can be incremented to simulate a dynamic system, including the release of nodal constraints to simulate crack advance.

2.4.2 FASTRAN II

One goal of this study is to correlate experimental fatigue life with the predictions of the FASTRAN II code in order to account for residual stress effects. The design of

this code makes it especially suitable for the modeling of fatigue crack growth predictions.

The FASTRAN II code is based upon the Dugdale strip yield model, which accounts for plasticity-induced crack closure effects. Modifications were made to allow plastically deformed material to remain on the surface as the crack propagates. The code also accounts for variable amplitude loading effects, such as crack acceleration and retardation. Plane strain and plane stress conditions, as well as intermediate conditions, can be simulated by placing a constraint factor on tensile yielding at the crack front, thus approximating three-dimensional conditions.

These features result in very realistic results, such as different crack growth rates in the depth and length directions for three-dimensional configurations. Failure can also be modeled for brittle, ductile, and intermediate materials. Almost any loading spectrum can be modeled, including compressive and tensile loads.

A module is currently under development to incorporate pre-existing residual stresses. The results from this study will be used to verify the results of that module.

2.4.3 Limitations of Numerical Methods

Despite the accuracy and usefulness of numerical methods, these models cannot replace experiments. Although conditions at the crack tip can be simulated, final fracture cannot be accurately predicted. These limitations are due to the continuum assumptions that the methods are based upon, which does not account for the imperfections of true engineering materials.

Continuum mechanics assumes that the material is uniform on all levels, which breaks down at the atomic level, since all materials are ultimately made up of discrete

elements. The benefit of this assumption is that stress can be defined at a point, enabling the use of differential calculus. Most engineering structures are so large that the atomic effects can be disregarded without losing any significant accuracy.

Discontinuities, however, exist on scales much larger than the atomic level. All engineering materials contain voids, inclusions, microcracks, and grain boundaries. When one considers that fatigue is a crack growth phenomenon, and that cracks begin on the micron level, these material imperfections suddenly become much larger in scale. The random nature of these imperfections prevents them from being incorporated into current numerical models.

Thus, finite element models produce sufficient predictions of the crack tip conditions, and even final failure (when the failure mode is specified) when a medium-sized crack of a given dimension is assumed, but cannot adequately predict the initiation of a crack in a component. This deficiency requires experimental testing to provide information about the overall behavior of engineering materials due to their random, discontinuous structure.

CHAPTER III: MATERIAL AND SPECIMENS

Each engineering application requires the careful selection of a suitable material. The choice of material depends on the design specifications, loading conditions, working environment, and cost. In aviation, these factors have led to the development of advanced materials from the common materials originally used in the first aircraft—from wood, to special alloys, to the new advanced composite materials that are still coming of age. In the same way, the material for this study had to be chosen to reflect the needs and realities of modern aircraft.

Material properties differ greatly, even between batches of the same alloys. It is therefore important to detail the properties of the chosen material, 2024-T3 aluminum, and the characteristics of the batch of material from which the test specimens are made.

Similarly, the specimen geometry and orientation affects the fatigue life of the specimens, and needs to be detailed. Specimen preparation has an effect as well, and deserves consideration. All of this information composes the subject matter of the present chapter.

3.1 History

Material weight has been an important consideration since the birth of aviation, as the first aircraft required lightweight construction just to get off the ground. The primary material of early airframes was wood, covered in varnished cloth. It had to be carefully protected from moisture, and did not provide much toughness. Aluminum became a

practical alternative after the discovery of precipitation hardening by Alfred Wilm in 1906. Several designers experimented with aluminum in the 1920's, but exfoliation corrosion was a problem until 1927, when anodizing was developed in England and Alcoa developed a cladding method [22].

Further material improvements were made largely by trial and error until the 1960's. About that time, the understanding of the properties of materials reached a point that advances could begin to be made purposefully. That purpose was provided by the desire to manufacture supersonic aircraft and by the growth of fracture mechanics, which identified specific properties governing the performance of materials. The 7050-T74 alloy was developed in the 1970's to balance the fracture toughness of 2024-T3, which had a significant weight penalty, with the high strength of 7075-T6, which was too brittle to be reliably used for tension-dominated applications. A host of other advanced alloys were then developed for specific use in wing and empennage structures. The 1980's saw the development of reliable aluminum-lithium alloys with the addition of magnesium[22].

The aging of the world's commercial aircraft fleets has prompted a new focus on life cycle cost and reliability, emphasizing the needs of commercial airlines that must not only purchase new aircraft at reasonable prices, but also cost-effectively maintain their aircraft for many years. These needs require materials that are cheap, reliable, and easily repaired.

Advanced composite materials have taken a spotlight in recent years, with their engineered load-bearing properties, ease of complex lay-up geometries, and light weight. Regardless, aluminum has remained the predominant material in the aircraft industry due to its extensive working history and material property data, as well as its ease of repair

and environmental friendliness compared with composites. These reasons, along with further advances in metallurgy, should keep aluminum competitive in aircraft construction for many years to come.

3.2 Material Properties

Aluminum was selected for this study, primarily because of the fact that it is in use by the majority of the current commercial aircraft fleet, as shown in Table 3-1. The alloy chosen was 2024-T3. The material stock was provided by NASA, and has been well documented in numerous other studies. The chemical composition of this stock of alloy is shown in Table 3-2.

Table 3-1 Material Composition By Weight in Commercial Aircraft[22]

Aircraft	Aluminum	Steel	Titanium	PMC's	Other
Boeing 747	81%	13%	4%	1%	1%
Boeing 757	78%	12%	6%	3%	1%
Boeing 767	80%	14%	2%	3%	1%
Boeing 777	70%	11%	7%	11%	1%
DC-10	78%	14%	5%	1%	2%
MD-11	76%	9%	5%	8%	2%
MD-12	70%	8%	4%	16%	2%

Table 3-2 Chemical Composition of 2024-T3 Aluminum Alloy[2]

Element	Percent
Silicon	0.16
Iron	0.33
Copper	4.61
Manganese	0.57
Magnesium	1.51
Chromium	0.02
Zinc	0.06
Aluminum	Balance

The T3 heat treatment designation signifies solution heat treatment plus cold-working. Its major precipitates are Guinier-Preston zones, which are coherent clusters of the solute elements and are of the same crystal structure as the matrix[22]. Average tensile properties are given in Table 3-3.

Table 3-3 Average Tensile Properties of 2024-T3 Aluminum Alloy Sheet[2]

Ultimate Tensile Strength	**Yield Stress (0.2 percent offset)**	**Modulus of Elasticity**	**Elongation Percent**
495 MPa	355 MPa	72,000 MPa	21
71.8 ksi	51.5 ksi	10,400 ksi	21

Material microstructure along the nominal dimension, perpendicular to the rolling direction, is shown in Figure 3-1. Typical grain dimensions in the LT nominal crack-growth direction, 2a and c, are 25 μm and 55 μm, respectively. In the rolling direction, the typical dimension is 95 μm^2.

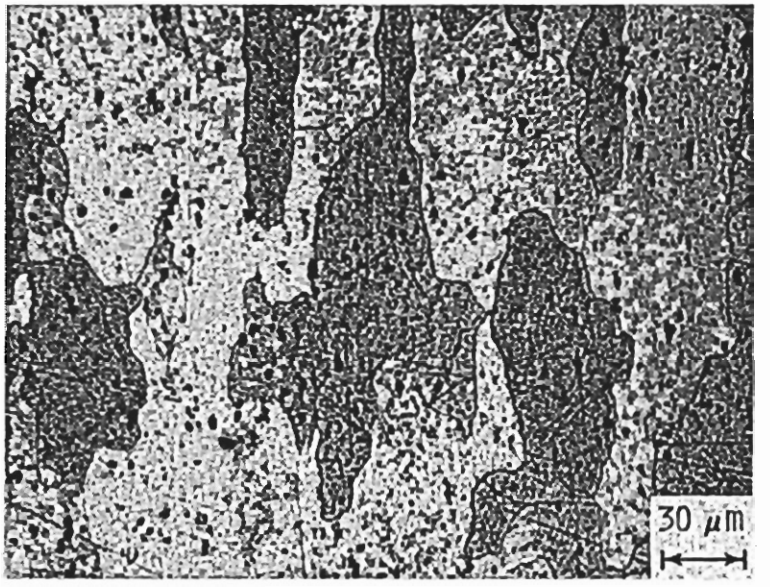

Figure 3-1 Microstructure Perpendicular to Rolling Direction[2]

3.3 Specimen Properties and Geometry

As with all the parameters of this study, the specimens were designed to represent real aircraft conditions, while still reducing the variables to those that are core to fatigue life and residual stresses. The design of the specimens reflects these desires by modeling a fastener hole in tension without introducing bending forces.

3.3.1 Microstructural Orientation

Coupons were of two different microstructural orientations. The majority of the coupons, including all hand- and machine-drilled fatigue coupons, were oriented in the LT direction. A few baseline coupons were oriented in the TL direction. All coupons in this paper are in the LT direction unless otherwise stated.

3.3.2 Specimen Geometry

All LT coupons had dimensions: length L = 11.00 inches (27.94 cm), width 2W = 2.00 inches (5.08 cm), and thickness B = 0.09 inches (2.3mm), as shown in Figure 3-2. The TL coupons had the same geometry, except that they were 12.00 inches long. All specimens were inscribed at the top and bottom with a unique identification number of the format A##N8-#(-TL), for example A92N8-8 for an LT sample or A34N7-9-TL for a TL sample. All specimens were filed at the edges to remove machining marks. The fatigue test specimens were through-the-thickness, center-hole coupons, as illustrated in Figure 3-2.

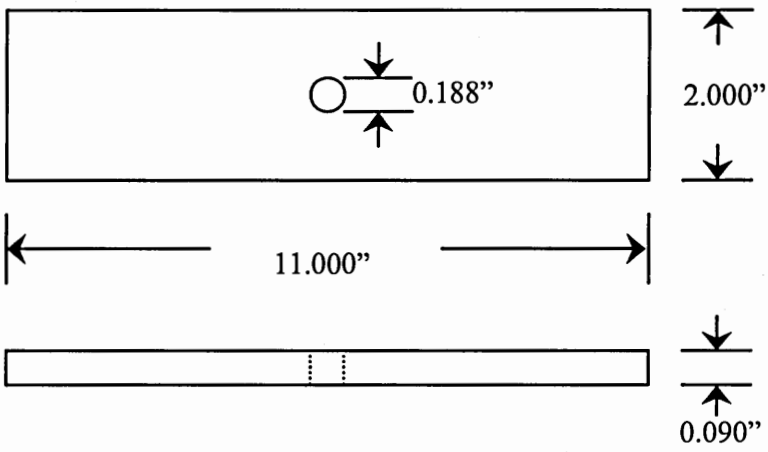

Figure 3-2 LT Specimen Geometry

3.4 Polishing Procedure

The baseline samples were chemically polished in accordance with the procedure used in AGARD R-732. The solution was 80 percent (by volume) phosphoric acid, 5 percent nitric acid, 5 percent acetic acid, and 10 percent water, heated to 105 degrees

Centigrade. A small hole was drilled near the end of the polished coupon, and a hanger was inserted in this hole to suspend the coupon in the polishing solution. All polished coupons were placed in the solution for five minutes, which smoothed the machining marks, burrs, and significant residual stresses, and mildly rounded the edges of the specimen, as shown in Figure 3-3[2].

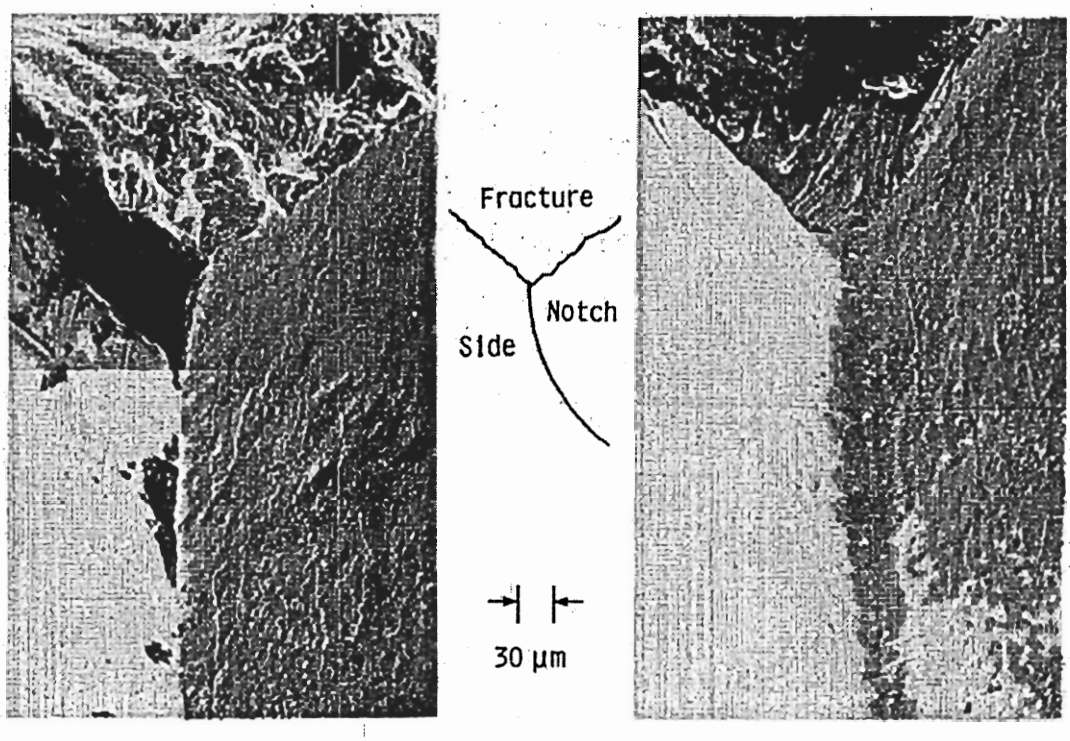

(a) One minute. (b) Five minutes.

Figure 3-3 Effect of Chemical Polishing on Surface Finish[2]

CHAPTER IV: HOLE QUALITY EXPERIMENT

Since hole quality is likely to have a large effect on fatigue life, a hole quality experiment was devised. The plan was to first identify the drilling factors most likely to significantly affect hole quality. Then a matrix of these drilling factors was designed and the holes were drilled using combinations of these factors. The holes were then cut and prepared for microscopy. Finally, the hole surfaces were measured for hole quality and compared.

One difficulty was that there was no standard method for determining hole quality. A metric or metrics needed to be established in order to quantify quality so that the effects of the factors could be compared objectively. Gouge marks and burrs were observed during initial inspections, and methods for incorporating them into the hole quality metrics were developed.

Measurement difficulties presented themselves, due to the curving geometry of the hole. Techniques had to be devised to accurately measure the quality according to the metrics in such a way that the curvature would not interfere.

A statistical technique called analysis of variance (ANOVA) was employed to determine the factors that produced significant differences in hole quality. The effects of the factors were compared using a normalization technique and statistical indicators of the confidence of hole quality differences. This also enabled the correlation of hole quality with fatigue life once the fatigue tests were completed.

4.1 Choice of Variables

Discussions were held with engineers and technicians at Lockheed and Delta to identify factors most likely to significantly affect the fatigue life of fastener holes. The production line of an aluminum-bodied aircraft was toured, and mechanics who drilled the fastener holes were interviewed to assess the factors identified and to elicit additional factors.

4.1.1 Bit Condition

The first probable factor identified was the condition of the drill bit. A sharp, new bit should quickly and easily cut through the workpiece. This, in turn, should reduce the amount that the operator's hand strays from drilling axis, resulting in a more cylindrical hole. A new bit should also be free of gouges, and therefore be less likely to score the surface.

An old bit, however, may have its own benefits. An old bit would also likely cause more tangential plastic deformation of the hole bore resulting in larger compressive residual hoop stresses, which would, in turn, retard fatigue crack growth. On the other hand, an older bit would be more likely to have gouges, which would score the bore surface. The longer drilling time would allow the operator's hand to stray more, and would also increase the heat generated in the hole, which may induce tensile residual hoop stresses upon cooling.

4.1.2 Pilot Hole

It is often advantageous to drill a small diameter hole in the fastener hole location prior to drilling the final fastener hole. This smaller hole is called a pilot hole. A smaller

diameter bit is easier to accurately drill in the right location since it is less likely to stray from its initial location, and this pilot hole then becomes a guide for the larger diameter bit. The disadvantage is that it is more time consuming, which becomes a major production concern when thousands of holes are drilled in the fuselage skin alone.

The use of a pilot hole may also affect hole quality, since the primary drill bit has less material to remove. This makes for faster, straighter drilling and less wear on the bit. Less heat is generated with the primary bit, and the pilot hole may allow for better cooling and chip removal. Since the drilling time, tool wear, and material removal concerns are reduced, scoring and rifling may also be reduced.

4.1.3 Bit Length

Two different length bits are typically used for fastener holes on the production line we visited. The standard bit is approximately 3.5 inches long, and the long bit is approximately 6 inches long. The long bit gives the operator better control over the straightness of the drill, but makes the tip more difficult to control when starting the hole, and may deflect along its axis when pressure is applied to the bit.

4.1.4 Operator Experience

Since fastener holes are drilled primarily by hand on the production line, human factors must come into play. It is unlikely that any two humans drill in exactly the same manner and, in fact, it is unlikely that any single human will ever drill any two holes exactly the same. The problem is that these human factors introduce a multitude of variables. Thus, to reduce the number of factors in the test matrix, it was thought that the greatest human difference in hole quality would be seen between an experienced operator

and a novice. If the human factors are significant to hole quality, the holes from the two different operators should be very different, and the experienced operator should drill a better quality hole than the novice.

4.1.5 Bit Pressure

It was also felt that a physically larger operator would probably apply greater pressure to the drill bit than a small operator. This should cause greater plastic deformation, and thus higher residual stresses in the axial direction. The greater pressure may also generate more heat, producing greater residual stresses. Additionally, if deformation in the bore of the hole affects burr formation, a higher pressure on the bit should increase the burr size.

4.1.6 Withdrawal Speed

It was observed on the assembly line that some operators release the trigger of the drill before the bit is withdrawn from the hole, allowing the bit to slow down as it was withdrawn. If scoring or rifling is a significant issue, then a drill bit rotating quickly would leave marks almost in the same plane as the fatigue loading, while the other extreme of a bit withdrawn after fully stopped would leave marks along the axis of the hole, which is in an ideal direction to initiate a crack.

4.1.7 Drill Block

Another method of drilling more accurate holes is to use a tool called a drill block. This tool has many different forms, but all serve the same purpose of providing a guide for the drill bit. The drill block has a hardened steel hole of slightly larger diameter than the bit. The bit is placed through the drill block and the tip of the bit is placed in the

desired hole location. The block is then moved down to the workpiece and held firmly against it while the hole is drilled. The only hole quality differences should be that the hole is more perpendicular and cylindrical.

4.1.8 Workpiece Material

The final factor identified was the material of the workpiece. Much new aircraft construction uses alloys other than 2024-T3 for the fuselage skin. The factors above may have much different results in different materials, depending on properties such as strength, toughness, and modulus.

After reviewing the list of probable factors, two were eliminated as variables in this study. The first was the drill block. This was eliminated because it only served to drill a straighter hole. This function is also served by the use of a pilot hole, and the drill block and pilot hole are not used simultaneously in practice. The second variable discarded was material type. Although this may have a significant effect, it introduced a level of complexity that was outside the scope of this project. The final choice of variables, then, was: bit condition, pilot hole, bit length, operator experience, bit pressure, and withdrawal speed.

4.2 Test Matrices

In order to test every combination of these six variables with a minimum of three holes per variable combination, 192 holes would have to be drilled. At an estimated lab time of two hours per hole to cut, mount, polish, photograph, and measure each hole, this

would require almost 400 hours. Therefore, a fractional factorial test matrix was constructed, which allowed fewer combinations of holes to be drilled while retaining the statistical significance of the results. The variable combinations are shown in Table 4-1. The matrix was designed to allow for the analysis of interactions between pairs of factors using a linear least squares fit model.

Table 4-1 Hand-Drilling Variable Combinations

Operator	Pilot Hole	Bit Length	Bit Condition	Pressure	Bit Speed
Experienced	No	Long	New	High	Stopped
Experienced	No	Long	New	Low	Full
Experienced	No	Long	Old	High	Full
Experienced	No	Long	Old	Low	Stopped
Experienced	No	Short	New	High	Full
Experienced	No	Short	New	Low	Stopped
Experienced	No	Short	Old	High	Stopped
Experienced	No	Short	Old	Low	Full
Experienced	Yes	Long	New	High	Full
Experienced	Yes	Long	New	Low	Stopped
Experienced	Yes	Long	Old	High	Stopped
Experienced	Yes	Long	Old	Low	Full
Experienced	Yes	Short	New	High	Stopped
Experienced	Yes	Short	New	Low	Full
Experienced	Yes	Short	Old	High	Full
Experienced	Yes	Short	Old	Low	Stopped
Novice	No	Long	New	High	Stopped
Novice	No	Long	New	Low	Full
Novice	No	Long	Old	High	Full
Novice	No	Long	Old	Low	Stopped
Novice	No	Short	New	High	Full
Novice	No	Short	New	Low	Stopped
Novice	No	Short	Old	High	Stopped
Novice	No	Short	Old	Low	Full
Novice	Yes	Long	New	High	Full
Novice	Yes	Long	New	Low	Stopped
Novice	Yes	Long	Old	High	Stopped
Novice	Yes	Long	Old	Low	Full
Novice	Yes	Short	New	High	Stopped
Novice	Yes	Short	New	Low	Full
Novice	Yes	Short	Old	High	Full
Novice	Yes	Short	Old	Low	Stopped

Each variable combination was replicated three times. The resultant matrix was partially randomized to reduce both sequencing effects and operator fatigue due to frequent bit changing. The complete test matrix as it was drilled can be found in Appendix A, Table A-1.

The above matrix was designed to test the range of the six variables in standard practice. It was hoped that the best and worst holes that humans could drill on the assembly line would be contained within the test. In order to eliminate the human variables, another matrix was developed for machine drilling. This eliminated the experienced/novice variable. The withdrawal speed variable was also eliminated because it is not standard practice, and because it had little effect, as will be shown later. The pressure variable was changed to feed rate. Humans have a difficult time responding to small variations in federate, but respond well to pressure. Drill presses, however, are not typically setup to sense pressure, but feed rate control is standard.

A fractional factorial matrix was again employed to reduce the number of required holes. Three replicates of each variable combination were drilled. The variable combinations used in the matrix are shown below in Table 4-2.

Table 4-2 Machine-Drilling Variable Combinations

Bit Condition	Bit Length	Pilot Hole	Feed Rate
Old	Short	No	Low
Old	Short	Yes	High
Old	Long	No	High
Old	Long	Yes	Low
New	Short	No	High
New	Short	Yes	Low
New	Long	No	Low
New	Long	Yes	High

4.3 Drilling Procedure

Each of the coupons to be drilled was first inscribed with a grid consisting of three columns running down the length of the coupon and 21 rows running across the width of the coupon, as shown in Figure 4-1. Each of the grid intersections was punched to help the operator drill the holes squarely on the grid, which would become important when the holes were later cut in half. An identifying mark was scribed on either side of each hole, referring to the row number and a column number, followed by a roman numeral referring to the coupon. For example 19-2 IV signified that the hole came from row 19, column 2 of the fourth coupon. Two of the coupons were then machine-drilled with a typical 3/32 inch pilot bit at each of the grid intersections. A punch was used to lightly mark the drilling positions in the coupons without pilot holes.

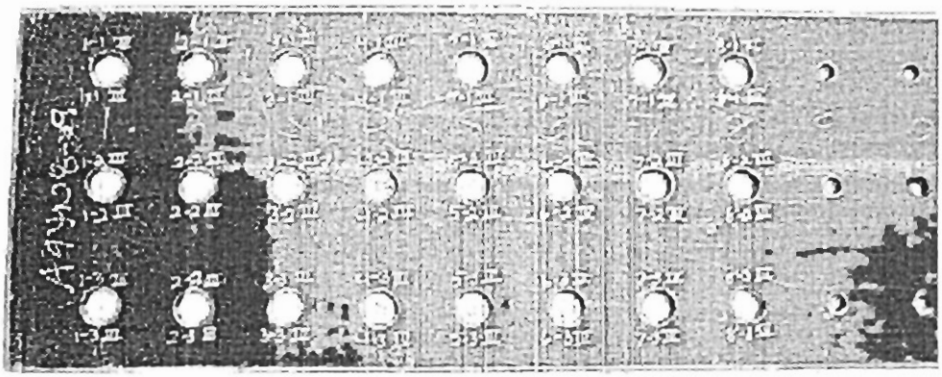

Figure 4-1 Hole Quality Coupon Drilling Layout

All of the hand-drilled holes were drilled at a Lockheed Martin test facility. A constant-speed (2800 rpm) pneumatic hand drill was used, identical to those used in

production, as shown in Figure 4-2. The coupon to be drilled was suspended over a wooden block to catch the bit as it penetrated the coupon. It was important that the coupon did not rest on the block, as it would interfere with the formation of the burr. This was done by placing two blocks about an inch apart and centering the hole to be drilled over the gap between the blocks.

Figure 4-2 Pneumatic Hand Drill Used for Tests

All of the final diameter drill bits were 3/16 inch (#10), 118 degree, high-speed twist drill bits, such as the type R1SA bit from the Precision Twist Drill Company. These primary drill bits were taken from the tool crib on the assembly floor to make sure that they were typical for fastener holes. The new bits were taken from a box of unopened new (not resharpened) bits, and a different bit was used each time a bit was replaced in the drill. The used bits were chosen from a group of discarded bits from the tool crib. The bits were chosen to be similar to the new bits with edges dull to the touch.

There was a noticeable difference in how long it took the operators to drill the holes with and without pilot holes, and the operators commented on how much easier it was to drill with the pilot holes. There was also a noticeable difference in the time it took to drill with the old bit compared with the new bit, although less noticeable than the pilot hole. The operators also commented on how much harder it was to drill with an old bit. Additionally, a difference in the chips between the old and new bits was noticed. The new bits did produce small chips, as expected, while the old bits produced long, spiraling chips.

All of the machine-drilled holes were drilled at Delta. The drilling setup is illustrated in Figure 4-3. The coupon was mounted in the grooves of a vise with sufficient pressure to hold the coupon firmly without causing it to bend. The short and long old drill bits were brought from the Lockheed test. For the new drill bits, bits of the same diameter were taken from the tool crib, but Delta did not have the bits in six-inch lengths, so the long bits were cut to size. The machine that was used had "high", "medium", and "low" feed rate speed presets, and the high and low presets were used. The high setting advanced three times faster than the low setting.

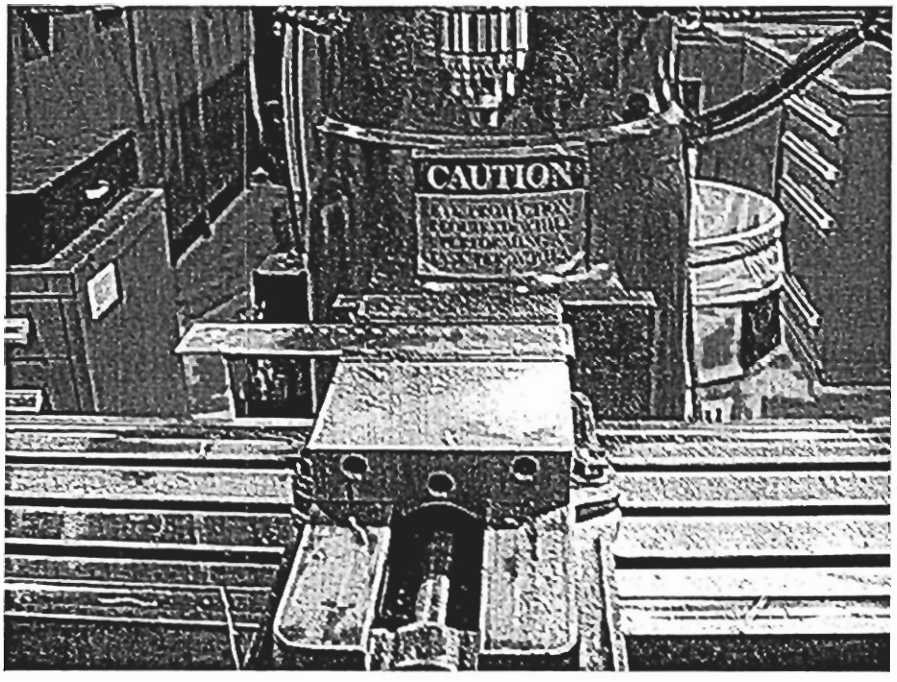

Figure 4-3 Machine Drilling Setup

4.3 Specimen Preparation

After the holes were drilled, they had to be prepared for microscopy. Each row was cut along the hole centers by electronic discharge machining (EDM). The rows were further cut into sections of two hole halves with a grinding wheel. The sections were mounted in epoxy with the edges of the holes exposed, two sections per hole, as shown in Figure 4-4. These mounts were polished to one micron to remove machining marks from the EDM and to provide a good material surface. The remaining set of hole halves were also divided up into sections of two, but were set aside for later analysis, and no further preparation was done to them.

Figure 4-4 Mounted Fastener Hole Sample

4.4 Hole Quality Metrics and Measurement Procedure

Hole quality was judged according to four metrics: surface Roughness, hole solid angle, number of gouge marks, and angle of gouge marks. In addition, burr sizes and geometries were recorded, since three distinct burr types were quickly distinguished, both at the entry and exit faces of the coupons.

4.4.1 Burr Geometry and Size

Burrs may act as crack initiation sites, since the material has hardened and become brittle. The most noticeable type of burr was called a "curling" burr, since it was long and slender and was usually found curled up like a cresting wave. This type of burr is illustrated in Figure 4-5(a). This burr is likely the result of material from the end of the hole being pushed out and away from the bit as it exits the coupon, and probably has little correlation with residual stress levels induced during drilling, since it would only be a local phenomenon, as modeled in Figure 2-9. The second burr type was called a "triangular" burr, and is similar to the curling burr, as illustrated in Figure 4-5(b).

However, the base of the burr is wider than the length of the burr. This burr may be more indicative of residual stresses, since its base extends farther away from the bore of the hole. The width of the base indicates that there is much more involved in its formation than local plasticity at the region shown in Figure 2-9. The final type of burr was called a "bulge" burr, because it was composed of a hump formed on the workpiece surface extending radially out from the bore, as illustrated in Figure 4-5(c). This burr is thought to have a significant correlation to stresses imposed deep inside the hole, especially in the axial direction. All of these burr types were observed on both exit and entry faces.

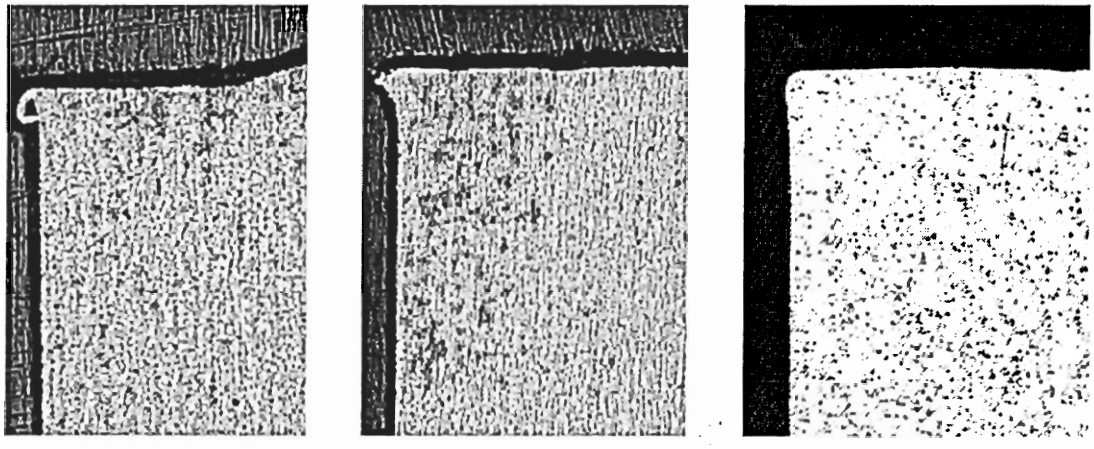

(a) (b) (c)

Figure 4-5 (a) Curling Burr, (b) Triangular Burr, and (c) Bulge Burr

The desire was to develop a metric that quantified hole quality, and since the effect of the size and shape of the burr could only be speculated about, as explained in Section 2.3.2, it was decided that burr geometry should not be used as a metric, but only recorded and compared with fatigue life and residual stresses.

The burrs were not classified according to their size, due to the difficulty of making such a measurement. The burrs were measured according to the length that they extended out from the coupon surface, but this was judged to be a poor measure of the burr. In the case of a curling burr, a small volume of material is left protruding a relatively long distance, even if it was a relatively small curling burr. Even a very large bulge burr, however, would not extend very far from the surface, but instead a long distance axially away from the bore of the hole. Burr length, then, depends on both the burr geometry and size. A better measure would be burr area. However, this is a difficult measurement on such a small scale with complex geometries.

The burrs were instead classified only according to type, and only the exit burrs were examined. The entry burrs were not considered because they were both relatively small and therefore often difficult to classify, and because they are likely to be dependent on both the drilling and withdrawal phases of the process, whereas the exit burrs would be primarily dependent only on the drilling phase. Since each hole was cut in half and two sides of the hole were examined, the number of each type was recorded for each side. For example, if both sides of the hole had a triangular exit burr, the entry would be zero for the curling burr, two for the triangular burr, and zero for the bulge burr. Likewise, if one side had a triangular burr and the other a bulge burr, the entry would be zero, one, and one, respectively. The maximum value for a particular burr type in any given hole is therefore two, and the minimum zero.

4.4.2 Surface Roughness

The curved geometry of the holes presented many challenges, and eliminated the use of several common measures of surface roughness, such as contact and laser

profilometry. The metric devised was the ratio of the traced surface length of the hole by the length of a straight line drawn across the bore, as shown in Figure 4-6. The holes were photographed with an optical microscope equipped with a digital camera, and analyzed with ImagePro software. The roughness was measured on both sides of the hole and the mean value was used. In order to determine the endpoints of the traced and straight lines used for measurement, two edge lines were drawn along the entry and exit faces. The ImagePro software was used to trace the surface of the hole from the intersection of the two edge lines and the surface of the hole. A straight line was then drawn between the same two intersection points used for the trace, and the length was again calculated with the ImagePro software. The traced length was then divided by the straight-line length (producing a number ≥ 1), the process was repeated for the opposite side of the hole, and the mean of the two values was calculated.

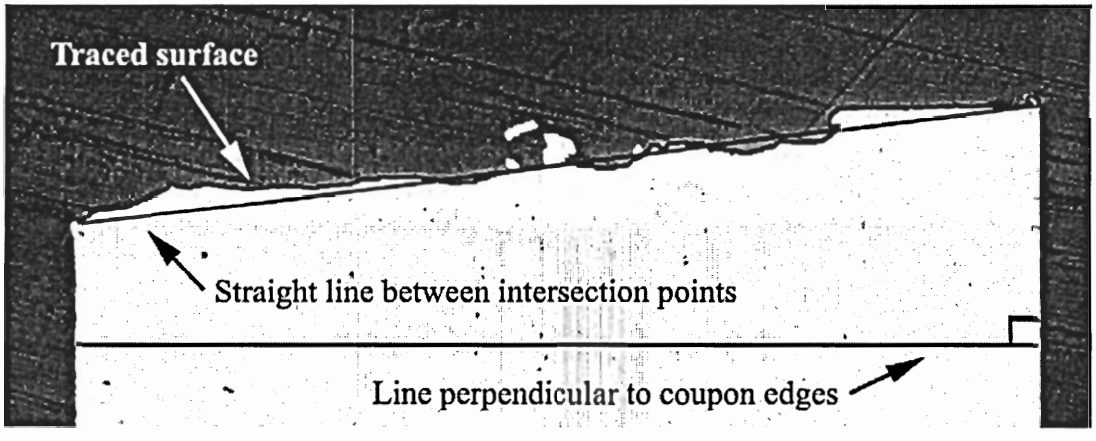

Figure 4-6 Sample Roughness Measurement

4.4.3 Solid Angle

It was quickly discovered that the typical hand-drilled hole is not only drilled at a slight angle from the surface normal, but also drilled wider in diameter at the entry side than the exit side so that, rather than a cylinder, the holes are more like sections of a cone. On the production line, the amount of deviation from the surface normal, or angularity, is important, because highly angular holes will not accept a rivet. This angularity is an issue of operator negligence rather than a result of drilling variables such as bit sharpness, and is unlikely to affect fatigue life. The cone shape is the result of drill "wobble," or a circular deviation from the surface normal. As the drill penetrates the workpiece at an angle, the cutting surfaces gouge out material along the bore, leaving deep scoring marks in the surface. These marks are much deeper than machining marks produced by the drill alone, likely influencing fatigue life more than surface Roughness.

Measuring this angle was straightforward. A line was added perpendicular to the two edge lines already drawn for the Roughness measurements, as shown in Figure 4-6, and the difference between the angle of this perpendicular line and the angle of the straight line connecting the endpoints was calculated. Again, ImagePro automatically gave the angle measurements. Since a larger entry diameter was typical, angles in this direction were considered positive. This same angle was calculated at on the opposite side of the bore, and the two angles were added together to give the resultant solid angle.

4.4.4 Gouge Marks and Plateau

The next two metrics apply specifically to characteristic deep scoring that was found in most drilled holes. The scoring was quickly observed in the mounted holes, and appeared as gouges in the surface of the hole bore, as shown in Figure 4-7, and was

therefore called "gouging." These gouges are much deeper than other types of scoring, and were clearly visible even without a microscope, but they spiraled down through the bore of the hole at the same angle as all the other marks. Another common characteristic noticeable to the eye is a relatively smooth, flat, and cylindrical section at the exit end of the holes. As viewed from the profile pictures, this region looked like a raised, flat region, as shown in Figure 4-7, and thus was labeled a "plateau". This plateau is likely the result of the drill punching through the material at the end as soon as the tip of the drill sufficiently pierces through the coupon. This is substantiated by the fact that there was no plateau in the baseline set, which was machine drilled at a constant feed rate. All of these marks were of slightly varying dimensions and geometry, making a single numeric quantification of them very difficult, so two simpler metrics were employed.

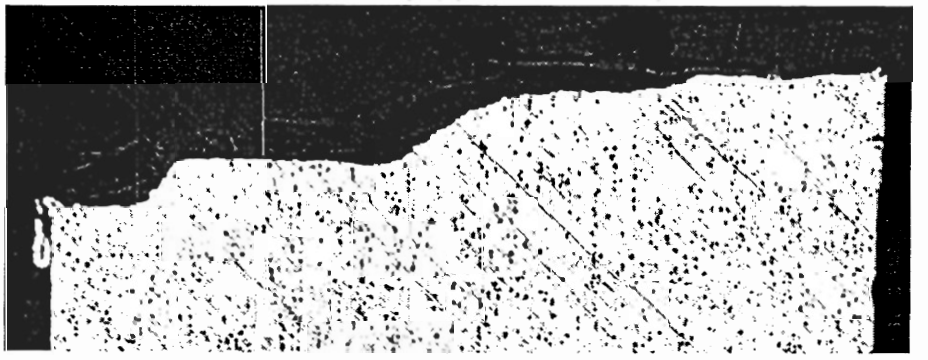

Figure 4-7 Profile Photograph of Gouge Marks and Plateau

4.4.5 Number of Gouge Marks

While there are much fewer gouge marks on the hole bores than the smaller scratches that cause general surface roughness, the gouge marks are larger, and therefore

likely to introduce higher stress concentrations. Thus, it follows that a higher number of these marks increase the likelihood of a fatigue crack initiating from one of them. The first metric for gouge marks, then, was simply a count of the number of gouge marks in the bore surface.

A different perspective on the hole was needed, so the unmounted hole halves were placed in the microscope so that the entire bore could be viewed, rather than the edge. The bore surface was lit from an angle to reduce glare and bring out the surface features. This readily identified the gouges, which contrasted well above the Roughness of the surrounding surface, as illustrated in Figure 4-8. The edge of the plateau region was counted as a gouge mark for this metric.

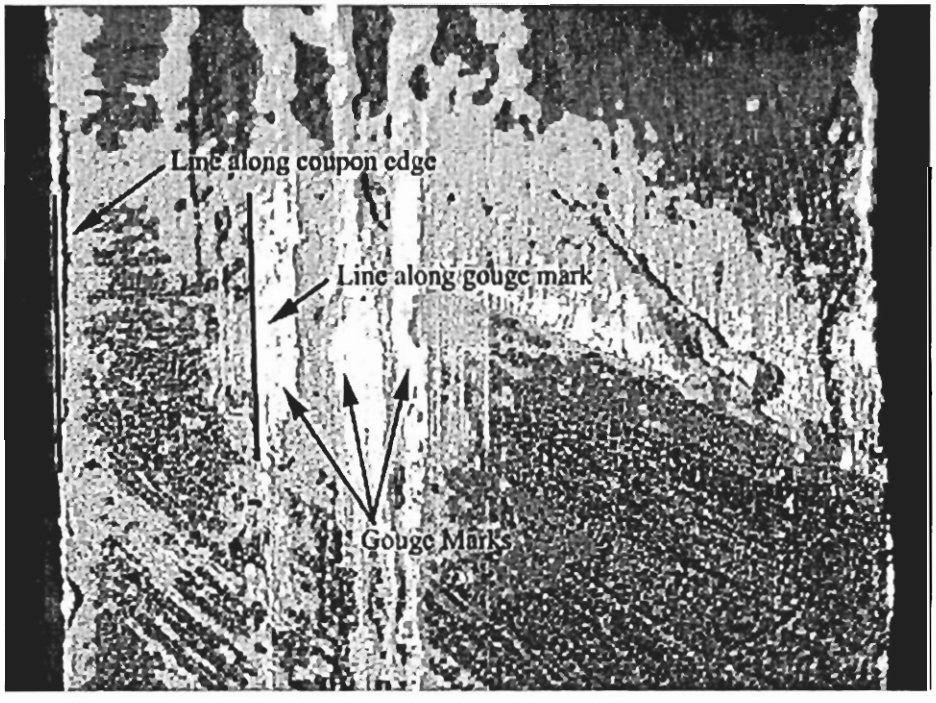

Figure 4-8 Gouge Mark Measurements

4.4.6 Gouge Mark Angle

The second metric measured the angle of the gouges. As the angle approaches ninety degrees, or along the drilling axis, the gouge becomes perpendicular to the loading axis, maximizing its effect. At zero degrees, the gouge is oriented along the loading axis, and has minimal effect.

To measure this angle, the hole was mounted as for the gouge mark count, and the bore was photographed, as in Figure 4-8. Using the ImagePro software, a line was first drawn along one face of the coupon, and another was drawn along a gouge mark. The difference between the angles of the two lines was calculated by the software, and recorded as the value for this metric.

4.5 Statistical Analysis

In order to compare such a complex combination of factors, a careful use of statistical techniques was necessary. First, each combination of factor and metric variable was analyzed. The factors were then compared with each other for each metric. A method of normalizing each metric according to its amount of variability was then employed. This allowed an overall comparison and ranking of the factors.

4.5.1 Ranking of Individual Metric Variables

The analysis was simplified somewhat by using a polar matrix construction in which each factor used a high/low or on/off "setting," which simulated the range of each factor under typical assembly line conditions. For example, each operator applied either

the highest or lowest realistic amount of pressure to the drill that he could. This allows the range of each factor's effect on each metric, or variable, to be calculated. To compute this range, the entire population of holes is sorted according to each factor, and the mean of each setting is calculated.

$$\bar{x} = \frac{\sum_{i=1}^{n} x_i}{n} \tag{4-1}$$

The difference in means is then calculated, and the absolute value yields the desired result. For example, all of the holes were sorted according to whether or not they used a pilot hole, the average roughness was calculated for those holes that had a pilot hole and for those holes that did not, and the lower average value was subtracted from the higher average value. The factors are then ranked according to their difference in means. This process is repeated for each metric.

$$\text{Difference in means} = \bar{x} - \bar{y} \tag{4-2}$$

4.5.2 Normalization

The difference in means allows the comparison of the different factor pairs for a given metric. It would, however, be more useful to compare the factor pairs across the set of metrics. In order to do this, the differences of means are divided by the pooled standard deviation of the two variables. The pooled standard deviation, s_p is found with the following equation:

$$s_p = \sqrt{\frac{(n-1)s_x^2 + (m-1)s_y^2}{n+m-2}} \tag{4-3}$$

where s_x is the standard deviation of the first population, given by:

$$s_x = \sqrt{\frac{\sum\left(x-\bar{x}\right)^2}{n-1}} \tag{4-4}$$

where n is the number of samples in the population and s_y is likewise the standard deviation of the second population with number of samples m. This pooled standard deviation yields a slightly more accurate result than would be achieved by dividing by the standard deviation of the entire population.

After the metrics have been normalized, the average of the variable values for each factor pair is calculated. The factors can then be ranked according to the amount of difference that each factor induces.

4.5.3 P-Value

The p-value is useful statistic for such analyses. It offers a convenient method for evaluating the difference produced by a factor. If the value is small, one can be reasonably confident that the factor produces a significant change in the dependent variable. This allows the investigator to boil all the variability down into a single number.

The p-value is the probability that there is in fact no difference between the variable means. A value of 0.10 or less is considered significant for most analyses. For a pooled variance procedure, the p-value is calculated with the t-statistic, which is computed by:

$$t = \frac{\bar{x}-\bar{y}}{s_p\sqrt{\frac{1}{n}+\frac{1}{m}}} \tag{4-5}$$

The p-value is then:

$$p\text{-value} = 2 \times P(X > |t|) \tag{4-6}$$

A word of caution should be said in about the application of the p-value. Statistics are tools for making statements with a given amount of certainty, but are based on uncertainty, and therefore can never be used to make a statement with absolute certainty. The specific use of this particular statistic is based upon the null hypothesis, which is that there is no difference in the sample means. A p-value of 0.05 can be interpreted by saying, "There is a 5% chance that there really is no difference in the sample means." It cannot be used to make the statement that a difference does exist, since there is always such a chance, no matter how small. The p-value does, however, provide a convenient measure of the amount of variation in the difference of means.

4.5.4 Confidence Intervals

The significance of the difference of means can also be evaluated graphically using confidence intervals. A confidence interval shows the range of values that the mean may have with a given degree of confidence. An example is shown below in Table 4-3. In this example, the factor variables are listed under the "Level" column, the number of samples in each population is listed in the "N" column, the mean value for each population is shown in the "Mean" column, and the "StDev" column gives the respective standard deviations. The confidence intervals are shown at the right of the table. The experimental mean value is shown with an asterisk at the center of the confidence intervals, and the range of the values that the mean may take with a 95% probability (the

confidence chosen for all confidence intervals in this paper) is represented by the dashes enclosed in parentheses. The mean value of the "Long" level, then, lies between about 4.5 and 6.2.

Table 4-3 Sample Confidence Interval

Level	N	Mean	StDev	------+---------+---------+---------+
Long	47	5.332	2.863	(--------*---------)
Short	47	7.162	4.920	(---------*--------)
				------+---------+---------+---------+
				4.8 6.0 7.2 8.4

The equation for calculating the confidence interval is given by:

$$\mu \in \left(\bar{x} - \frac{t_{\alpha/2,n-1} s}{\sqrt{n}}, \bar{x} + \frac{t_{\alpha/2,n-1} s}{\sqrt{n}} \right) \tag{4-7}$$

where μ is the actual mean value of the population, $\bar{x}$ is the experimental mean value, $t_{\alpha/2,n-1}$ is the student's *t*-distribution with α the confidence (0.05 for 95% confidence) and *n* the number of samples in the population, *s* is the experimental standard deviation. For the set in this example, the number of samples is the same, and thus the *t*-distributions are equivalent. The confidence intervals, then, are proportional to $s/\sqrt{n}$, so that the intervals increase with the standard deviation and decrease with the square of the number of samples.

The example in Table 4-3 has overlapping intervals, demonstrating that it is possible that there is in fact no difference in means (or even an opposite difference). However, the means are assumed to have a *t*-distribution, which is very similar to the normal distribution, and in fact reduces to the normal distribution as the number of samples approaches infinity. With such a distribution, the true mean is much more likely

to fall closer to the experimental mean than the edge of the confidence interval. This is reflected by the *p*-value, which for this example is 0.030, reflecting that there is a 3% chance that there really is no difference in means.

Appendix B contains the statistical analyses for a large variety of factor combinations. The significant confidence intervals are duplicated in Chapter 7, Results and Discussion, with minor alterations for readability. The "Level" columns are renamed "Factor", and the factor names are expanded for clarity. The "N" columns have been deleted since the number of samples is already reflected in the standard deviation, and the *p*-values are included in the tables, since it is such a meaningful statistic.

Thus, confidence intervals include a lot of information in a compact form that is easy to interpret visually. They are used extensively in the discussions of the experimental results because they offer such a wealth of statistical information.

CHAPTER V: X-RAY DIFFRACTION

X-ray diffraction is a non-destructive technique that can be used to measure residual stresses in metals. It was employed in this study to attempt to measure the relative residual hoop stresses in order to compare the effects of the drilling factors listed in Chapter 4. This chapter describes the principals of the technique and the experimental methods employed in this study.

5.3 The X-Ray Diffraction Technique

X-ray diffraction, in its essence, measures the intensity of rays diffracted from crystallographic planes. Figure 5-1 shows the principal of x-ray diffraction, in which an incident beam enters a crystal, strikes the atoms arranged in lattice planes, and is diffracted back through the material. At most incident angles, the diffracted rays destructively interfere with each other and cancel out, but diffract out through the lattice planes without interference at certain principal angles that are unique to each material. If one irradiates a crystal with an x-ray beam at a large range of incident angles, and places a detector at corresponding angles of incidence, a graph of the intensity of the detected rays versus the angle of incidence will result in peaks at the principal angles, as shown in Figure 5-2.

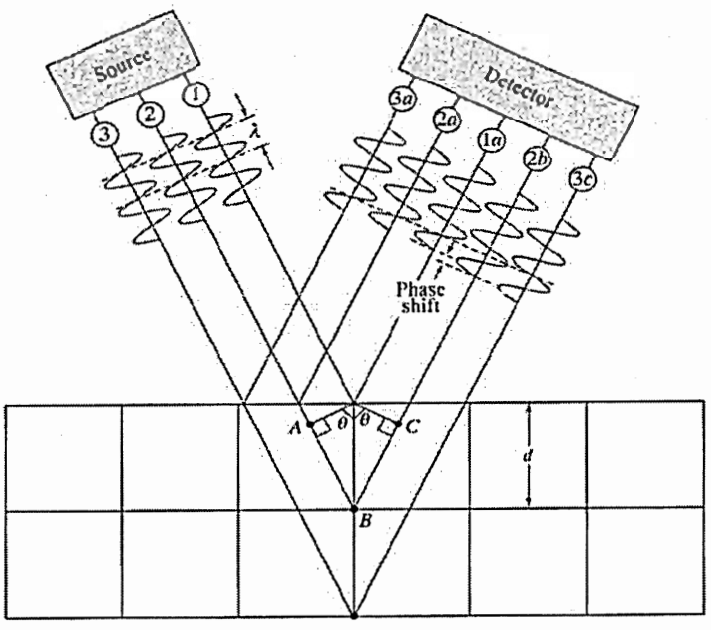

Figure 5-1 The Principal of X-Ray Diffraction[23]

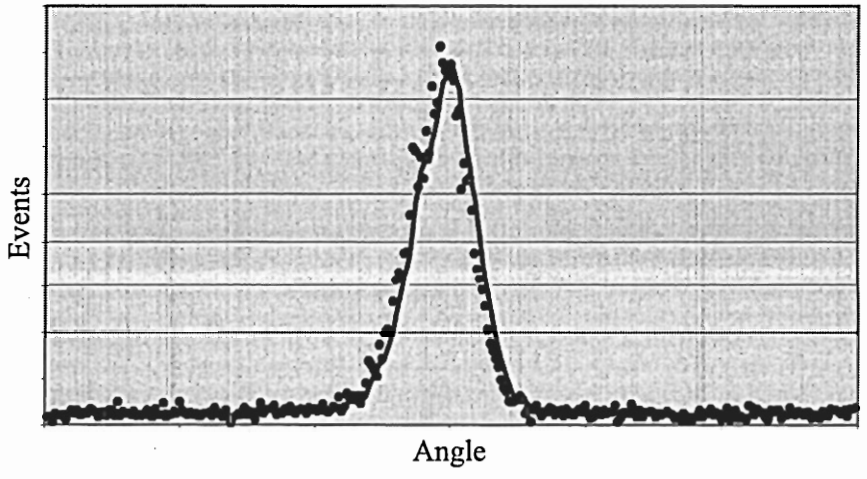

Figure 5-2 Sample Diffraction Line

A uniform stress applied to a bulk material strains the lattice planes and increases the distance between the planes in the direction of the stress. This uniform strain results

in a shift of the corresponding peaks on the diffraction line, as shown in Figures 5-3(a-b). This shift gives a measure of the relative strain, and therefore stress, applied to the material.

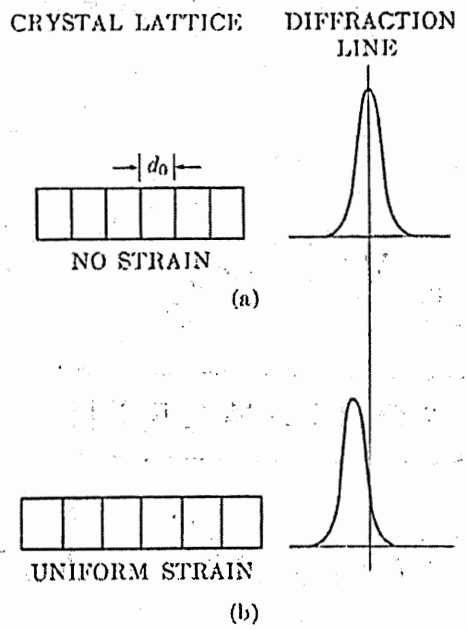

Figure 5-3 Diffraction Lines of (a) Unstrained and (b) Strained Lattices[24]

Figure 5-1 is simplified, because most metals form a polycrystalline structure with the lattice planes of the crystals oriented in random directions. These crystals are generally very small in comparison with the bulk material, and an x-ray beam irradiating a bulk material will strike a number of crystals oriented parallel to the specimen surface, as Figure 5-4 illustrates.

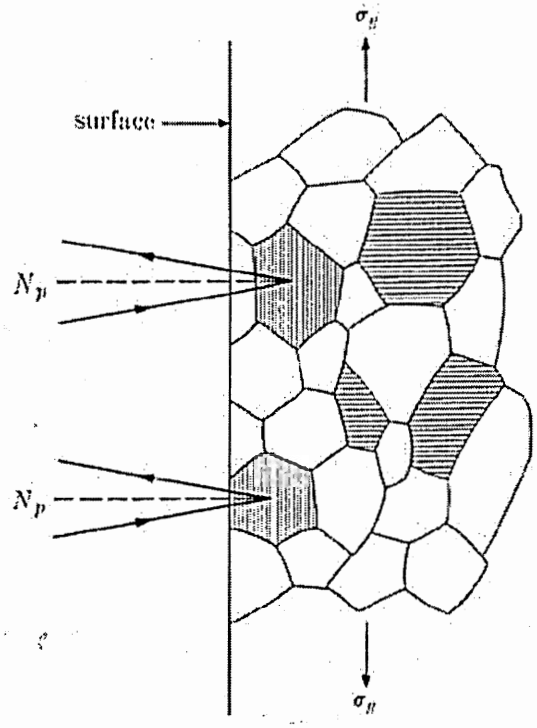

Figure 5-4 Diffraction of a Bulk Material Specimen

5.2 Design of Experiment

The unmounted hole halves from the hole quality experiment provided the sample set for the x-ray diffraction experiment. Both the hand-drilled and machine-drilled holes were to be used. One sample from each of the combinations of hand-drilling and machine-drilling factor variables were to be used, as well as one polished sample each of the LT and TL coupons. This would limit the number of specimens to be tested while still providing a sufficiently large sample population.

5.3 Experimental Procedure

The samples were mounted to the x-ray goniometer stage such that the length of the specimen was vertical (the y-direction), the width of the specimen was horizontal (x-direction), and the depth protruded out of the stage in the z-direction, as illustrated in Figure 5-5. Rotation about the x-axis is the Ψ (Psi) angle, and rotation about the y-axis are the 2θ/Ω (2 Theta / Omega) angles.

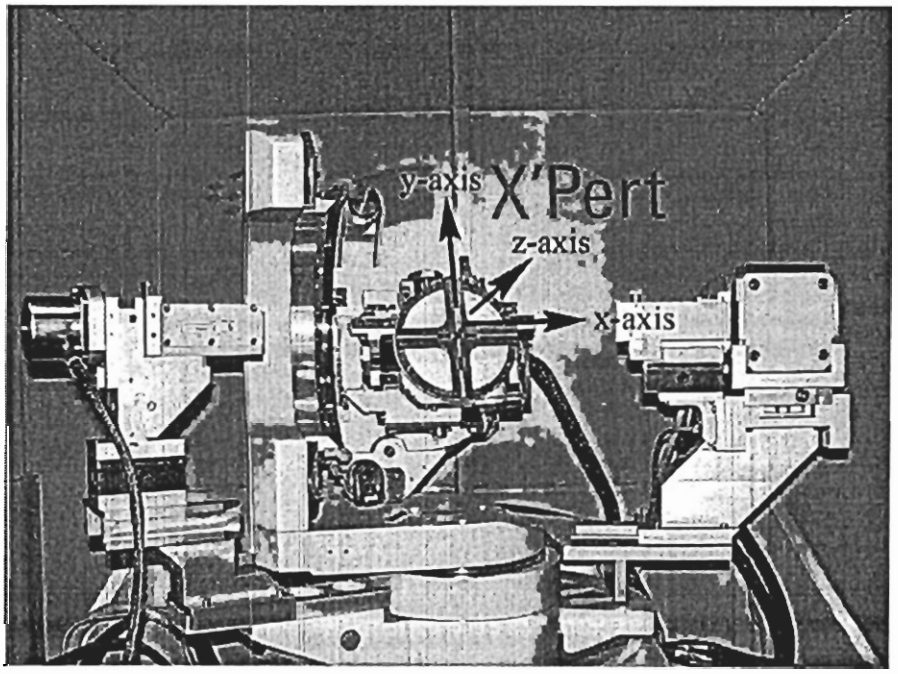

Figure 5-5 X-Ray Machine Coordinates

The x-ray beam optics were specially chosen for the sample geometry. The Cu-kα x-ray tube was rotated to produce a spot beam, which allowed the entire beam intensity to be focused in a smaller area, rather than spread out over a line, which is typical. In order to optimize the height and width of the beam, a crossed-slits collimator

(Figure 5.6(a)) was employed, which allowed the beam size to be adjusted both vertically and horizontally from 0 to 10 mm at increments of 0.01 mm. A nickel attenuator was inserted into the crossed-slits collimator to prevent damage to the detector. The sample stage was also aluminum, and so a parallel plate collimator (Figure 5-6(b)) with a 0.027 mm slit was chosen for the detector to reduce the chance of collecting signals from the stage.

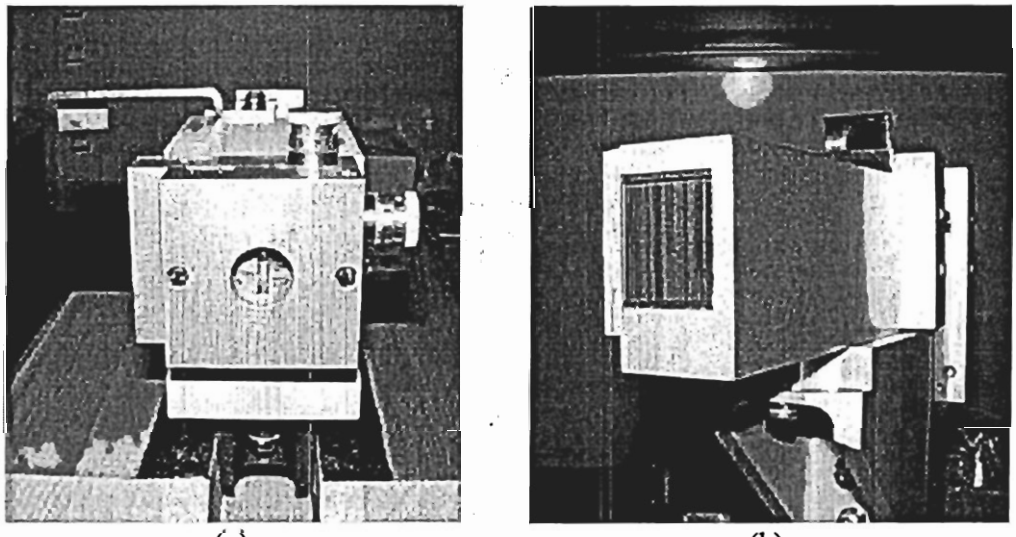

(a) (b)

Figure 5-6 (a) Crossed-Slits Collimator and (b) Parallel Plate Collimator

The placement of the beam on the sample is illustrated in Figure 5-7. The x-ray beam was directed into the center of the hole half to minimize any hoop stress relaxation due to cutting of the hole in half. The nominal beam cross-section was 0.25 mm^2, and was determined by reducing the beam size to the minimum allowable to clearly distinguish the peaks above the signal noise. Flat specimen surfaces are preferred so that the incident beam angle is the same throughout the beam cross-section. The curved

geometry of the hole therefore presented a continuously variable angle of incidence. To reduce this effect, the beam width was maximized so that the height could be reduced to the minimum possible, while still retaining the nominal cross-section. In aluminum, the [111] plane gives the strongest diffraction, corresponding to a principal angle of 38.47 degrees. At a 38 degree angle, the width of the incident beam spot width will be about 1.6 times the emitted width. Because of this, the width of the emitted beam was maximized at 1.1 mm, or about 0.043 inches, which corresponds to an incident spot width of about 0.070 inches, allowing 0.01 inches on either side of the beam for specimen nonuniformity, misalignment of the beam, and plane stress conditions at the free surfaces. In order to maintain the 0.25 mm^2 spot cross-section, the height of the emitted beam spot was set at 0.23 mm.

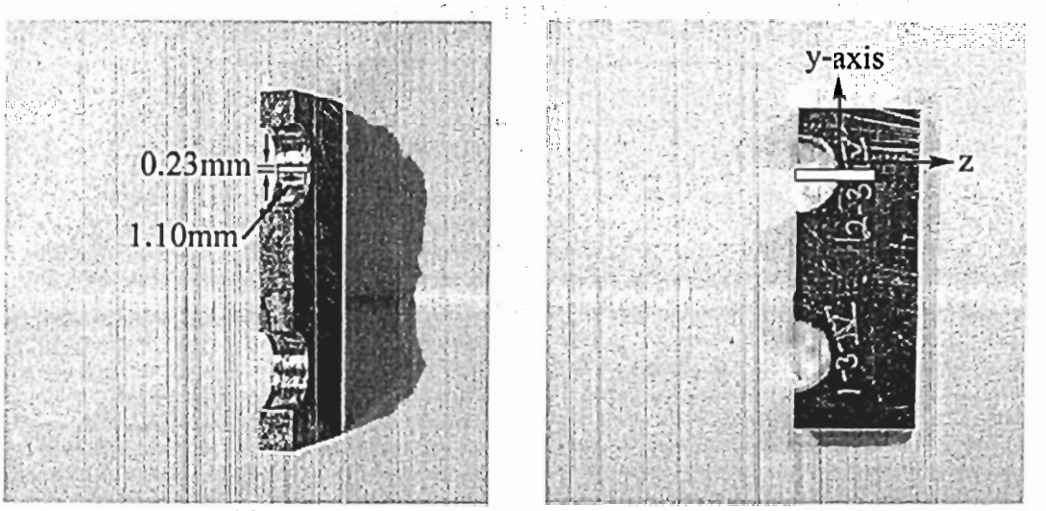

Figure 5-7 (a) Placement and (b) Alignment of Exaggerated X-Ray Beam

Before a specimen could be scanned, the specimen needed to be aligned and the system optimized. The specimen was loaded onto the stage as illustrated in Figure 5-5. The specimen was always offset in the x-direction by 0.84 mm, which was accounted for first in the alignment. The x-ray beam shutter was then opened and the intensity was noted. In order to center the beam horizontally, the sample was adjusted along the z-axis until the intensity was halved, as illustrated in Figure 5-7(b). To center the beam vertically, the specimen was adjusted along the y-axis until the intensity was maximized. The z-axis was then adjusted again until the intensity was half of the original value. To align the system, a 2θ scan was run in one degree about the current 0 degree position, and the system was offset to match the diffraction line peak. An Ω scan was then run in six degrees about the current position, and the system was again offset to match the peak. Finally, an Ω/2Θ scan was run in one degree about the 38.47 degree principal angle, and 2Θ was offset to half of Ω.

Once this was accomplished, a residual stress scan could be run. Scans were conducted by varying the 2Θ/Ω angles, and tilting the sample at nine different Ψ angles. The peaks of each of the nine resulting curves were identified, and the corresponding lattice distance, or *d*-spacing, was recorded. The results were plotted as $\sin^2\Psi$ versus *d*, and the angle of the resultant slope represented the relative residual stress.

CHAPTER VI: FATIGUE TESTING

The fatigue tests are the capstone of this study, since the ultimate objective was to assess the fatigue life of aircraft fastener holes. The first goal of the tests was to compare the fatigue life of as-drilled holes with holes polished in accordance with the AGARD R-732 procedure. The second goal was to compare the fatigue effects of the factors from the hole quality study.

These tests also had to answer a number of different questions while making efficient use of time and material. The test parameters needed to be consistent with those of the AGARD R-732 study, as discussed in Section 2.1.1, which concluded that drilling induced significant compressive residual hoop stresses that could be removed through a chemical polishing procedure. Consistency in loading parameters would enable the comparison of the results of this study with those of the AGARD study. The tests also needed to represent the conditions to which actual production fastener holes are subjected in order to provide meaningful application to the industry.

6.1 Design of Experiments

The fatigue tests were broken up into two segments. The first segment tested only as-drilled and polished coupons. In the second segment, rivets were inserted into the coupon holes in order to assess whether the fastening process eliminated drilling effects or modified them.

The first test was designed to investigate the effect of residual stresses, which were assumed to exist in the as-drilled holes. Two factors were to be chosen, which would result in four possible combinations. Six replicates of each combination were to be drilled to provide statistical significance of the results while allowing for a variety of loading conditions. This yielded twenty-four holes, which was less than one-third of the available test coupons, and could be fatigue tested in a reasonable amount of time.

The three most significant hole quality factors were 1) Pilot Hole, 2) Operator, and 3) Bit Condition, as will be shown in Section 7.1. The use of a pilot hole resulted in the largest hole quality variations, and was thus chosen as a factor for the fatigue tests. The operator factor was included in the hole quality experiment to represent the human factors involved in drilling. These factors are likely extremely complex, and out of the scope of this study. The operator factor was therefore eliminated as a factor for this test matrix. The drill bit condition also resulted in significant variations in hole quality, and it was also suspected that a dull drill bit would induce greater residual stresses than a sharp bit. Bit condition was therefore chosen as the second factor for the first test.

Due to the small number of samples to be prepared, a factorial matrix was not required. The four factor combinations are show in Table 6-1. The twelve coupons that used a pilot hole were predrilled before the fastener holes were drilled. The twenty-four coupons were randomized to reduce sequencing effects, and the randomized matrix is shown below, in Table 6-2.

Table 6-1 Fatigue Test As-Drilled Factor Combinations

Bit Condition	Pilot Hole
New	Yes
New	No
Old	Yes
Old	No

Table 6-2 Randomized Hand-Drilling Matrix

Bit Condition	Pilot Hole	Coupon
Old	Yes	A96N8-6
New	No	A93N8-4
New	Yes	A91N8-14
New	No	A95N8-2
Old	No	A91N8-8
New	Yes	A94N8-12
New	No	A96N8-3
Old	Yes	A89N8-3
Old	No	A95N8-3
New	No	A89N8-9
New	Yes	A91N8-3
Old	Yes	A95N8-14

Bit Condition	Pilot Hole	Coupon
New	Yes	A90N8-10
Old	Yes	A94N8-6
Old	Yes	A93N8-3
Old	Yes	A93N8-15
New	Yes	A94N8-14
New	Yes	A91N8-12
New	No	A90N8-15
Old	No	A96N8-10
Old	No	A93N8-8
Old	No	A89N8-14
Old	No	A93N8-10
New	No	A95N8-7

All of the as-drilled coupons provided were in the LT orientation. Coupons polished according to the AGARD R-732 five-minute-polishing procedure were provided in both the LT and TL orientations for the purpose of establishing a baseline comparable to the AGARD study. Another set of machine-drilled coupons was prepared at Delta for the purpose of establishing an as-drilled baseline. The factor combinations for the machine-drilled coupons were chosen based on the theoretical best quality hole parameters—short bit, low feed rate, and with a pilot hole. Since it was unknown

whether an old bit would increase the fatigue life, both an old bit and new bit were used. Loads were chosen to be the same as those in the AGARD study, which were R = 0 with a maximum remote stress of 17.5 ksi, 21 ksi, and 25 ksi. The complete test matrix is shown in Table 6-3.

Table 6-3 Fatigue Test Matrix

Specimen Type	Max Load (ksi)	Number
Polished, LT	17.5	2
Polished, TL	17.5	2
Hand-Drilled, New Bit, No Pilot Hole	17.5	1
Hand-Drilled, New Bit, Pilot Hole	17.5	1
Hand-Drilled, Old Bit, No Pilot Hole	17.5	1
Hand-Drilled, Old Bit, Pilot Hole	17.5	1
Machine-Drilled, Old Bit, No Pilot Hole	17.5	3
Machine-Drilled, New Bit, No Pilot Hole	17.5	3
Polished, LT	21	5
Polished, TL	21	4
Hand-Drilled, New Bit, No Pilot Hole	21	5
Hand-Drilled, New Bit, Pilot Hole	21	5
Hand-Drilled, Old Bit, No Pilot Hole	21	5
Hand-Drilled, Old Bit, Pilot Hole	21	5*
Polished, LT	25	2
Polished, TL	25	2

*Due to operator error, one specimen tested at 25 ksi

The net section stress is calculated by the equation in Figure 6-1, where P is the load, which is the remote stress multiplied by the cross sectional area of the coupon, and the other dimensions are as shown in the figure. Using a hole diameter of 3/16 inch, or 0.1875 inches, a coupon width of 2.000 inches, and a coupon thickness of 0.0900 inches, the remote stress levels 17.5, 21, and 25 ksi correspond to net section stress levels of 19.3, 23.2, and 27.6 ksi. The figure shows that a d/w value of 0.09 from the coupon

dimensions corresponds to a k_t value of approximately 2.8. Thus, the corresponding stress levels at the notch root are 54.1, 64.9, and 77.2 ksi.

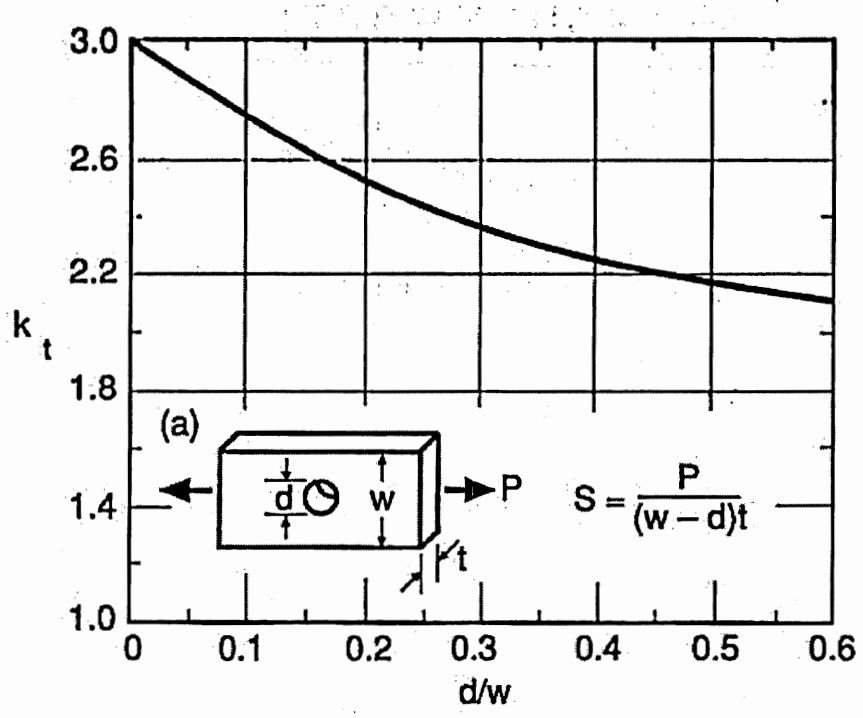

Figure 6-1 Stress Concentration Calculation[25]

In addition, underload and overload tests were to be conducted in order to help correlate the results of the FASTRAN K3DL residual stress code. Eight of these tests were conducted, as shown in Table 6.4. A spike underload or overload was applied to each specimen on the first cycle. The specimens were then tested at 21 ksi maximum load at R = 0.

Table 6-4 Underload and Overload Fatigue Test Matrix

Specimen Type	Spike Load (ksi)	Max Fatigue Load (ksi)	Number
Polished, LT, Overload	35.7	21	2
Polished, LT, Underload	-35.7	21	2
Polished, TL Overload	35.7	21	2
Polished, TL Underload	-35.7	21	2

6.2 Experimental Procedure

6.2.1 Drilling

All hand drilling was done according to the procedure used for the hole quality experiment, as detailed in Section 4.3. The old bit was the same bit used in the previous study, and the new bit was an unused bit provided by Lockheed Martin, both the same type bit as before. The pilot holes were 3/32 inch diameter, also as before. The holes were not deburred prior to testing.

6.2.2 Crack Detection Gages

Crack detection gages were successfully installed on several as-drilled specimens and polished specimens at various loads. The gages were Micro-Measurements type CD-23-10A, which is an isoelastic nickel-chromium alloy laminated to a glass-fiber-reinforced backing, remaining essentially linear to approximately 5000 με, and a fatigue life of approximately 10^5 cycles at 3000 με. The gages were attached by first applying a conditioner formula and polishing the material adjacent to the hole, being careful not to disturb any burrs. A neutralizer was then applied, and any residue was removed. The

gages were then mounted next to the notch root using a cyanoacrylate adhesive. Lead wires were soldered to the ends of the gage, as show in Figure 6-2. A circuit was constructed to monitor the gages, as shown in Figure 6-3. The circuit illuminated a LED as long as the gage remained intact. Once the gage failed, the relay switched current away from the LED and through either a siren or the test frame computer. Four of these circuits were constructed in parallel—one for each detection gage.

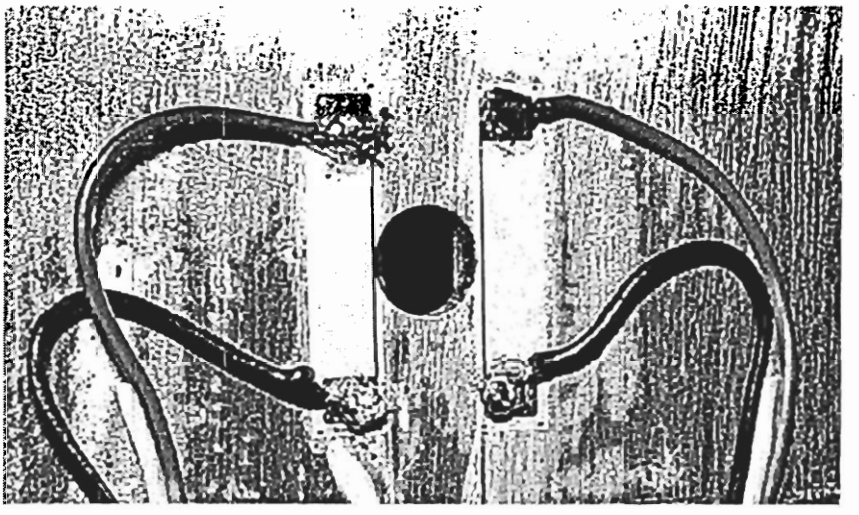

Figure 6-2 Crack Detection Gage Mounting

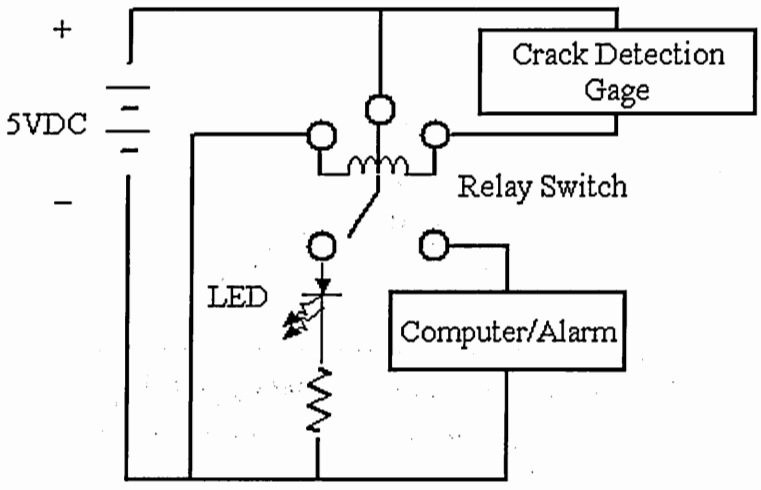

Figure 6-3 Crack Detection Circuit

6.2.3 Fatigue Testing and Data Collection

In order to calculate the loading parameters, the width and thickness of each specimen was measured near each end and at the middle, and the average cross-sectional thickness was calculated. This area was multiplied by the maximum stress to be applied in order to determine the maximum load. All tests were conducted at R = 0 at a maximum of 10 Hz.

Specimens were tested with a 20,000 lbf MTS hydraulic test frame at room temperature. The specimens were mounted in hydraulic wedge grips so that $L \geq 4a$, i.e. so that there was at least twice the width, or four inches, between grips, as shown in Figure 6-4. The specimens were adjusted on the grips so that the hole was at the center of the load line.

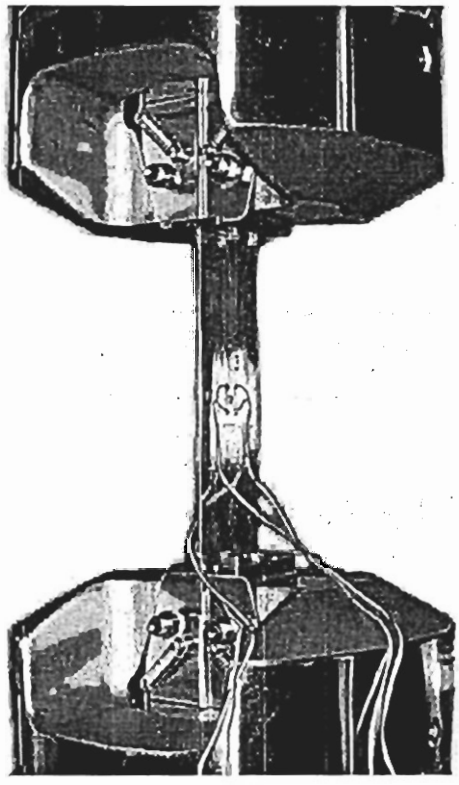

Figure 6-4 Typical Fatigue Test Setup

Cycles to failure, N_f, for the fatigue tests was the number of cycles to separation of the specimen. Cycles to initiation, N_i, was considered number of cycles to indication of the first crack detection gage (to the nearest 100 cycles).

The overload and underload tests used polished LT specimens. The "spike" overload was applied with a single cycle of 1.7 times the maximum tensile fatigue stress of 21 ksi, which equals 35.7 ksi. The underload was applied in a single compressive cycle of the same magnitude, or –35.7 ksi. Actions were taken to prevent buckling, as will be described below.

The overloaded specimens were tested in the same way as the standard specimens, except that tabs were attached to the specimens to prevent breakage at the

grips due to grip tooth indentations and cycles exceeding one million. The tabs were phenolic board attached with epoxy, as shown in Figure 6-5.

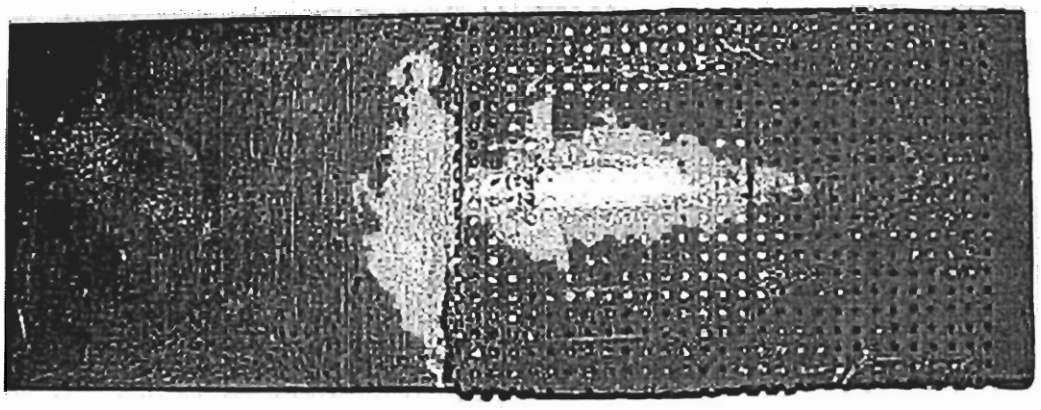

Figure 6-5 Overload Specimen With Tabs

The specimens were could not support the spike underload, so two actions were taken to prevent specimen damage. The first action was to reduce the length of the specimen. Equation 6-1 was used to calculate the critical buckling length of a specimen 0.09 inches thick and two inches wide, where E is Young's Modulus; K is the effective-length factor, which is 0.5 for a column fixed at both ends; σ is the buckling stress, which is 35.7 ksi; I is the least moment of inertia for the cross-sectional area; and A is the cross-sectional area. Calculations showed that a maximum distance between the grips of 2.6 inches would be sufficient. The test grips were 1.75 inches long, and the minimum distance allowable between the grips during fatigue testing was four inches. Therefore, any specimen length below 7.5 inches would require increased gripping pressure during fatigue testing. A test on a blank specimen showed that the specimen buckled at a length

of 2.2 inches between the grips. This was probably due to slight warping of the specimen and imperfect alignment of the grips. Cutting the specimen down to any shorter length would require gripping pressures high enough to damage the specimen and increase the likelihood of breakage at the grips.

$$L_{cr} = \frac{\pi \cdot \sqrt{E} \cdot r}{K \cdot \sqrt{\sigma}} \tag{6-1}$$

$$r = \sqrt{\frac{I}{A}} \tag{6-2}$$

In order to maintain an acceptable specimen length and gripping pressure, an anti-buckling plate was made. The device was constructed of aluminum plate with Teflon sheeting sandwiched between the plates and the specimen. The arrangement was fastened at the corners with washers and bolts adjusted to finger tightness, so that the device could be moved across the specimen without much force, as shown in Figure 6-6. The specimens were then loaded with 2.2 inches between the grips and the underloads were successfully applied.

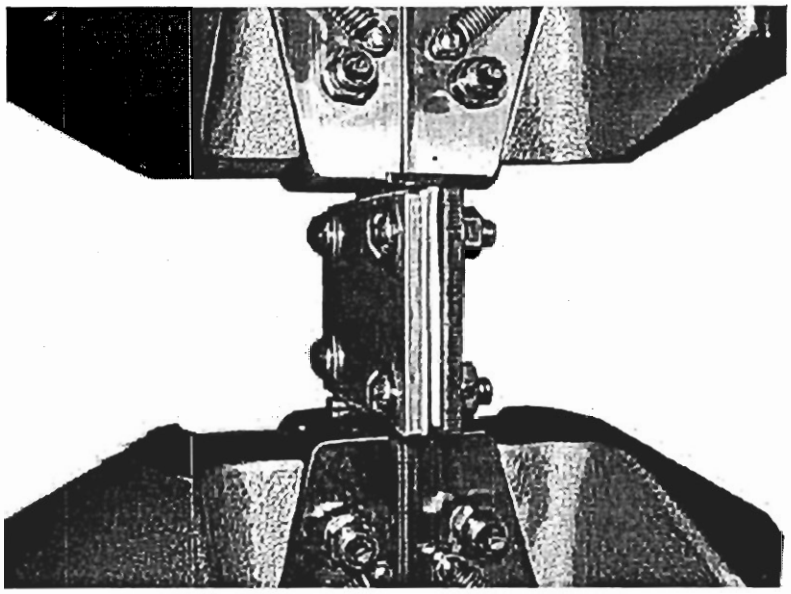

Figure 6-6 Underload Setup With Anti-Buckling Plates

Specimens were inspected after failure to determine the initiation site. The specimens were viewed at low power and lit from the side to reveal surface features. In the majority of specimens, a large crack formed on both sides of the hole before the specimen failed, therefore only specimens with crack detection gages were used, and the side of the hole that first indicated a crack was examined. Crack initiation sites were determined visually, and was categorized as either a corner or center crack.

6.3 Data Reduction

Fatigue is a complex phenomenon consisting of three primary stages: crack initiation, crack growth, and failure. A number of analyses are needed to sufficiently describe the nature of fatigue in this study. These analyses have been performed both

graphically and statistically (as laid out in Section 4.5), although the statistical receives the most attention in this paper.

Failure was the easiest measure to define, at least in this study. It was specified as the number of cycles to separation of the specimen into two halves from a crack initiating at the hole, as was designated N_f. This represents the total life of the specimen, and encompasses crack initiation and growth, as well as failure.

Crack growth is the stage between initiation and failure. It is defined in this study by the difference between failure and initiation, $N_f - N_i$. Residual stresses can retard the growth of the crack until it extends beyond the residual stress field. In order to account for loading differences, the crack growth stage can also be normalized by dividing by the cycles to failure $(N_f - N_i)/N_f$.

Crack initiation can be a difficult quantity to define. Every material contains flaws and stress concentrations before the first cycle is applied, and often the critical crack must be identified after failure and some method must be employed to trace that crack back to its initial size. The crack detection gages simplified the problem in this test by defining initiation as the appearance of the first surface crack, N_{i1}. The disadvantage is that this definition is mildly dependant upon the crack initiation site, since a corner crack would be detected immediately and a center crack must grow to the surface before it would be detected. This problem makes the statistical analysis of multiple samples necessary. The initiation can also be normalized by failure, N_i/N_f. As the first crack grows, the stress at the notch root and crack tip increases since all tests were stress controlled. This increase in stress will eventually cause a crack to form at the notch root opposite the initial crack. The initiation of this crack was designated N_{i2}. If N_{i2} occurs

shortly after N_{i1}, then the stress will not have risen significantly, and the second crack is more dependent on surface features than on the stress increase. Therefore, $N_{i2} - N_{i1}$ was also used, as well as the normalized quantity $(N_{i2} - N_{i1})/N_f$. This quantity was also normalized by the cycles to initiation, $(N_{i2} - N_{i1})/(N_f - N_{i1})$, in order to eliminate crack growth effects.

6.4 Fatigue Crack Surface Microscopy

In order to better model crack growth, it is important to specify the location and shape of the initial crack. Therefore, crack surfaces were inspected with an optical microscope. Since the most critical crack is the one that initiates first, only those coupons were inspected in which the crack detection gages successfully operated, and only on the side of the hole that cracked first.

These surfaces were digitally photographed in an optical microscope at 10x magnification. The initiation sites were then categorized as either corner cracks or center cracks. The results were then analyzed statistically in reference to whether the specimens were polished, hand-drilled, or machine-drilled.

In addition, since the crack detection gages have not been proven in this laboratory, the reliability of their operation was in question. In particular, it was important to know the size of a detectable crack. In order to determine this, the crack surface needed to be inspected while under sufficient load to open the crack, but without destroying the specimen.

Replicating tape, purchased from Ernest F. Fullam, Inc., was employed for this purpose. The tape was prepared before the test by cutting a length of tape approximately

three inches long and rolling it into a cylinder the same diameter as the hole. The test was stopped as soon as a crack was detected, the load was set to zero, and the cylinder of tape was inserted into the hole. The specimen load was then set to two-thirds of the maximum load. This load was chosen because the crack detection gages typically required at least half of the maximum load to reopen when they initially failed, indicating that the crack was completely closed at half-load. The tape was then wetted with acetate, which softened the material, and the butt end of a 5/32 inch drill bit was used to press the tape against the cracked surface, starting from the opposite side of the hole so that the cylinder was collapsed upon itself. After about one minute the tape was carefully peeled away from the surface and set aside, and the test was immediately resumed. Five of these replicates were made with both thin and thick replicating tape. The thin tape gave the best results and was used for microscope inspection.

The replicates were first inspected with an optical microscope. The specimens were placed on the stage and viewed at low magnification until the crack could be found. Once found, the crack was digitally photographed at 50x magnification and the width of the crack was measured. The clear tape proved to be problematic for this type of inspection because the crack was difficult to find and the back surface of the replicate was often confused with the front. In addition, the edges of the crack were difficult to define for measurement.

The replicates were then inspected with a scanning electron microscope (SEM). The tape was sputtered with gold to permit conductivity. The crack was readily visible under the SEM, and the edges of the crack were easy to define. The cracks were photographed at 40x magnification to provide a global view of the entire hole surface,

200x to illustrate the conditions at the edge of the hole, and at 1000x to measure the width of the crack.

CHAPTER VII: RESULTS AND DISCUSSION

The three tests of hole quality, x-ray diffraction, and fatigue life were conducted as prescribed in Chapters 4, 5, and 6, respectively. The hole quality tests found that the pilot hole produced the greatest difference in hole quality, and that the use of a pilot hole improved hole quality in every respect. The x-ray diffraction tests could not yield acceptable results due to the specimen geometry, the machining marks, and the properties of the aluminum. The fatigue tests found that drilling appears to produce compressive residual hoop stress, but that hole quality predominantly determines fatigue life.

7.1 Hole Quality

Difference of means calculations were performed as described in Section 4.5, and the results are tabulated for the hand-drilled and machine-drilled holes in Tables 7-1 and 7-2, respectively. In these tables, the mean values for each factor/response combination are listed in the first two rows of each factor/response combination. The absolute values of the differences are shown in the rows entitled "Difference", and the *p*-values for the differences of means are displayed in the rows labeled "*p*-value". The standard deviations for the individual factor/response combinations are listed in the "StDev" rows. The normalized differences in means are calculated in the "Score" rows. These averages of the scores for each factor are shown in the final column, entitled "Overall Score". The raw data for the hole quality measurements can be found in Appendix A, Table A-2. It

should be noted that only five of the twenty-four factor/response combinations have *p*-values less than 0.1

A statistical analysis package called MiniTab was used to calculate these values using the same equations given in Section 4.5. The complete output created by the MiniTab package for these analyses can be found in Appendix B. MiniTab was also used to plot the 95% confidence intervals for each factor/response combination, some of which will be shown below.

Two graphical comparisons of these results are shown in Figures 7-1(a-b). These charts plot the average normalized differences in means for each of the two tests, giving a measure of the relative significance of each factor. It is interesting to note that machine drilling resulted in more overall variability than did hand drilling.

Table 7-1 Hole Quality Results

Factor	Roughness	Conicality	Gouge Angle	Gouge Number	Overall Score
Experienced	1.049	6.2	4.3	1.9	
Novice	1.051	6.3	2.8	1.1	
Difference	0.002	0.0	1.5	0.8	
p-value	0.955	0.968	0.127	**0.002**	
StDev	0.158	4.130	4.597	1.187	
Score	0.012	0.008	0.318	0.645	**0.246**
No Pilot	1.065	7.8	5.4	1.3	
Pilot Hole	1.035	4.8	1.8	1.7	
Difference	0.031	3.0	3.5	0.4	
p-value	0.341	**0.000**	**0.000**	0.159	
StDev	0.157	3.833	4.301	1.235	
Score	0.197	0.794	0.821	0.294	**0.526**
Long Bit	1.048	5.3	3.7	1.4	
Short Bit	1.051	7.2	3.5	1.6	
Difference	0.003	1.8	0.2	0.2	
p-value	0.926	**0.030**	0.827	0.509	
StDev	0.158	4.025	4.655	1.246	
Score	0.020	0.455	0.045	0.136	**0.164**
New Bit	1.024	5.7	3.5	1.3	
Old Bit	1.045	6.7	3.7	1.7	
Difference	0.021	1.0	0.2	0.4	
p-value	0.117	0.240	0.848	**0.097**	
StDev	0.155	4.099	4.655	1.230	
Score	0.133	0.244	0.040	0.346	**0.191**
High Press	1.044	5.6	3.0	1.4	
Low Press	1.055	6.8	4.1	1.5	
Difference	0.012	1.2	1.1	0.1	
p-value	0.720	0.157	0.264	0.679	
StDev	0.157	4.085	4.625	1.248	
Score	0.074	0.294	0.232	0.086	**0.172**
Full Speed	1.047	6.3	3.6	1.5	
Stopped	1.053	6.2	3.6	1.5	
Difference	0.006	0.0	0.0	0.1	
p-value	0.860	0.970	0.999	0.806	
StDev	0.158	4.130	4.656	1.248	
Score	0.037	0.008	0.000	0.051	**0.024**

Table 7-2 Machine-Drilled Hole Quality Results

Factor	Roughness	Conicality	Gouge Angle	Gouge Number	Overall Score
No Pilot	1.074	3.9	6.0	1.9	
Pilot Hole	1.076	0.7	3.2	0.8	
Difference	0.003	3.2	2.9	1.2	
p-value	0.804	**0.001**	0.218	**0.069**	
StDev	0.026	2.045	5.558	1.495	
Score	0.104	1.577	0.517	0.781	**0.745**
Long Bit	1.089	3.2	6.5	1.7	
Short Bit	1.061	1.5	2.7	1.0	
Difference	0.028	1.7	3.7	0.7	
p-value	**0.004**	**0.108**	**0.105**	0.311	
StDev	0.022	2.495	5.416	1.576	
Score	1.316	0.685	0.691	0.423	**0.779**
New Bit	1.069	2.6	5.5	1.3	
Old Bit	1.081	2.0	3.7	1.3	
Difference	0.013	0.7	1.9	0.0	
p-value	0.240	0.546	0.427	1.000	
StDev	0.025	2.627	5.674	1.614	
Score	0.494	0.251	0.330	0.000	**0.269**
High Feed	1.078	1.6	4.7	1.9	
Low Feed	1.072	3.0	4.5	0.8	
Difference	0.006	1.3	0.3	1.2	
p-value	0.589	0.212	0.913	**0.069**	
StDev	0.026	2.555	5.756	1.495	
Score	0.224	0.525	0.045	0.781	**0.394**

(a)

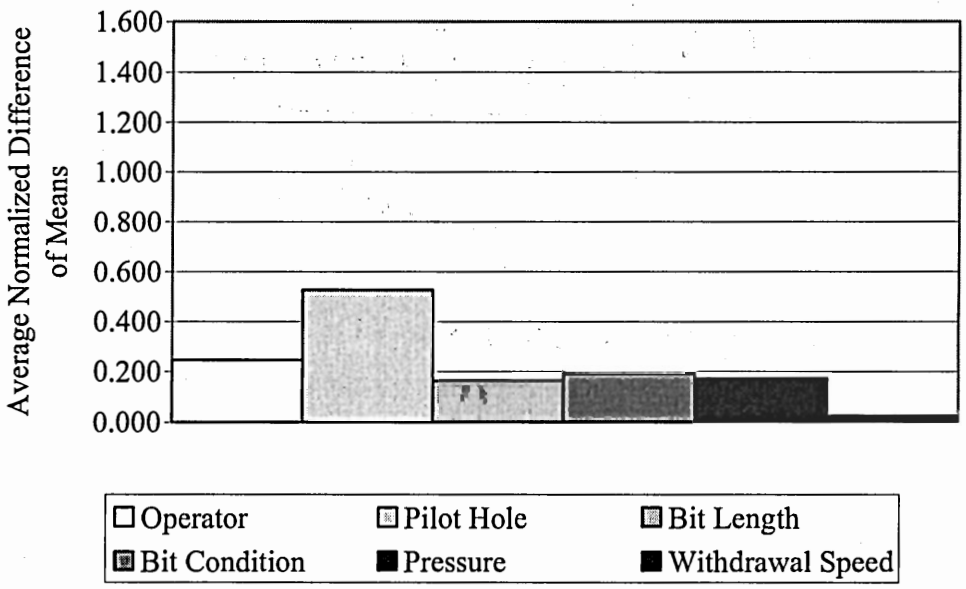

(b)

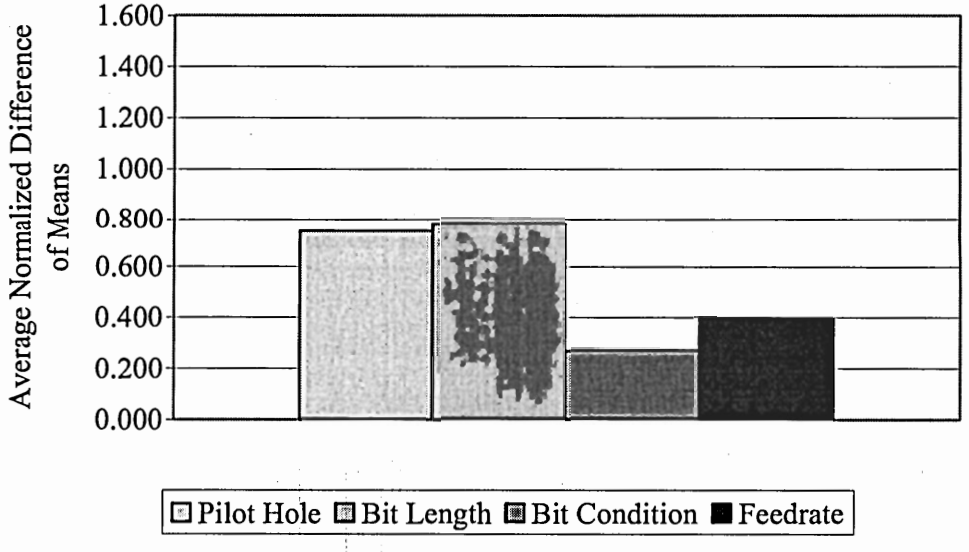

Figure 7-1 Comparison of Overall Variability in (a) Hand Drilling and (b) Machine Drilling

7.1.1 Pilot Hole Results

As Figures 7-1(a-b) illustrate, the pilot hole produced the greatest overall variability in the hole quality tests. This factor resulted in more than twice as much variability as the next most significant factor in the hand-drilled holes, and scored a close second in the machine-drilled holes. In particular, the pilot hole resulted in clearly significant differences in means in the hand-drilled tests in both conicality and gouge mark angle. In the machine-drilled holes, it yielded a significant difference in the conicality and number of gouge marks.

The effects of the pilot hole on conicality are shown in the 95% confidence intervals in Tables 7-3 and 7-4. Confidence intervals are described in Section 4.5.4. It should be noted that the scales of the confidence interval plots for the two tables are different. These results clearly show that the use of a pilot hole reduces the conicality of the final hole. In fact, comparing these two tables shows that hand drilling with a pilot hole is roughly equivalent to machine drilling without a pilot hole. Thus, using a pilot hole makes hand drilling equivalent to machine drilling in the case of conicality.

Table 7-3 Effect of Pilot Hole on Conicality (Hand Drilling)

Factor	Mean	StDev	------+---------+---------+---------+
No Pilot Hole	7.800	4.768	(------*------)
Pilot Hole	4.758	2.646	(-------*------)
			------+---------+---------+---------+
p-value = 0.000			4.5 6.0 7.5 9.0

Table 7-4 Effect of Pilot Hole on Conicality (Machine Drilling)

Factor	Mean	StDev	----+---------+---------+---------+--
No Pilot Hole	3.925	2.798	(-------*------)
Pilot Hole	0.700	0.732	(------*-------)
			----+---------+---------+---------+--
p-value = 0.001			0.0 1.6 3.2 4.8

This effect of the pilot hole on conicality is likely due to three factors: the quick biting of the bit into the workpiece, the increased forward speed of the bit, and the guiding effect of the pilot hole. When the drilling begins, the pilot hole provides a definite starting location for the bit, which can then instantly bite into the edges of the hole. Without a pilot hole the bit can wander across the surface before finding purchase, sometimes in the wrong location. Not only does the cutting start more quickly with a pilot hole, but it also proceeds more quickly because less material must be removed, reducing the opportunity for the bit to "wobble" at the beginning of the drilling, when the bit is least constrained. Once the bit enters the workpiece the pilot hole guides the bit throughout the remainder of the drilling, providing the bit with a predetermined path. In the case of machine drilling, the drill press constrains the end of the bit, reducing the amount that the tip can wander from its path, which produces less conicality than hand drilling. However, the pilot hole significantly improves conicality even when the hole is drilled by machine.

The gouge mark angle was also significantly affected by the use of the pilot hole, reducing the angle in hand drilling, as shown in Table 7-5. An interesting insight into the cause of gouging can be made from these results. The angle of the gouge marks was originally thought to be directly related to the forward speed of the bit, so that a higher speed would produce a higher angle. However, the use of a pilot hole increases the forward speed in hand drilling since less material has to be removed, but it reduces the angle of the gouge marks, suggesting that the forward speed of the drill does not affect the gouge mark angle. This is confirmed by the result of the machine drilling feed rate in

Table 7-6, which shows essentially no difference on the gouge mark angle even though the speed of drilling was increased threefold.

Table 7-5 Effect of Pilot Hole on Gouge Angle (Hand Drilling)

Factor	Mean	StDev	2.0	4.0	6.0
No Pilot Hole	5.378	5.849		(-----*-----)	
Pilot Hole	1.848	1.857	(-----*-----)		
p-value = 0.000					

Table 7-6 Effect of Feed Rate on Gouge Angle (Machine Drilling)

Factor	Mean	StDev	2.0	4.0	6.0	8.0
High	4.725	4.598		(----------*----------)		
Low	4.467	6.717	(----------*----------)			
p-value = 0.913						

The use of a pilot hole also reduced the number of gouge marks. This was evident in machine drilling, where there were more than twice as many gouge marks on average in the holes drilled without a pilot hole than those drilled with the pilot hole, as shown in Table 7-7. The combined results of the number and angle of gouge marks show that the formation of these marks is highly dependent on the use of the pilot hole, suggesting that the formation of gouges is dependent upon the orientation of the bit in relation to the workpiece, rather than the speed or quality of the drill bit.

Table 7-7 Effect of Pilot Hole on Gouge Number (Machine Drilling)

Factor	Mean	StDev	0.00	0.80	1.60	2.40
No Pilot Hole	1.917	1.730		(----------*----------)		
Pilot Hole	0.750	1.215	(----------*----------)			
p-value = 0.069						

7.1.2 Bit Length Results

The bit length produced a great amount of variability in machine drilling, as shown in Figure 7-1(b), and is approximately equal to the effect produced by the pilot hole. In hand drilling, however, the next four most significant factors after the pilot hole are approximately equal and much less significant, as shown in Figure 7-1(a). The greatest variability due to bit length is found in surface roughness—the only factor that significantly affected roughness in either of the two tests. The bit length also significantly affected conicality in both hand drilling and machine drilling. It caused approximately equal variability in the gouge mark angle and conicality in machine drilling.

The large surface roughness effect in machine drilling is confirmed in Table 7-8, which shows that the longer bits increased surface roughness—probably due to "chatter" of the bit, which was audibly very apparent during drilling. The difference in surface quality was also visibly very apparent, as shown in Figures 7-2(a-b), which illustrates the characteristic rippled surface caused by chattering. This effect does not appear in hand drilling because the rear end of the bit is held in place only by the operator, so any bucking of the bit is absorbed by the operator's hand. In machine drilling, however, the rear of the bit is firmly constrained by the massive drill press so that vibrations must be absorbed by the workpiece. The longer the drill bit, the more it can deflect, increasing chatter and, therefore, surface roughness.

Table 7-8 Effect of Bit Length on Surface Roughness (Machine Drilling)

```
Factor            Mean     StDev  --+---------+---------+---------+----
Long Bit          1.0891   0.0263                    (--------*--------)
Short Bit         1.0608   0.0152   (-------*--------)
                                  --+---------+---------+---------+----
p-value = 0.004                    1.050     1.065     1.080     1.095
```

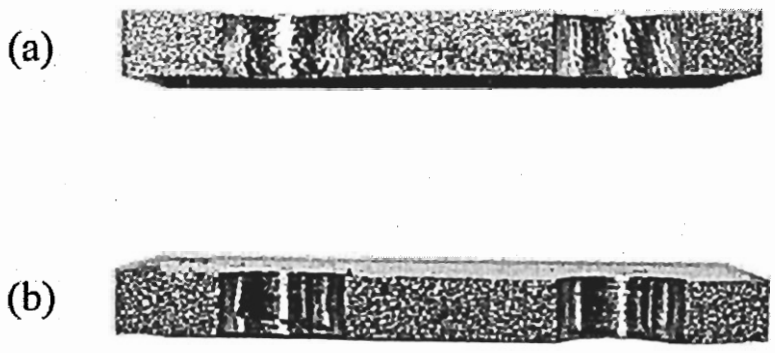

Figure 7-2 Bore of Hole Drilled With (a) Long Bit and (b) Short Bits

Conicality was affected by the bit length in both hand drilling and machine drilling, although in opposite ways. A longer bit produces less conicality in hand drilling, as shown in Table 7-9, and greater conicality in machine drilling, as shown in Table 7-10. This can be explained in part by the different ways that the bit is more constrained, as discussed in the paragraph above. In hand drilling, the tip of the bit is constrained and the long bit gives the operator more control over the angle of the bit, as he can see and feel the orientation of the drill to the workpiece more accurately with a longer bit. Additionally, as the length of the bit increases, any straying of the hand produces a smaller angle relative to the workpiece. Conversely, in machine drilling the rear end of the bit is constrained, and a longer bit allows the tip of the bit to deflect more, cutting into

the material around the entrance of the hole. In fact, the longer bits used in this experiment tended to produce slightly triangular hole bores, as shown previously in Figure 7-3(a-b), giving evidence of increased deflection of the bit.

Table 7-9 Effect of Bit Length on Conicality (Hand Drilling)

Factor	Mean	StDev	------+---------+---------+---------+
Long Bit	5.332	2.863	(--------*---------)
Short Bit	7.162	4.920	(---------*--------)
			------+---------+---------+---------+
p-value = 0.030			4.8 6.0 7.2 8.4

Table 7-10 Effect of Bit Length on Conicality (Machine Drilling)

Factor	Mean	StDev	-+---------+---------+---------+-----
Long Bit	3.167	3.355	(---------*---------)
Short Bit	1.458	1.091	(---------*---------)
			-+---------+---------+---------+-----
p-value = 0.108			0.0 1.5 3.0 4.5

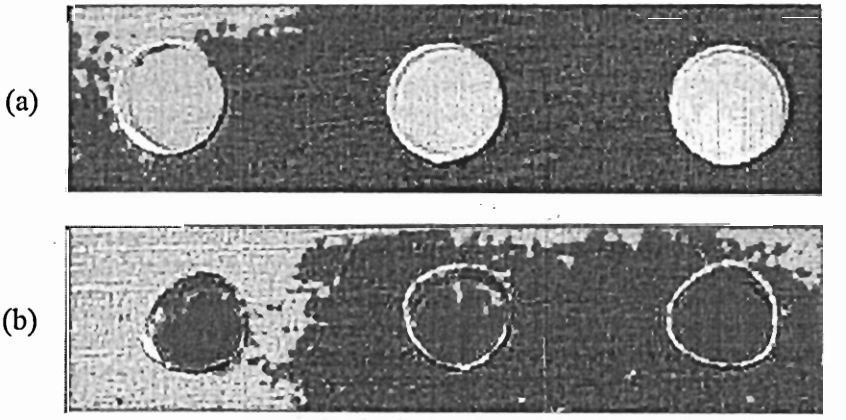

Figure 7-3 (a) Round and (b) Triangular Holes

The gouge mark angle was affected by bit length in machine drilling. The bit length was the only factor in this study that significantly affects the gouge mark angle in

machine drilling (the pilot hole, as discussed in Section 7.1.1, is the only factor of the six identified that significantly affects this angle in hand drilling). As shown in Table 7-11, the long bit produces a steeper gouge mark angle.

Table 7-11 Effect of Bit Length on Gouge Mark Angle (Machine Drilling)

Factor	Mean	StDev	--+---------+---------+---------+----
Long Bit	6.467	6.270	(----------*---------)
Short Bit	2.725	4.399	(----------*----------)
			--+---------+---------+---------+----
p-value = 0.105			0.0 3.0 6.0 9.0

In addition, the analysis of variances revealed that the bit length interacted with the pilot hole factor in hand drilling in conicality. Figure 7-4 shows that the conicality of the holes was equivalent when drilled with a long bit, but was strongly affected by the pilot hole when drilled with a short bit. Not surprisingly, the pilot hole reduced the conicality of the holes in the case of the short bit. This is probably due to the less amount of control that an operator has with a shorter bit.

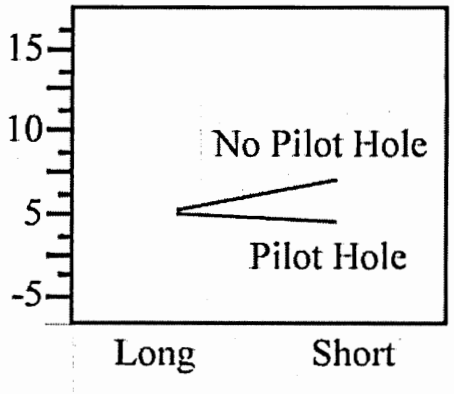

Figure 7-4 Interaction of the Bit Length and Pilot Hole Factors

7.1.3 Bit Condition Results

The condition of the bit, along with pressure/feed rate, produced moderate hole quality variability in both hand drilling and machine drilling. It was thought that duller drill bits would produce more plastic deformation and therefore higher residual compressive hoop stress in drilling than would a sharp bit. However, residual stresses are not visible to the eye, and it was not supposed that the bit condition would greatly affect hole quality. The mechanics commented on the longer drilling time required for an old bit. The only hole quality metric that was significantly affected by bit condition was the number of gouge marks in hand drilling.

Table 7-12 shows the confidence intervals for bit condition on the number of gouge marks, and shows that the new bit produced fewer gouge marks than did the old bit. This is most likely due to the same effect that caused the reduction in the number of gouge marks due to the use of a pilot hole, since the new bit drills more quickly through the workpiece.

Table 7-12 Effect of Bit Condition on Gouge Mark Number (Hand Drilling)

Factor	Mean	StDev	----+---------+---------+---------+--
New Bit	1.277	1.057	(---------*---------)
Old Bit	1.702	1.382	(---------*---------)
			----+---------+---------+---------+--
p-value = 0.097			1.05 1.40 1.75 2.10

7.1.4 Pressure/Feed Rate Results

The overall hole quality variability of the feed rate factor in machine drilling is due primarily to the number of gouge marks. Table 7-13 gives the factor confidence intervals, showing that high feed rate produces more gouge marks than does low feed

rate. Although the bit does cut through the workpiece more quickly with a high feed rate, it is forced to do so, in contrast to the effect of the new bit, which allows the bit to cut through the workpiece more easily. The higher applied pressure likely causes more deflection of the tip of the bit, gouging the surface more often. This effect is not replicated in hand drilling probably due to the lower maximum pressure that can be applied by an operator compared to a machine.

Table 7-13 Effect of Feed Rate on Gouge Mark Number (Machine Drilling)

Factor	Mean	StDev	--+---------+---------+---------+----
High Feed Rate	1.917	1.730	(----------*----------)
Low Feed Rate	0.750	1.215	(----------*----------)
			--+---------+---------+---------+----
p-value = 0.069			0.00 0.80 1.60 2.40

7.1.5 Operator Experience Results

In hand drilling, operator experience produced the second greatest amount of overall variability, due primarily to gouging effects. This factor was not included in machine drilling since machine drilling by definition removes this human factors. Most of the overall variability produced by the operator factor is attributed to the number of gouge marks, as this was the only response with a *p*-value below 0.1, as shown in Table 7-14, below. Surprisingly, the experienced operator produced more gouge marks (about 2 per hole) than did the novice (about 1). Operator experience also produced a marginal effect on the gouge mark angle, but the scatter is too large to make any conclusions.

Table 7-14 Effect of Operator Experience on the Number of Gouge Marks

Factor	Mean	StDev	-+---------+---------+---------+-----
Experienced	1.872	1.361	(--------*-------)
Novice	1.106	0.983	(--------*-------)
			-+---------+---------+---------+-----
p-value = 0.002			0.80 1.20 1.60 2.00

7.1.6 Withdrawal Speed Results

No measurable effect was produced by the withdrawal speed factor in hand drilling. This factor was not included in the machine drilling matrix because the drill rotation is always kept at full speed in machine operations. Especially surprising is the fact that there was no difference in the angle of the gouge marks, since it was thought that stopping the bit would deeply score the surface of the hole at a ninety degree angle. This is further evidence that gouging is a factor of the orientation of the bit to the workpiece rather than a factor of the drill or bit parameters.

Thus, the pilot hole factor results in the largest change in hole quality, and the use of a pilot hole generally improves hole quality. The bit length stands out in machine drilling, where a long bit significantly roughens the surface. Otherwise, the bit length produced a mild hole quality difference roughly equivalent to that made by the bit condition, pressure/feed rate, and the operator. The speed of the bit upon withdrawal made no significant difference in hole quality.

7.1.7 Burr Types

Section 4.4.1 discussed the three different types of burrs observed in the sectioned holes. Those types were the curling burr, the triangular burr, and the bulge burr. As

detailed in the procedure, burr geometries were recorded for each sectioned hole. The data shows that the curling burr is dependent on the operator and pilot hole factors; the triangular burr is only dependent on the use of a pilot hole; and the bulge burr is dependent on the pilot hole, pressure, and operator.

The curling burr is most dependent on the operator, with a *p*-value of 0.000. Table 7-15 shows that machine drilling was the factor most likely to result in a curling burr. The average number of curling burrs observed in machine-drilled holes was 0.96. Since a maximum of two exit burrs could be observed for each hole, machine drilling was 48% likely to create a curling burr. The curling burr also appears to be operator dependent.

Table 7-15 Effect of Operator on Curling Burr

Factor	Mean	StDev	---+---------+---------+---------+---
Experienced	0.4792	0.7143	(---*---)
Machine	0.9583	0.7506	(-----*-----)
Novice	0.0638	0.2471	(----*---)
			---+---------+---------+---------+---
p-value = 0.000			0.00 0.40 0.80 1.20

Table 7-16 shows that a curling burr is also much more likely to be formed when a pilot hole is not employed, with a *p*-value of 0.034. Approximately 27% of those holes drilled without a pilot hole resulted in a curling burr, while approximately 14% of those drilled with a pilot hole showed curling burrs.

Table 7-16 Effect of Pilot Hole on Curling Burr

Factor	Mean	StDev	-----+---------+---------+---------+-
No Pilot Hole	0.5424	0.6778	(-------*--------)
Pilot Hole	0.2833	0.6402	(-------*--------)
			-----+---------+---------+---------+-
p-value = 0.034			0.20 0.40 0.60 0.80

The triangular burr showed a strong correlation to the use of a pilot hole, with a *p*-value of 0.000. As with the curling burr, the triangular burr is more likely to form when a pilot hole is not used, which suggests that the two burrs are related to each other. About 53% of the holes drilled without a pilot hole formed a triangular burr, while only about 14% of those drilled with a pilot hole formed a triangular burr. The combined probability of a triangular and curling burr resulting from the use of a pilot hole is about 80%, which is the strongest correlation in this study. This correlation, along with the similar shapes of the burrs, suggests that the curling burr is a precursor to the triangular burr, while the bulge burr is based on a separate phenomenon.

Table 7-17 Effect of Pilot Hole on Triangular Burr

Factor	Mean	StDev	-------+---------+---------+---------
No Pilot Hole	1.0508	0.7526	(-----*-----)
Pilot Hole	0.2833	0.5552	(----*-----)
			-------+---------+---------+---------
p-value = 0.000			0.30 0.60 0.90

The use of a pilot hole also affected the formation of the bulge burr, but in this case a bulge burr is more likely to form when a pilot hole is used, with a *p*-value of 0.000. Approximately 32% of the holes drilled with a pilot hole formed a bulge burr, while only about 8% of those drilled without a pilot hole formed a bulge burr, as shown in Table 7-18.

Table 7-18 Effect of Pilot Hole on Bulge Burr

```
Factor            Mean     StDev  ----------+---------+---------+------
No Pilot Hole   0.1695    0.3784  (------*------)
Pilot Hole      0.6333    0.8431                    (-----*------)
                                  ----------+---------+---------+------
p-value = 0.000                          -0.25      0.50      0.75
```

The pressure applied to the drill appears to contribute to the formation of the bulge burr, with a *p*-value of 0.014. High pressure is about 28% likely to produce a bulge burr, which low pressure resulted in bulge burrs in less than 13% of the hole. These results are displayed below, in Table 7-19. The shape of the bulge burr suggests that it results from a large deformation in the axial direction of the material surrounding the hole. The pressure results clearly agree with this hypothesis. The pilot hole results may also substantiate this hypothesis, since a pilot hole would allow the bit to proceed through the hole by its own twisting action, rather than being pushed through.

Table 7-19 Effect of Pressure on Bulge Burr

```
Factor            Mean     StDev  -------+---------+---------+---------
High Pressure   0.5593    0.7938                   (--------*--------)
Low Pressure    0.2500    0.5407   (-------*--------)
                                   -------+---------+---------+---------
p-value = 0.014                  0.20      0.40      0.60
```

Hand drilling also appears more likely to result in a bulge burr, with a *p*-value of 0.020. About 24% of the holes drilled by hand resulted in a bulge burr, while only about 4% of the machine-drilled holes resulted in such a burr, as shown in Table 7-20.

Table 7-20 Effect of Operator Versus Bulge Burr

Factor	Mean	StDev	--------+---------+---------+---------
Experienced	0.5625	0.7964	(------*-----)
Machine	0.0833	0.2823	(--------*--------)
Novice	0.4043	0.6808	(-----*------)
			--------+---------+---------+---------
p-value = 0.020			0.00 0.30 0.60

Thus, the curling burr and triangular burr appear to be directly related to each other, such that the curling burr is a precursor to the triangular burr. These burrs may be the result of both local deformation of residual exit face material and plastic flow within the bore of the hole. The bulge burr appears to be related to the amount of axial deformation of the material surrounding the hole.

7.2 X-Ray Diffraction

The material and specimen geometry proved too problematic to obtain consistent residual stress results using x-ray diffraction. These problems persisted despite trying a large variety of testing parameters. The problems were attributed to the material properties, curvature of the hole, and roughness of the drilled surface.

After testing a number of different samples, it was decided that one sample would be tested until consistent results could be obtained. A hole that had been machine drilled using an old bit, and which had a very smooth surface relative to the other holes, was chosen because it would minimize roughness effects and have a high chance of containing a residual hoop stress field. A variety of different optics and beam sizes were tried before the wide and narrow geometry discussed in Section 5.3 was decided upon. The narrowness of the beam minimized the effect of the curvature of the hole surface, and the width of the beam maintained sufficient beam intensity while still ensuring that

the beam was only incident on the specimen and not on the aluminum stage. A scan was run without a sample and compared to the results of a scan run with the exact same parameters with a sample to ensure that the inconsistencies were not due to readings from the stage.

When all of the parameters were optimized, three scans were run on the same specimen on three different days using the same procedure. The resultant graphs of $\sin^2\Psi$ versus *d* are shown in Figures 7-5 through 7-7, below. All of the graphs have significant scatter, although two of the three have approximately equivalent slopes, suggesting residual hoop stress. A composite of these three graphs is shown in Figure 7-8, and shows that the two graphs with similar slopes have widely different average *d*-spacings, while two of the graphs with differing slopes have very similar *d*-spacings. This amount of variability among scans would prevent meaningful comparison between samples.

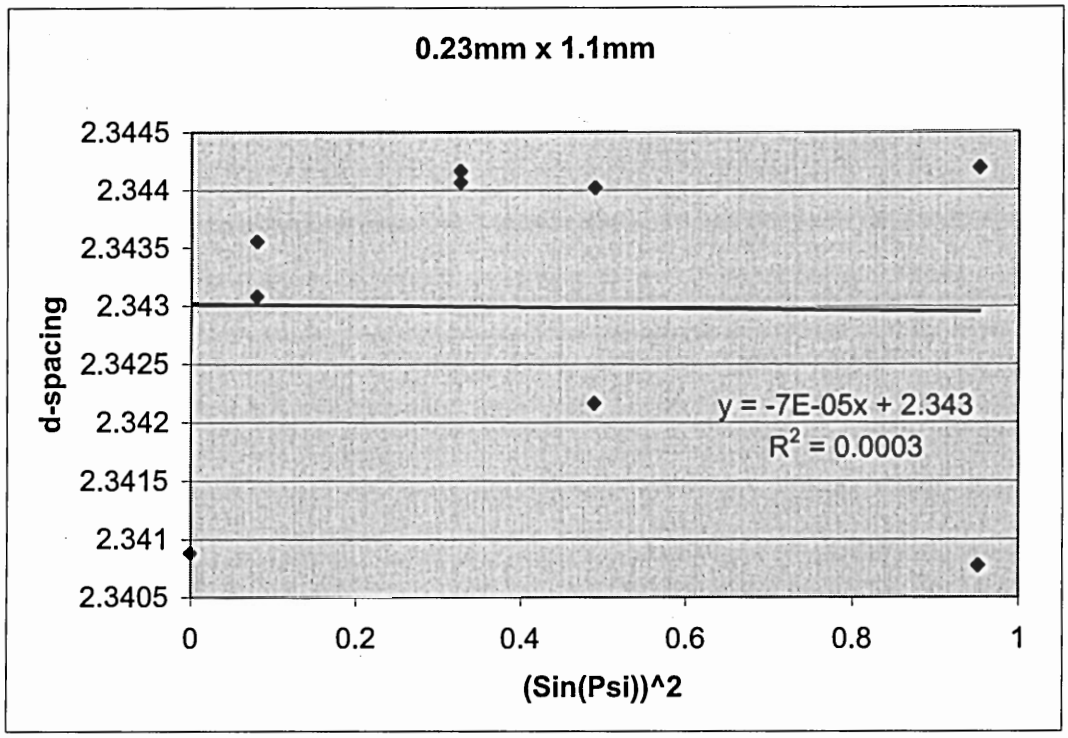

Figure 7-5 First X-Ray Scan of Sample 2-1, Coupon A89N8-10

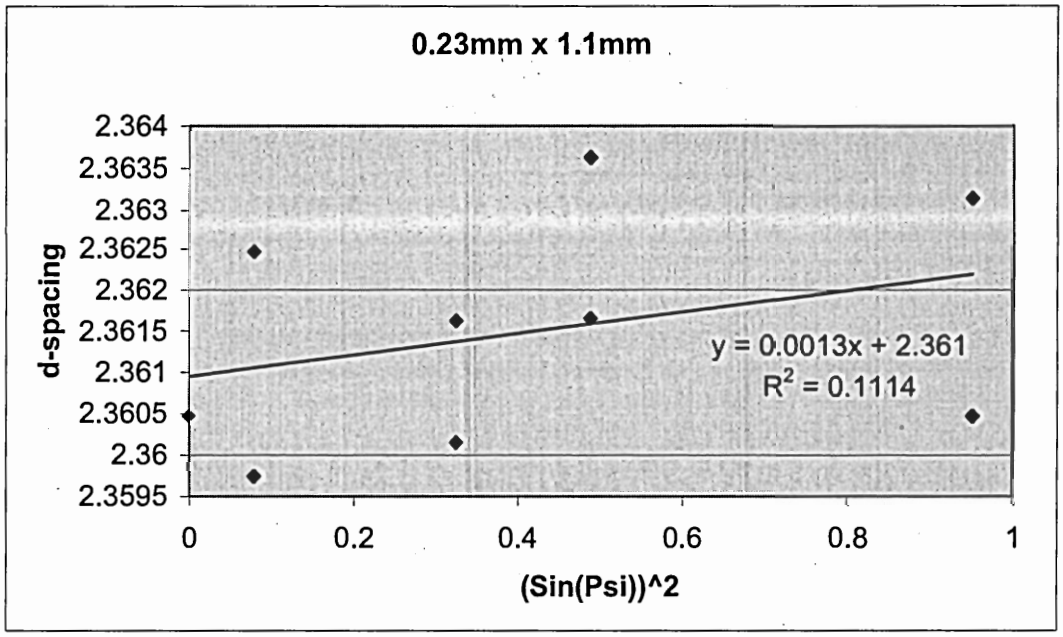

Figure 7-6 Second X-Ray Scan of Sample 2-1, Coupon A89N8-10

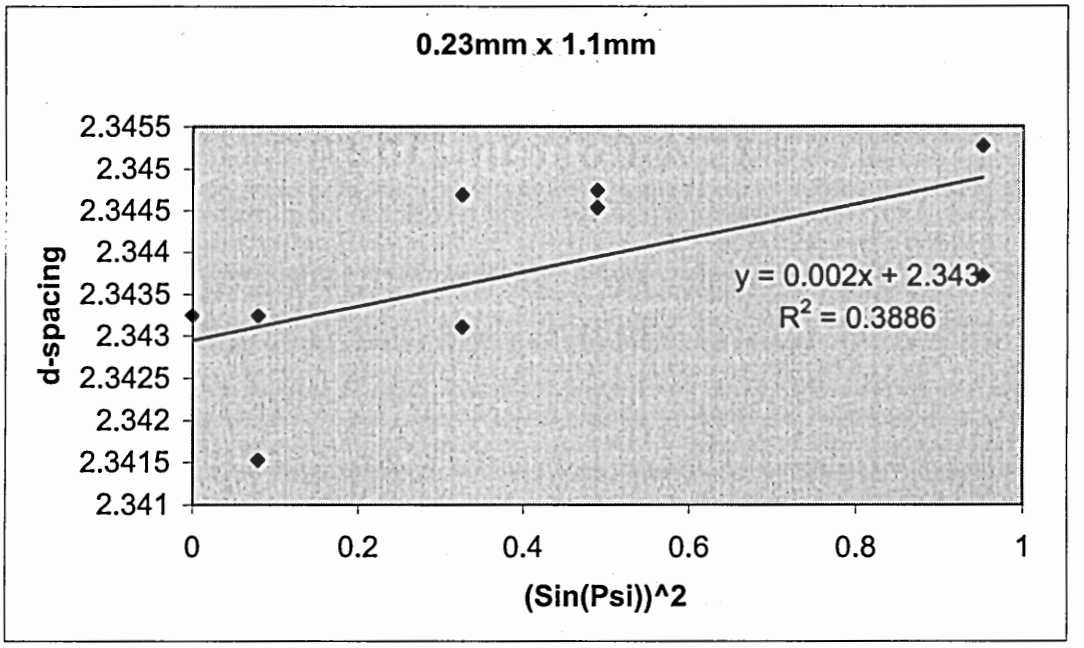

Figure 7-7 Third X-Ray Scan of Sample 2-1, Coupon A89N8-10

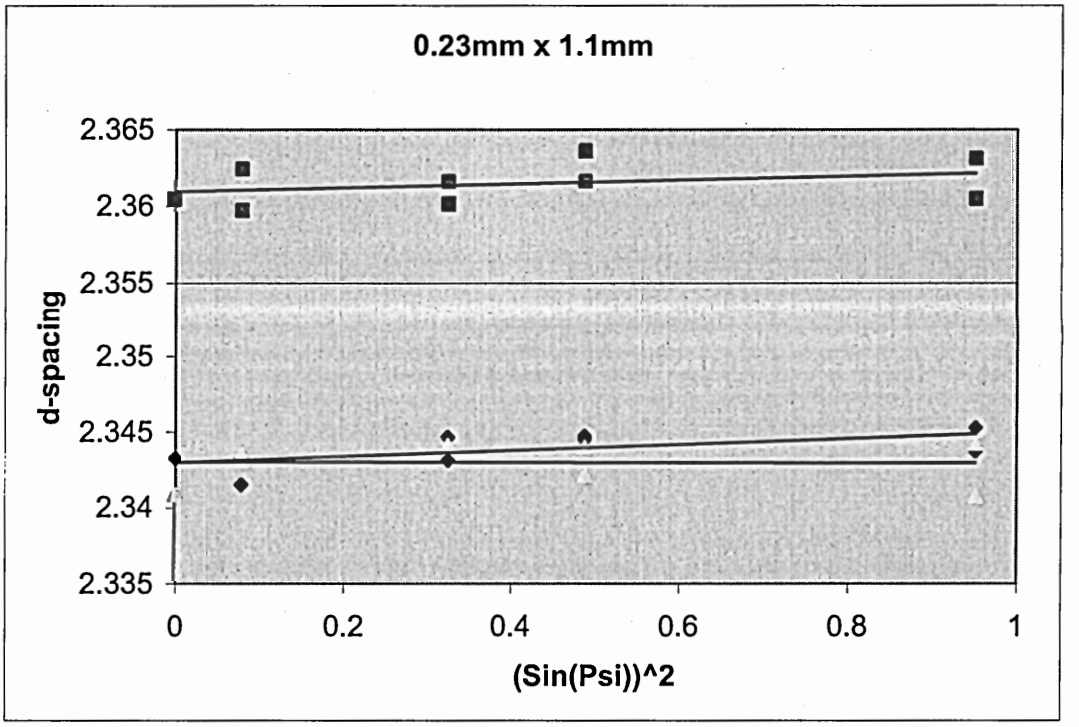

Figure 7-8 Composite of Three X-Ray Scans of Sample 2-1, Coupon A89N8-10

These inconsistencies can be attributed to three factors: material properties, curvature of the hole, and roughness of the drilled surface. Two material property concerns are the depth of x-ray penetration and sample texture. The low relative density of aluminum allows x-ray to penetrate several hundred microns into the surface. The residual stresses induced by drilling are only on the order of about twenty microns. Since x-ray diffraction averages over the depth of penetration, the effect of the residual stresses will be greatly reduced. Sample texture refers to the quality of the material grains. Since the batch of aluminum provided for this study was rolled, its grains are highly textured. This texturing can produce a large amount of scatter in x-ray diffraction results. X-ray diffraction also produces the best results on flat surfaces. The curvature of the hole bore causes the beam to strike the sample at different angles, causing additional scatter. In addition, the curvature may cause the beam to strike the sample at unpredictable angles as the sample is tilted, which may cause a large amount of scatter if the sample is rotated so much as a few microns off-axis. Although using a narrow beam minimized this effect, it cannot be completely eliminated. Finally, surface of the hole is invariably roughened to some degree by machining marks. Just as the curvature of the sample causes scatter, so does the roughness of the surface scatter the beam. This could be reduced by chemically polishing the samples, but the polishing would also eliminate the greatest residual stresses—those nearest the machine surface.

The overall effect was probably the result of a combination of these factors, two of which were minimized by the geometry of the beam and the choice of a smooth sample. Regardless, the variability of the scans remained too great to permit meaningful

comparisons between samples. Therefore, x-ray diffraction had to be eliminated as a method of determining relative residual stresses.

7.3 Fatigue Testing

Fatigue tests were conducted at three stress levels, corresponding to three conditions relative to the yield stress of the material at the notch root: 17.5 ksi, which is well below the yield stress; 21 ksi, just below the yield stress; and 25 ksi, well above the yield stress. Since the pilot hole was the most significant factor affecting hole quality and the bit condition was believed to most significantly affect the magnitude of residual stresses, these two factors were chosen for the initial tests, and chemically polished specimens were used as a baseline. Additional polished samples were later used to provide more data at the 17.5 ksi level. A set of specimens was also machine drilled, three with an old bit and three with a new bit, for testing at 17.5 ksi. Both drill bits were short bits, and all six specimens used a pilot hole and the low feed rate.

The cycles to failure for the various tests are shown below in Figure 7-9, where failure was considered specimen separation. These results show that the polished specimens lasted much longer than the as-drilled specimens. This difference is attributed primarily to machining marks, which provide stress concentrations. Within the sets of as-drilled specimens, results indicate that the dull bit did induce residual compressive hoop stresses, increasing fatigue life of the fastener holes.

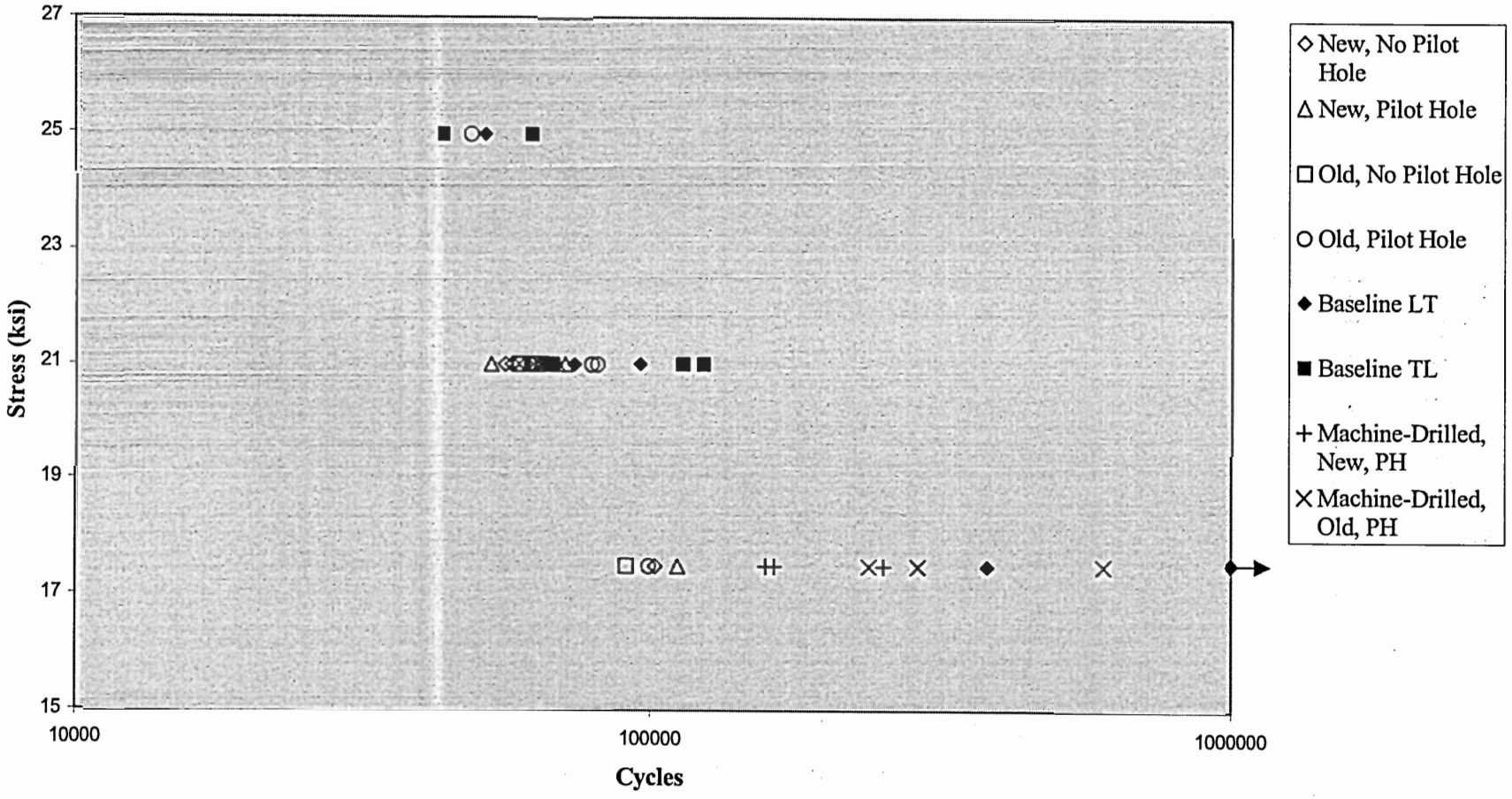

Figure 7-9 Fatigue Test Cycles To Failure

7.3.1 Testing at 21 ksi

The primary fatigue tests were conducted at 21 ksi, which is just below the yield stress of the material at the notch root. Any residual stresses in a polished sample would effectively reduce the applied stress to a level below the yield stress and retard crack initiation and early crack growth. The tests included five specimens each of the as-drilled combinations of new bit, no pilot hole; new bit, pilot hole; and old bit, no pilot hole; and four of the old bit, pilot hole specimens (one was tested at 25 ksi due to operator error). Three polished specimens each in the LT and TL directions, which were assumed to be without residual stresses, were tested at this level to provide a baseline. Additionally, four underloaded and four overloaded specimens (two each in the TL and LT directions) were tested to be used for correlation with FASTRAN predictions.

A comparison of the cycles to failure of the polished LT specimens and the 24 as-drilled specimens is shown in Table 7-21. The fatigue life of the as-drilled specimens is clearly reduced, despite the large standard deviation of the polished specimens, which is due to the fact that there were only two polished LT specimens tested. The reduction in fatigue life appears to be about 20%, although more polished specimens would need to be tested to reduce the standard deviation. The difference is most likely due to hole quality, in particular the gouge marks, since even one of these large stress concentrations would would provide a large enough stress concentration to quickly initiate a crack.

Table 7-21 As-Drilled Versus Polished LT Cycles to Failure (21 ksi)

```
Factor            Mean     StDev  --+---------+---------+---------+----
Polished         91438     28532                (--------*--------)
Hand Drilled     64484      6989   (---*---)
                                   --+---------+---------+---------+----
p-value = 0.001                    60000     75000     90000    105000
```

In light of this apparent hole quality effect, a closer look at the fatigue life of the as-drilled holes is warranted. The difference in fatigue lives was found to be due to crack initiation. Table 7-22 shows that the holes drilled with the old bit lasted longer than those drilled with the new bit, while the pilot hole had little effect on fatigue life. In fact, the analysis of variance of cycles to initiation for the pilot hole factor resulted in a *p*-value of only 0.401, while the bit condition resulted in a *p*-value of 0.011, as shown in Table 7-23. These two tables show that the old bit resulted in a longer life than did the new bit. It should be recalled that the old bit produced significantly more gouge marks and a marginally greater surface roughness, while having no significant effect on conicality or gouge mark angle. Thus, this longer fatigue life produced by the old bit contrasted with its poorer hole quality suggests that the old bit does indeed produced higher compressive residual stresses. The fact that the holes drilled with the old bit took about 40% longer to initiate a crack proves that this effect is not insignificant.

Table 7-22 N_i For As-Drilled Holes (21 ksi)

Factor	Mean	StDev	36000	48000	60000
New Bit, No Pilot	37700	8227	(---------*---------)		
New Bit, Pilot	39575	9871	(---------*---------)		
Old Bit, No Pilot	48333	9500	(---------*---------)		
Old Bit, Pilot	57550	9088	(---------*---------)		
p-value = 0.054			36000	48000	60000

Table 7-23 Bit Condition Versus N_i (21 ksi)

Factor	Mean	StDev	40000	50000	60000
New Bit	38771	8502	(-------*-------)		
Old Bit	53600	9780	(-------*-------)		
p-value = 0.011			40000	50000	60000

After the first crack initiates, an interesting phenomenon takes place to equalize the fatigue lives. Table 7-24 shows that the cycles from initiation to failure are higher for the new bit than for the old bit, reversing the above trends. The most probable reason for this is that multiple cracks are forming simultaneously in the holes drilled with the old bit, due to the higher number of gouge marks, whereas cracks tend to form more in series in the holes drilled with a new bit. Table 7-25 shows the confidence intervals for the normalized difference between the cycles to initiation of the first surface crack and initiation of a surface crack on the opposite side of the hole. This theory appears plausible, but the *p*-value of 0.131 provides only marginal confidence, due primarily to the low number of initiation data points in these tests.

Table 7-24 Bit Condition Versus N_f-N_i (21 ksi)

Factor	Mean	StDev	----------+---------+---------+------
New Bit	23021	7465	(---------*---------)
Old Bit	15341	3282	(----------*---------)
			----------+---------+---------+------
p-value = 0.040			15000 20000 25000

Table 7-25 Bit Condition Versus $(N_{i2}-N_{i1})/N_f$ (21 ksi)

Factor	Mean	StDev	-+---------+---------+---------+-----
New Bit	0.1921	0.1210	(----------*----------)
Old Bit	0.0946	0.0602	(------------*-----------)
			-+---------+---------+---------+-----
p-value = 0.131			0.000 0.080 0.160 0.240

The combined effect of the above two competing trends of crack initiation and growth approximately equalize the as-drilled hole fatigue lives. It is important to remember that the overall differences in cycles to failure for the as-drilled specimens are small in comparison to those of the polished specimens, as shown in Table 7-21 and Figure 7-8, above. So, while residual stresses do appear to be a factor, they are offset by

the detrimental effects of machining marks. This may be a mixed blessing when it comes to aircraft production, for although the residual stresses do not provide a great improvement in fatigue life, they do appear to reduce the effects of machining marks, and essentially equalize the variables involved in the manufacturing process.

7.3.2 Testing at 17.5 ksi

As shown in Figure 7-8, the as-drilled specimens had much shorter fatigue lives than did the polished specimens, as predicted from the 21 ksi test results. All of the polished specimens were run-outs to three million cycles except for one, which initiated a crack on one side and fractured before initiating a crack on the opposite side, suggesting that either the hole was drilled off-center or that there was a flaw at the notch root. These results confirm that machining marks play a larger role in fatigue life than does residual stress.

Figure 7-8 also clearly shows that the machine-drilled holes lasted longer than did the hand-drilled holes, as does Table 7-26. All of the machine-drilled holes used a pilot hole, which in machine drilling showed an average of 0.8 gouges per hole in machine drilling compared with and overall average of 1.5 gouges per hole in hand drilling, as shown in Tables 7-1 and 7-2. This hole quality difference likely accounts for the difference in fatigue lives. Table 7-27 shows that crack initiation accounted for about 84% of the life of the machine-drilled holes, while it accounted for only 62% of the life of hand-drilled holes. Cycles from initiation to failure, however, show no real difference between hand-drilled and machine-drilled holes, as displayed in Table 7-28. The fact that crack initiation was the difference between the fatigue lives of the two drilling methods

supports the hypothesis that hole quality is the major factor in fatigue life of as-drilled holes.

Table 7-26 Drilling Method Versus N_f (17.5 ksi)

Factor	Mean	StDev
Hand Drilled	100795	8445
Machine Drilled	283135	163791

p-value = 0.061

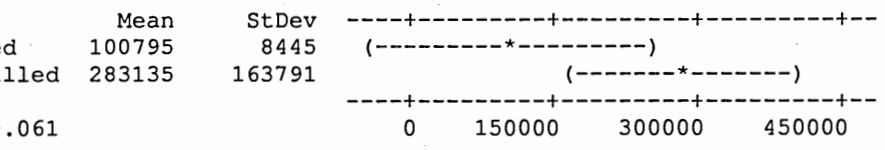

Table 7-27 Drilling Method Versus N_i/N_f (17.5 ksi)

Factor	Mean	StDev
Hand Drilled	0.62345	0.03444
Machine Drilled	0.83858	0.06214

p-value = 0.004

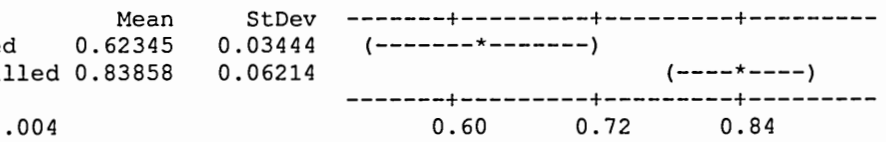

Table 7-28 Drilling Method Versus N_f-N_i (17.5 ksi)

Factor	Mean	StDev
Hand Drilled	35677	1017
Machine Drilled	44751	24372

p-value = 0.635

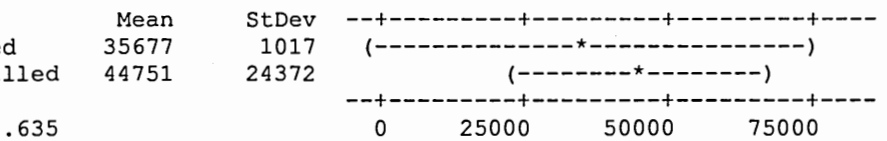

7.3.3 Testing at 25 ksi

Fatigue testing at 25 ksi was conducted primarily for correlation with FASTRAN predictions. The test was composed of two each of polished TL and LT specimens and one as-drilled specimen (due to operator error). As expected, all specimens failed at similar numbers of cycles, ranging from about 45,000 to 60,000 cycles. The results corresponded well with the model predictions. The high stress level yielded the material at the notch root and resulted in rapid failure. This level of stress eliminated any residual stress or material effects.

7.3.4 Overload and Underload Tests

The underloaded and overloaded specimens were tested at 21 ksi. Figure 7-10 shows a comparison of the fatigue lives of the various hole types at 21 ksi. The average life of the polished baseline samples is represented by the solid line, and the average lives of the other sample types are represented by the corresponding dashed lines. The polished, as-drilled, and underload samples failed within fairly tight scatter bands, while the overload tests showed a surprising amount of scatter. The underload test resulted in about a 40% decrease in fatigue life while the overload test resulted in fatigue lives about a factor of 18 longer, which were both greater than the FASTRAN respective predictions of 23% and a factor of 10.

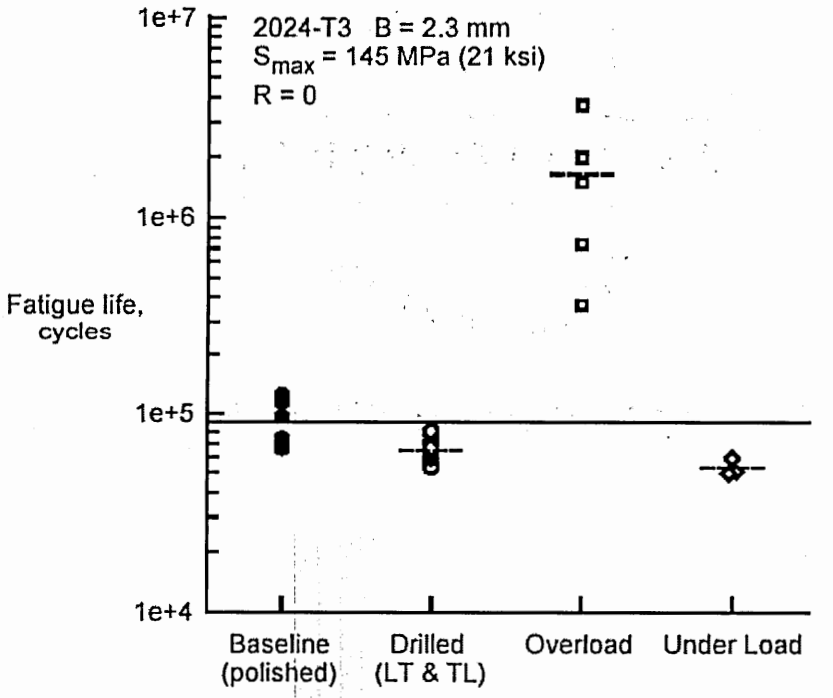

Figure 7-10 Fatigue Lives At 21 ksi

7.3.5 Fatigue Crack Surface Microscopy

No correlation could be found between the crack initiation site and the type of specimen. Of the twenty specimens inspected, fourteen (70%) had center cracks, which suggests that the cracks are not as likely to initiate at the corners. In addition, none of the twenty specimens showed evidence of cracks initiating at the burrs.

SEM inspection of the initiation crack replicates corresponded fairly well with the optical microscopy estimates. The optical results gave an average approximate crack size at the edge of the hole of about four microns. The SEM measurements show a crack size of about ten microns, as shown in Figures 7-11.

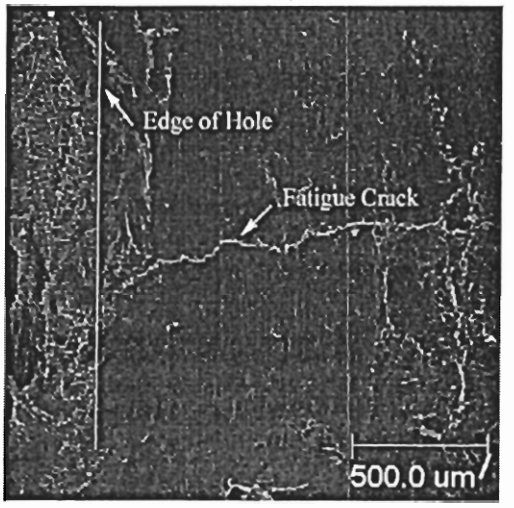

(a)

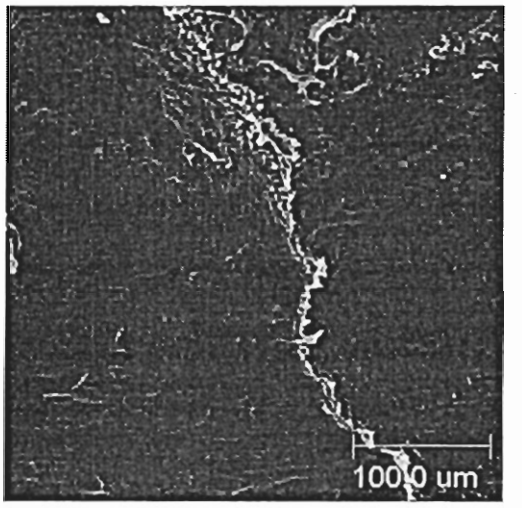

(b)

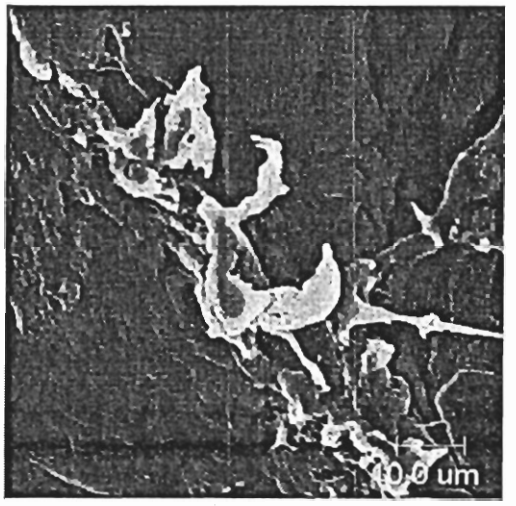

(c)

Figure 7-11 SEM micrograph of crack replicate at (a) 40x (b) 200x and (c) 1000x

In summary, fatigue tests suggest that dull bits do induce residual compressive hoop stresses, resulting in longer lives, but machining marks create stress intensities that reduce the fatigue life much more than the extension caused by residual stresses. Machining effects, however, appear to balance out, so that there is not a large difference in the fatigue lives due to the different factors. This means that, although production conditions detract from the performance of aircraft fastener holes, there is no production condition that is extremely detrimental, and which great care should be taken to avoid.

CHAPTER VIII: CONCLUSIONS

This study investigated several production fastener hole drilling factors and their effects on hole quality, residual stress, and fatigue life. These tests were conducted with production quality hand and machine drills and drill bits on 11 inch by 2 inch by 0.09 inch coupons of 2024-T3 aluminum, and were compared with similar laboratory quality coupons that had been chemically polished to remove machining marks and residual stresses.

Hole quality was quantified in four categories: surface roughness, conicality, the number of gouge marks, and the angle of the gouge marks. The tests found that the use of a pre-drilled half-diameter hole, or pilot hole, most affected overall hole quality, and that hole quality was improved by its use. Other factors that affected hole quality were the length of the bit, the sharpness of the bit, the feed rate, and the experience of the operator.

X-ray diffraction was employed to attempt to measure residual stresses directly and non-destructively. A number of tests were conducted, and it was found that the best method was to concentrate the beam across the width of the hole bore while minimizing the height of the beam, and to use 2Theta/Omega scans with Psi tilts. Unfortunately, the tests gave inconsistent results due to a number of factors. One major factor was the curved geometry of the hole, which caused the beam to be incident upon the surface at continuously changing angles. Another factor was that the drilling process produced a rough surface. Both of these factors can alter the beam, giving misleading results. Another factor is that the aluminum has been rolled, creating texture, which can also give

poor results. The overall effect led to such inconsistency that no meaningful comparison could be made between samples.

Fatigue tests showed that the production-quality holes failed faster than did the laboratory-quality holes. It was concluded that machining marks caused crack initiation sites, accounting for this difference. Among the as-drilled holes, those drilled with the old, or dull, bit lasted longer in fatigue compared with those drilled with new, sharp bits. This is especially revealing in the set of machine-drilled holes, which were all drilled with a pilot hole, because this produced the best quality in the hole quality tests. In these machine-drilled holes, the only difference was that some of the holes were drilled with the old bit and some with the new bit, which showed no discernable difference in hole quality. Those drilled with the old bit lasted longer in fatigue, suggesting that the old bit induced more beneficial hoop stresses. However, hole quality remained a more significant factor in fatigue life than did residual stress.

CHAPTER IX: RECOMMENDATIONS

Often in seeking answers, one finishes with more questions than when they started. Thus science advances. This project was no different, and many questions arose which were either out of the scope of the research or required additional resources that could not be justified. Recommendations for future work fall into two categories: additional testing, and better models.

9.1 Additional Testing

One goal of this research is to improve manufacturing procedures. The drilling of the fastener holes is only one part of the whole process of joining parts, and other parts of the procedure should be examined. In particular, the next step of riveting should be investigated. Riveting is a highly dynamic procedure that consists of inserting or driving the rivet into the hole and plastically deforming the rivet by hammering. The rivet is obviously deformed, but the fastener hole may also be deformed axially, radially, or randomly. These deformations may pinch the collar of the hole or induce compressive residual hoop stresses, benefiting the fatigue life; or they may form cracks or additional crack initiation sites, or result in fretting fatigue during cycling. All of these factors, and more, may either wipe out, negate, or intensify the drilling effects, and the fatigue performance of riveted fastener holes should be investigated. Many studies have already been conducted on the riveting process, but again, they often are sterilized by laboratory procedures, eliminating many manufacturing effects that may prove critical. In response

to this need, samples have been prepared in the same manner as the fatigue tests, and a MS20470D6 rivet was installed at the Delta repair hanger. These samples will be tested as part of another study at 17.5 ksi.

The AGARD R-732 study suggested that holes polished for one minute lasted much longer than predicted because the machining marks had been eliminated or greatly diminished while the residual stresses remained. Additional fatigue testing of coupons drilled under the same conditions as those in the fatigue tests, but polished for one minute, may provide better evidence of the effect of the residual stresses apart from the effects of hole quality. This would allow for a more rigorous comparison to the polished holes on the basis of residual stress effects alone, providing a reasonable estimate of the magnitude of the stress.

Residual stress formation and hole quality may be material dependent. Since the industry now commonly uses the 7050 series aluminums, identical hole quality and fatigue tests with that material would be advisable.

9.2 Mechanical Modeling

Residual stress analysis is complicated in this study by the hole quality effects. If an initial flaw size could be assumed, the fatigue life could then be used to estimate the magnitude of the residual stress. Due to the different shapes of the gouge marks, it would be difficult to estimate such a flaw size. What is needed is a model relating stress intensity to the gouge mark geometry. This model would need to take into account the size of the gouge, the angle of incidence of the gouge to the bore, and the shape of the gouge.

The cause of the gouging is still a mystery. The independence of the gouge angle to the feed rate of the bit eliminates the most obvious guesses. The straying of the operator's hand and the deflection of the tip of the bit seem to explain the angle of the gouges, but cannot explain the regularity of angle. Explaining the formation of the gouges would help determine how to eliminate the gouges, thus extending fatigue life.

9.3 Improved Burr Formation Model

Existing models of the formation of the burr only take into account localized bending of excess material at the exit face of the hole. The presence of burrs on the entry face and the geometry of the bulge burrs are evidence that axial plastic deformation contributes to the formation of the burr, and material from deeper inside the bore of the hole may make up the burr. An improved burr formation model is needed to more accurately represent the condition of the hole after drilling, and especially the residual stresses induced by the drilling process.

9.4 Fastener Hole Production

Production of fastener holes can be improved to increase the fatigue life of aircraft structural joints, and to improve the quality of the holes. The use of pilot holes as standard practice would be the most beneficial practice. This requires more production time, however, and a serious analysis of the cost-benefit should be performed before making such a change.

Individual drill bits should be used as long as practical in production, since they offer improved fatigue life without a significant reduction in hole quality. This practice

would not greatly increase drilling time, and the increase will be partially offset by the reduced frequency of changing bits, as well as the purchase of fewer bits.

APPENDIX A: EXPERIMENTAL TEST DATA

Table A-1 Complete Hole Quality Test Matrix

Operator	Pilot Hole	Bit Length	Bit Condition	Pressure	Bit Speed
Experienced	No	Long	New	High	Stopped
Experienced	No	Long	New	Low	Full
Experienced	No	Long	New	High	Stopped
Experienced	No	Long	New	High	Stopped
Experienced	No	Long	New	Low	Full
Experienced	No	Long	New	Low	Full
Experienced	No	Long	Old	Low	Stopped
Experienced	No	Long	Old	Low	Stopped
Experienced	No	Long	Old	High	Full
Experienced	No	Long	Old	Low	Stopped
Experienced	No	Long	Old	High	Full
Experienced	No	Long	Old	High	Full
Experienced	No	Short	New	Low	Stopped
Experienced	No	Short	New	Low	Stopped
Experienced	No	Short	New	High	Full
Experienced	No	Short	New	High	Full
Experienced	No	Short	New	High	Full
Experienced	No	Short	New	Low	Stopped
Experienced	No	Short	Old	Low	Full
Experienced	No	Short	Old	High	Stopped
Experienced	No	Short	Old	Low	Full
Experienced	No	Short	Old	High	Stopped
Experienced	No	Short	Old	High	Stopped
Experienced	No	Short	Old	Low	Full
Experienced	Yes	Long	New	High	Full
Experienced	Yes	Long	New	High	Full
Experienced	Yes	Long	New	Low	Stopped
Experienced	Yes	Long	New	Low	Stopped
Experienced	Yes	Long	New	High	Full
Experienced	Yes	Long	New	Low	Stopped
Experienced	Yes	Long	Old	High	Stopped
Experienced	Yes	Long	Old	Low	Full
Experienced	Yes	Long	Old	Low	Full

Table A-1 (cont'd)

Operator	Pilot Hole	Bit Length	Bit Condition	Pressure	Bit Speed
Experienced	Yes	Long	Old	Low	Full
Experienced	Yes	Long	Old	High	Stopped
Experienced	Yes	Long	Old	High	Stopped
Experienced	Yes	Short	New	High	Stopped
Experienced	Yes	Short	New	High	Stopped
Experienced	Yes	Short	New	Low	Full
Experienced	Yes	Short	New	Low	Full
Experienced	Yes	Short	New	Low	Full
Experienced	Yes	Short	New	High	Stopped
Experienced	Yes	Short	Old	Low	Stopped
Experienced	Yes	Short	Old	High	Full
Experienced	Yes	Short	Old	High	Full
Experienced	Yes	Short	Old	Low	Stopped
Experienced	Yes	Short	Old	High	Full
Experienced	Yes	Short	Old	Low	Stopped
Novice	No	Long	New	High	Stopped
Novice	No	Long	New	Low	Full
Novice	No	Long	New	High	Stopped
Novice	No	Long	New	High	Stopped
Novice	No	Long	New	Low	Full
Novice	No	Long	New	Low	Full
Novice	No	Long	Old	Low	Stopped
Novice	No	Long	Old	Low	Stopped
Novice	No	Long	Old	High	Full
Novice	No	Long	Old	Low	Stopped
Novice	No	Long	Old	High	Full
Novice	No	Long	Old	High	Full
Novice	No	Short	New	Low	Stopped
Novice	No	Short	New	Low	Stopped
Novice	No	Short	New	High	Full
Novice	No	Short	New	High	Full
Novice	No	Short	New	High	Full
Novice	No	Short	New	Low	Stopped
Novice	No	Short	Old	Low	Full
Novice	No	Short	Old	High	Stopped
Novice	No	Short	Old	Low	Full
Novice	No	Short	Old	High	Stopped

Table A-1 (cont'd)

Operator	Pilot Hole	Bit Length	Bit Condition	Pressure	Bit Speed
Novice	No	Short	Old	High	Stopped
Novice	No	Short	Old	Low	Full
Novice	Yes	Long	New	High	Full
Novice	Yes	Long	New	High	Full
Novice	Yes	Long	New	Low	Stopped
Novice	Yes	Long	New	Low	Stopped
Novice	Yes	Long	New	High	Full
Novice	Yes	Long	New	Low	Stopped
Novice	Yes	Long	Old	High	Stopped
Novice	Yes	Long	Old	Low	Full
Novice	Yes	Long	Old	Low	Full
Novice	Yes	Long	Old	Low	Full
Novice	Yes	Long	Old	High	Stopped
Novice	Yes	Long	Old	High	Stopped
Novice	Yes	Short	New	High	Stopped
Novice	Yes	Short	New	High	Stopped
Novice	Yes	Short	New	Low	Full
Novice	Yes	Short	New	Low	Full
Novice	Yes	Short	New	Low	Full
Novice	Yes	Short	New	High	Stopped
Novice	Yes	Short	Old	Low	Stopped
Novice	Yes	Short	Old	High	Full
Novice	Yes	Short	Old	High	Full
Novice	Yes	Short	Old	Low	Stopped
Novice	Yes	Short	Old	High	Full
Novice	Yes	Short	Old	Low	Stopped

Table A-2 Complete Hole Quality Data

Operator	Pilot Hole	Bit Length	Bit Condition	Pressure / Feed Rate	Bit Speed	Hole	Coupon	Gouge Angle	Gouge Number	Roughness	Solid Angle	Curling Burr	Triangular Burr	Bulge Burr
Machine	No	Short	Old	Low	Full	01-1	A89N8-10	12.3	1	1.065	3.6	0	2	0
Machine	No	Short	Old	Low	Full	02-1	A89N8-10	0	0	1.041	1.7	0	2	0
Machine	No	Short	Old	Low	Full	03-1	A89N8-10	0	0	1.044	1.1	1	1	0
Machine	Yes	Short	Old	High	Full	04-1	A89N8-10	6.1	1	1.054	0.2	1	1	0
Machine	Yes	Short	Old	High	Full	05-1	A89N8-10	9.9	1	1.096	0.2	2	0	0
Machine	Yes	Short	Old	High	Full	06-1	A89N8-10	0	0	1.064	1.5	2	0	0
Machine	No	Long	Old	High	Full	07-1	A89N8-10	2.3	2	1.069	2.7	0	1	1
Machine	No	Long	Old	High	Full	08-1	A89N8-10	2.3	4	1.112	5.4	1	1	0
Machine	No	Long	Old	High	Full	09-1	A89N8-10	10.4	3	1.147	4.3	0	2	0
Machine	Yes	Long	Old	Low	Full	10-1	A89N8-10	0	0	1.125	1.3	1	1	0
Machine	Yes	Long	Old	Low	Full	11-1	A89N8-10	0.6	4	1.067	1.2	1	1	0
Machine	Yes	Long	Old	Low	Full	12-1	A89N8-10	0	0	1.089	0.6	2	0	0
Machine	No	Short	New	High	Full	13-1	A89N8-10	0	0	1.070	3.2	1	1	0
Machine	No	Short	New	High	Full	14-1	A89N8-10	3.9	5	1.053	1.6	0	1	1
Machine	No	Short	New	High	Full	15-1	A89N8-10	0.5	4	1.046	0.8	0	2	0
Machine	Yes	Short	New	Low	Full	16-1	A89N8-10	0	0	1.074	0.3	0	2	0
Machine	Yes	Short	New	Low	Full	17-1	A89N8-10	0	0	1.066	2	1	1	0
Machine	Yes	Short	New	Low	Full	18-1	A89N8-10	0	0	1.056	1.3	2	0	0
Machine	No	Long	New	Low	Full	19-1	A89N8-10	16.8	2	1.063	9.6	1	1	0
Machine	Yes	Long	New	High	Full	19-3	A89N8-10	9.2	2	1.082	-0.4	1	1	0
Machine	No	Long	New	Low	Full	20-1	A89N8-10	14.8	1	1.079	4.6	1	0	0
Machine	Yes	Long	New	High	Full	20-3	A89N8-10	12.1	1	1.074	0.1	2	0	0

Table A-2 (cont'd)

Operator	Pilot Hole	Bit Length	Bit Condition	Pressure / Feed Rate	Bit Speed	Hole	Coupon	Gouge Angle	Gouge Number	Roughness	Solid Angle	Curling Burr	Triangular Burr	Bulge Burr
Machine	No	Long	New	Low	Full	21-1	A89N8-10	9.1	1	1.094	8.5	1	1	0
Machine	Yes	Long	New	High	Full	21-3	A89N8-10	0	0	1.067	0.1	2	0	0
Experienced	No	Long	New	High	Stopped	01-1	A90N8-12	0	0	1.085	6.4	0	0	1
Experienced	No	Long	New	Low	Full	01-2	A90N8-12	10.8	3	1.061	7.3	0	0	2
Experienced	No	Long	New	Low	Full	02-2	A90N8-12	5	2	0.046	9.7	0	0	2
Experienced	No	Long	New	Low	Full	02-3	A90N8-12	6.1	2	1.089	5.5	0	2	0
Experienced	No	Long	New	High	Stopped	05-1	A90N8-12	0	0	1.084	9.3	2	0	0
Experienced	No	Long	New	High	Stopped	05-2	A90N8-12	2.2	1			0	1	0
Experienced	No	Short	New	Low	Stopped	05-3	A90N8-12	9.2	1	1.088	14	0	1	0
Experienced	No	Short	New	Low	Stopped	06-1	A90N8-12	0.6	1	1.146	11.8	0	0	1
Experienced	No	Short	New	High	Full	06-2	A90N8-12	0	0	1.090	12.8	0	0	1
Experienced	No	Short	New	High	Full	06-3	A90N8-12	14.8	2	1.056	5.1	0	1	0
Experienced	No	Short	New	High	Full	07-1	A90N8-12	24.1	1	1.106	6.6	0	0	0
Experienced	No	Short	New	Low	Stopped	07-2	A90N8-12	4.9	3	1.127	7.1	0	0	0
Experienced	No	Short	Old	Low	Full	08-1	A90N8-12	9	2	1.095	18.1	0	0	0
Experienced	No	Short	Old	High	Stopped	08-2	A90N8-12	13	3	1.109	6	0	0	0
Experienced	No	Short	Old	Low	Full	08-3	A90N8-12	2.2	1	1.122	6.3	0	2	0
Experienced	No	Short	Old	High	Stopped	09-1	A90N8-12	6.9	1	1.059	5.6	0	1	1
Experienced	No	Short	Old	High	Stopped	09-2	A90N8-12	3.4	2	1.058	2.8	0	0	2
Experienced	No	Short	Old	Low	Full	09-3	A90N8-12	3.8	3	1.151	8.4	1	1	0
Experienced	No	Long	Old	Low	Stopped	10-1	A90N8-12	4.5	3	1.082	6.1	0	2	0
Experienced	No	Long	Old	Low	Stopped	10-2	A90N8-12	5.3	3	1.152	9.3	0	0	1

Table A-2 (cont'd)

Operator	Pilot Hole	Bit Length	Bit Condition	Pressure / Feed Rate	Bit Speed	Hole	Coupon	Gouge Angle	Gouge Number	Roughness	Solid Angle	Curling Burr	Triangular Burr	Bulge Burr
Experienced	No	Long	Old	High	Full	10-3	A90N8-12	2.3	3	1.079	3.7	0	2	0
Experienced	No	Long	Old	Low	Stopped	11-1	A90N8-12	3.8	2	1.071	5.5	0	2	0
Experienced	No	Long	Old	High	Full	11-2	A90N8-12	7	3	1.097	7.9	0	2	0
Experienced	No	Long	Old	High	Full	11-3	A90N8-12	0.9	1	1.074	5.9	0	2	0
Experienced	Yes	Long	New	High	Full	01-1	A90N8-3	0	0	1.054	1.7	0	0	2
Experienced	Yes	Long	New	High	Full	01-2	A90N8-3	1.5	2	1.046	3.9	0	1	1
Experienced	Yes	Long	New	Low	Stopped	01-3	A90N8-3	0.5	1	1.063	3.1	0	2	0
Experienced	Yes	Long	New	Low	Stopped	02-1	A90N8-3	4.4	2	1.042	0.3	0	1	1
Experienced	Yes	Long	New	High	Full	02-2	A90N8-3	1.8	1	1.028	5.2	0	0	1
Experienced	Yes	Long	New	Low	Stopped	02-3	A90N8-3	2	1	1.038	2.1	0	2	0
Experienced	Yes	Long	Old	High	Stopped	03-1	A90N8-3	1.7	5	1.064	4.1	0	0	1
Experienced	Yes	Long	Old	Low	Full	03-2	A90N8-3	2.3	2	1.075	5.7	0	0	0
Experienced	Yes	Long	Old	Low	Full	03-3	A90N8-3	4.9	1	1.047	7.5	0	0	1
Experienced	Yes	Long	Old	Low	Full	04-1	A90N8-3	4.8	2	1.038	6.8	0	0	0
Experienced	Yes	Long	Old	High	Stopped	04-2	A90N8-3	4.2	2	1.051	12.4	0	1	0
Experienced	Yes	Long	Old	High	Stopped	04-3	A90N8-3	4	1	1.047	6.9	0	0	2
Experienced	Yes	Short	New	High	Stopped	05-1	A90N8-3	0	0	1.041	2.4	0	0	2
Experienced	Yes	Short	New	High	Stopped	05-2	A90N8-3	7	1	1.037	3.4	0	0	2
Experienced	Yes	Short	New	Low	Full	05-3	A90N8-3	0.1	1	1.058	3.5	0	0	1
Experienced	Yes	Short	New	Low	Full	06-1	A90N8-3	1.4	1	1.029	3.7	0	0	2
Experienced	Yes	Short	New	Low	Full	06-2	A90N8-3	4.5	3	1.023	2.2	0	0	0
Experienced	Yes	Short	New	High	Stopped	06-3	A90N8-3	0.4	1	1.052	1.3	0	0	2

Table A-2 (cont'd)

Operator	Pilot Hole	Bit Length	Bit Condition	Pressure / Feed Rate	Bit Speed	Hole	Coupon	Gouge Angle	Gouge Number	Roughness	Solid Angle	Curling Burr	Triangular Burr	Bulge Burr
Experienced	Yes	Short	Old	Low	Stopped	07-1	A90N8-3	0.8	1	1.080	7.1	0	0	0
Experienced	Yes	Short	Old	High	Full	07-2	A90N8-3	2.8	4	1.046	6.1	0	0	0
Experienced	Yes	Short	Old	High	Full	08-2	A90N8-3	0.8	7	1.051	0.6	0	0	2
Experienced	Yes	Short	Old	Low	Stopped	08-3	A90N8-3	5	3	1.059	6.7	0	1	1
Experienced	Yes	Short	Old	High	Full	09-1	A90N8-3	5.2	1	1.050	8.1	0	0	2
Experienced	Yes	Short	Old	Low	Stopped	09-2	A90N8-3	4.7	3	1.047	6.8	0	0	2
Novice	Yes	Long	New	High	Full	01-1	A94N8-9	1.5	3	1.058	3.9	0	0	2
Novice	Yes	Long	New	High	Full	01-2	A94N8-9	0	2	1.057	3.9	0	0	1
Novice	Yes	Long	New	Low	Stopped	01-3	A94N8-9	0.3	1	1.081	5.5	0	0	2
Novice	Yes	Long	New	Low	Stopped	02-1	A94N8-9	0.9	2	1.077	4.2	0	0	0
Novice	Yes	Long	New	High	Full	02-2	A94N8-9	0	0	1.004	4.2	0	0	0
Novice	Yes	Long	New	Low	Stopped	02-3	A94N8-9	3.5	1	1.087	5.5	0	1	1
Novice	Yes	Long	Old	High	Stopped	03-1	A94N8-9	0	0	1.090	7.4	0	0	2
Novice	Yes	Long	Old	Low	Full	03-2	A94N8-9	0.3	2	1.098	7.1	0	1	0
Novice	Yes	Long	Old	Low	Full	03-3	A94N8-9	2.5	1	1.113	2.7	0	0	1
Novice	Yes	Long	Old	Low	Full	04-1	A94N8-9	1.5	1	1.056	5.1	0	0	0
Novice	Yes	Long	Old	High	Stopped	04-2	A94N8-9	0.6	1	1.093	12	0	0	0
Novice	Yes	Long	Old	High	Stopped	04-3	A94N8-9	1.7	1	1.050	1.5	0	0	2
Novice	Yes	Short	New	High	Stopped	05-1	A94N8-9	0	0	1.042	6.2	0	0	0
Novice	Yes	Short	New	High	Stopped	05-2	A94N8-9	1.2	4	-0.013	3.4	0	0	0
Novice	Yes	Short	New	Low	Full	05-3	A94N8-9	2.9	3	1.074	5.2	0	0	0
Novice	Yes	Short	New	Low	Full	06-1	A94N8-9	0	0	1.051	3.2	0	0	0

Table A-2 (cont'd)

Operator	Pilot Hole	Bit Length	Bit Condition	Pressure / Feed Rate	Bit Speed	Hole	Coupon	Gouge Angle	Gouge Number	Roughness	Solid Angle	Curling Burr	Triangular Burr	Bulge Burr
Novice	Yes	Short	New	Low	Full	06-2	A94N8-9	0	0	1.046	2.5	0	0	0
Novice	Yes	Short	New	High	Stopped	06-3	A94N8-9	0.2	3	1.041	2.2	0	0	0
Novice	Yes	Short	Old	Low	Stopped	07-1	A94N8-9	2.9	1	1.059	4.6	0	0	0
Novice	Yes	Short	Old	High	Full	07-2	A94N8-9	2.7	2	1.094	8.7	0	0	0
Novice	Yes	Short	Old	High	Full	07-3	A94N8-9	0	0	1.060	2.1	0	0	2
Novice	Yes	Short	Old	Low	Stopped	08-1	A94N8-9	0.6	2	1.056	5.4	0	0	0
Novice	Yes	Short	Old	High	Full	08-2	A94N8-9	0.4	2	1.028	2.3	0	0	0
Novice	Yes	Short	Old	Low	Stopped	08-3	A94N8-9	0.2	2	1.093	8	0	0	0
Novice	No	Long	New	High	Stopped	01-1	A96N8-11	0	0	1.206	0.4	0	0	0
Novice	No	Long	New	Low	Full	01-2	A96N8-11	0	0	1.072	5.2	1	0	0
Novice	No	Long	New	High	Stopped	01-3	A96N8-11	3.2	1	1.079	2.6	0	2	0
Novice	No	Long	New	High	Stopped	02-1	A96N8-11	3.8	2	1.052	5.7	0	1	1
Novice	No	Long	New	Low	Full	02-2	A96N8-11	12	1	1.051	6.4	0	0	1
Novice	No	Long	New	Low	Full	02-3	A96N8-11	12.5	1	1.056	7.4	0	2	0
Novice	No	Long	Old	Low	Stopped	03-1	A96N8-11	5.4	1	1.061	7.9	0	2	0
Novice	No	Long	Old	Low	Stopped	03-2	A96N8-11	15.4	1	1.033	0.8	1	0	0
Novice	No	Long	Old	High	Full	03-3	A96N8-11	0	0	1.042	2.2	0	1	0
Novice	No	Long	Old	Low	Stopped	04-1	A96N8-11	14	1	1.106	8.5	0	2	0
Novice	No	Long	Old	High	Full	04-2	A96N8-11	16.1	1	1.072	0	0	0	0
Novice	No	Long	Old	High	Full	04-3	A96N8-11	0	0	1.056	4.2	0	1	1
Novice	No	Short	New	Low	Stopped	05-1	A96N8-11	16.2	1	1.097	10.8	0	0	1
Novice	No	Short	New	Low	Stopped	05-2	A96N8-11	2.1	2	1.092	10.4	0	1	0

Table A-2 (cont'd)

Operator	Pilot Hole	Bit Length	Bit Condition	Pressure / Feed Rate	Bit Speed	Hole	Coupon	Gouge Angle	Gouge Number	Roughness	Solid Angle	Curling Burr	Triangular Burr	Bulge Burr
Novice	No	Short	New	High	Full	05-3	A96N8-11	0.9	1	1.051	5.4	0	2	0
Novice	No	Short	New	High	Full	06-1	A96N8-11	1.3	1	1.117	13.9	0	0	1
Novice	No	Short	New	High	Full	06-3	A96N8-11	0	0	1.095	14.6	0	2	0
Novice	No	Short	New	Low	Stopped	07-1	A96N8-11	2.1	2	1.082	9	1	1	0
Novice	No	Short	Old	Low	Full	08-1	A96N8-11	0.9	1	1.048	6.6	0	2	0
Novice	No	Short	Old	Low	Full	08-2	A96N8-11	0	0	1.120	26.3	0	2	0
Novice	No	Short	Old	High	Stopped	08-3	A96N8-11	3.9	1	1.128	13.7	0	1	1
Novice	No	Short	Old	High	Stopped	09-1	A96N8-11	0	0	1.046	10.4	0	2	0
Novice	No	Short	Old	High	Stopped	09-2	A96N8-11	0	0					
Novice	No	Short	Old	Low	Full	09-3	A96N8-11	0	0	1.119	5.2	0	1	0

Table A-3 Complete Fatigue Test Data

Sample	Type	Test	Load (ksi)	Ni1	Ni2	Nf	Crack Site	Comments
A89N8-14	HD	Old, No PH	21	48400	55400	64856	Center	
A89N8-3	HD	Old, PH	21	48200	50900	59420	Corner	
A89N8-9	HD	New, No PH	21	36400	46200	57692	Corner	
A90N8-10	HD	New, PH	21	45600	55700	68953	Center	
A90N8-15	HD	New, No PH	21			67622		
A91N8-12	HD	New, PH	17.5			111309		
A91N8-14	HD	New, PH	21	50300	51900	64183	Center	
A91N8-3	HD	New, PH	21			71148		
A91N8-8	HD	Old, No PH	21	57800	63400	63400		
A93N8-10	HD	Old, No PH	21			62340		
A93N8-15	HD	Old, PH	25	31000	46000	49078	Center	
A93N8-3	HD	Old, PH	21	66400	69000	78957	Corner	
A93N8-4	HD	New, No PH	21			56163		
A93N8-8	HD	Old, No PH	17.5	54400		90796	Center	
A94N8-12	HD	New, PH	21	31800	40900	53209	Corner	
A94N8-14	HD	New, PH	21	30600	57400	65254	Center	
A94N8-6	HD	Old, PH	21	64200		80885	Center	
A95N8-14	HD	Old, PH	17.5	64300		99258		
A95N8-2	HD	New, No PH	21	30200	47000	60884	Center	
A95N8-3	HD	Old, No PH	21			62523		
A95N8-7	HD	New, No PH	17.5			101817		
A96N8-10	HD	Old, No PH	21	38800	49700	59208	Center	
A96N8-3	HD	New, No PH	21	46500	55600	62373	Corner	
A96N8-6	HD	Old, PH	21	51400	58200	66119	Center	
A92N8-1	LT	Baseline	21			96064		
A92N8-10	LT	Baseline	21	56400	63400	73777		
A92N8-11	LT	Underload	21			50969		
A92N8-12	LT	Baseline	25			51888		
A92N8-13	LT	Overload	21			1997564		
A92N8-15	LT	Overload	21			737452	Center	
A92N8-2	LT	Underload	21			52016		
A92N8-4	LT	Baseline	21	61900				Overloaded
A92N8-5	LT	Baseline	21	108500		129768		
A92N8-6	LT	Baseline	17.5			4942664		Run-out
A92N8-7	LT	Baseline	25	16800	18800	62269	Center	
A92N8-8	LT	Baseline	17.5			380187		Crack on one side ONLY
A92N8-9	LT	Baseline	21	20100	51400	66144	Corner	

Table A-3 (cont'd)

Sample	Type	Test	Load (ksi)	Ni1	Ni2	Nf	Crack Site	Comments
A90N8-14	MD	Old, PH	17.5	211100	280200	288603		
A91N8-2	MD	Old, PH	17.5	532800	596100	600672		
A91N8-6	MD	New, PH	17.5	208900	247200	251573		
A93N8-7	MD	Old, PH	17.5	195100	222100	237331		
A96N8-5	MD	New, PH	17.5	134200	139700	157655		
A97N8-3	MD	New, PH	17.5	148200	149700	162974		Initiation suspect due to low battery
A34N7-12-TL	TL	Overload	21			1500732		
A34N7-13-TL	TL	Overload	21					Failed at grips
A34N7-15-TL	TL	Baseline	21			123463		
A34N7-2-TL	TL	Baseline	25	16100	40400	43809	Center	
A34N7-4-TL	TL	Underload	21			58888		
A34N7-5-TL	TL	Overload	21			366014		
A34N7-6-TL	TL	Baseline	21			113694		
A34N7-8-TL	TL	Baseline	25			62231		
A34N7-9-TL	TL	Baseline	21	44600		67844	Center	
A97N8-11-TL	TL	Overload	21			3655454		Run-out
A97N8-14-TL	TL	Overload	21					Bent
A97N8-5-TL	TL	Baseline	17.5			3027062		Run-out
A97N8-6-TL	TL	Underload	21			49612		
A97N8-7-TL	TL	Baseline	17.5			3005205		Run-out

APPENDIX B: MINITAB STATISTICAL OUTPUT

Hand-Drilled Hole Quality

One-way ANOVA: Roughness versus Operator

Analysis of Variance for Roughnes

Source	DF	SS	MS	F	P
Operator	1	0.0001	0.0001	0.00	0.955
Error	92	2.2824	0.0248		
Total	93	2.2825			

Level	N	Mean	StDev
A	47	1.0487	0.1528
B	47	1.0506	0.1621

Pooled StDev = 0.1575

Individual 95% CIs For Mean Based on Pooled StDev

```
------+---------+---------+---------+
(---------------*--------------)
 (--------------*--------------)
------+---------+---------+---------+
    1.020     1.050     1.080     1.110
```

One-way ANOVA: Roughness versus Pilot Hole

Analysis of Variance for Roughnes

Source	DF	SS	MS	F	P
Pilot Ho	1	0.0225	0.0225	0.92	0.341
Error	92	2.2600	0.0246		
Total	93	2.2825			

Level	N	Mean	StDev
No Pilot	46	1.0654	0.1575
Pilot Ho	48	1.0345	0.1560

Pooled StDev = 0.1567

Individual 95% CIs For Mean Based on Pooled StDev

```
--------+---------+---------+---------
          (------------*-----------)
 (------------*-----------)
--------+---------+---------+---------
      1.015     1.050     1.085
```

One-way ANOVA: Roughness versus Bit Length

Analysis of Variance for Roughnes

Source	DF	SS	MS	F	P
Bit Leng	1	0.0002	0.0002	0.01	0.926
Error	92	2.2823	0.0248		
Total	93	2.2825			

Level	N	Mean	StDev
Long	47	1.0481	0.1528
Short	47	1.0512	0.1621

Pooled StDev = 0.1575

Individual 95% CIs For Mean Based on Pooled StDev

```
------+---------+---------+---------+
(--------------*--------------)
 (--------------*--------------)
------+---------+---------+---------+
    1.020     1.050     1.080     1.110
```

One-way ANOVA: Roughness versus Bit Condition

Analysis of Variance for Roughnes

Source	DF	SS	MS	F	P
Bit Cond	1	0.0603	0.0603	2.50	0.117
Error	92	2.2222	0.0242		
Total	93	2.2825			

Level	N	Mean	StDev
New	47	1.0243	0.2176
Old	47	1.0750	0.0307
Pooled StDev =		0.1554	

Individual 95% CIs For Mean Based on Pooled StDev

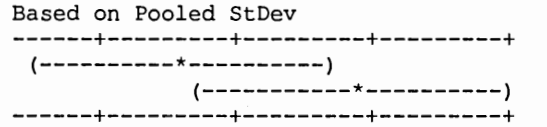

One-way ANOVA: Roughness versus Pressure

Analysis of Variance for Roughnes

Source	DF	SS	MS	F	P
Pressure	1	0.0032	0.0032	0.13	0.720
Error	92	2.2793	0.0248		
Total	93	2.2825			

Level	N	Mean	StDev
High	46	1.0437	0.1627
Low	48	1.0554	0.1522
Pooled StDev =		0.1574	

Individual 95% CIs For Mean Based on Pooled StDev

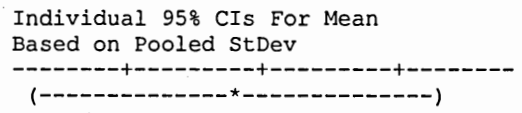

One-way ANOVA: Roughness versus Bit Speed

Analysis of Variance for Roughnes

Source	DF	SS	MS	F	P
Bit Spee	1	0.0008	0.0008	0.03	0.860
Error	92	2.2817	0.0248		
Total	93	2.2825			

Level	N	Mean	StDev
Full	48	1.0468	0.1506
Stopped	46	1.0526	0.1643
Pooled StDev =		0.1575	

Individual 95% CIs For Mean Based on Pooled StDev

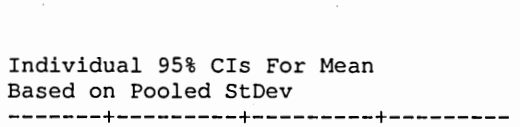

One-way ANOVA: Conicality versus Operator

Analysis of Variance for Conicali

Source	DF	SS	MS	F	P
Operator	1	0.0	0.0	0.00	0.968
Error	92	1569.2	17.1		
Total	93	1569.3			

Level	N	Mean	StDev
A	47	6.230	3.566
B	47	6.264	4.626
Pooled StDev =		4.130	

Individual 95% CIs For Mean Based on Pooled StDev

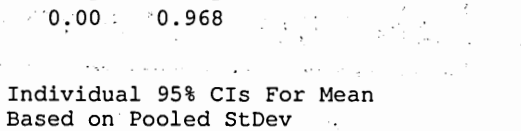

One-way ANOVA: Conicality versus Pilot Hole

Analysis of Variance for Conicali

Source	DF	SS	MS	F	P
Pilot Ho	1	217.3	217.3	14.79	0.000
Error	92	1352.0	14.7		
Total	93	1569.3			

Level	N	Mean	StDev
No Pilot	46	7.800	4.768
Pilot Ho	48	4.758	2.646
Pooled StDev =		3.833	

Individual 95% CIs For Mean
Based on Pooled StDev

```
------+---------+---------+---------+
                        (------*------)
(-------*------)
------+---------+---------+---------+
    4.5       6.0       7.5       9.0
```

One-way ANOVA: Conicality versus Bit Length

Analysis of Variance for Conicali

Source	DF	SS	MS	F	P
Bit Leng	1	78.7	78.7	4.86	0.030
Error	92	1490.6	16.2		
Total	93	1569.3			

Level	N	Mean	StDev
Long	47	5.332	2.863
Short	47	7.162	4.920
Pooled StDev =		4.025	

Individual 95% CIs For Mean
Based on Pooled StDev

```
------+---------+---------+---------+
 (--------*---------)
                (---------*--------)
------+---------+---------+---------+
    4.8       6.0       7.2       8.4
```

One-way ANOVA: Conicality versus Bit Condition

Analysis of Variance for Conicali

Source	DF	SS	MS	F	P
Bit Cond	1	23.5	23.5	1.40	0.240
Error	92	1545.8	16.8		
Total	93	1569.3			

Level	N	Mean	StDev
New	47	5.747	3.639
Old	47	6.747	4.513
Pooled StDev =		4.099	

Individual 95% CIs For Mean
Based on Pooled StDev

```
-----+---------+---------+---------+-
 (----------*----------)
           (----------*----------)
-----+---------+---------+---------+-
   5.0       6.0       7.0       8.0
```

One-way ANOVA: Conicality versus Pressure

Analysis of Variance for Conicali

Source	DF	SS	MS	F	P
Pressure	1	34.0	34.0	2.04	0.157
Error	92	1535.3	16.7		
Total	93	1569.3			

Level	N	Mean	StDev
High	46	5.633	3.817
Low	48	6.835	4.326
Pooled StDev =		4.085	

Individual 95% CIs For Mean
Based on Pooled StDev

```
------+---------+---------+---------+
(-----------*-----------)
             (----------*-----------)
------+---------+---------+---------+
    5.0       6.0       7.0       8.0
```

One-way ANOVA: Conicality versus Bit Speed

Analysis of Variance for Conicali

Source	DF	SS	MS	F	P
Bit Spee	1	0.0	0.0	0.00	0.970
Error	92	1569.2	17.1		
Total	93	1569.3			

Level	N	Mean	StDev
Full	48	6.263	4.601
Stopped	46	6.230	3.572

Pooled StDev = 4.130

Individual 95% CIs For Mean
Based on Pooled StDev

```
---------+---------+---------+-------
   (---------------*----------------)
 (----------------*----------------)
---------+---------+---------+-------
       5.60      6.30      7.00
```

One-way ANOVA: Gouge Angle versus Operator

Analysis of Variance for Gouge An

Source	DF	SS	MS	F	P
Operator	1	50.2	50.2	2.38	0.127
Error	92	1944.3	21.1		
Total	93	1994.5			

Level	N	Mean	StDev
A	47	4.306	4.509
B	47	2.845	4.684

Pooled StDev = 4.597

Individual 95% CIs For Mean
Based on Pooled StDev

```
--------+---------+---------+--------
             (----------*----------)
  (----------*----------)
--------+---------+---------+--------
      2.4       3.6       4.8
```

One-way ANOVA: Gouge Angle versus Pilot Hole

Analysis of Variance for Gouge An

Source	DF	SS	MS	F	P
Pilot Ho	1	292.8	292.8	15.83	0.000
Error	92	1701.8	18.5		
Total	93	1994.5			

Level	N	Mean	StDev
No Pilot	46	5.378	5.849
Pilot Ho	48	1.848	1.857

Pooled StDev = 4.301

Individual 95% CIs For Mean
Based on Pooled StDev

```
-------+---------+---------+---------
                  (-----*-----)
(-----*-----)
-------+---------+---------+---------
      2.0       4.0       6.0
```

One-way ANOVA: Gouge Angle versus Bit Length

Analysis of Variance for Gouge An

Source	DF	SS	MS	F	P
Bit Leng	1	1.0	1.0	0.05	0.827
Error	92	1993.5	21.7		
Total	93	1994.5			

Level	N	Mean	StDev
Long	47	3.681	4.303
Short	47	3.470	4.982

Pooled StDev = 4.655

Individual 95% CIs For Mean
Based on Pooled StDev

```
----+---------+---------+---------+--
   (----------------*----------------)
(----------------*----------------)
----+---------+---------+---------+--
  2.40      3.20      4.00      4.80
```

One-way ANOVA: Gouge Angle versus Bit Condition

Analysis of Variance for Gouge An

Source	DF	SS	MS	F	P
Bit Cond	1	0.8	0.8	0.04	0.848
Error	92	1993.7	21.7		
Total	93	1994.5			

Level	N	Mean	StDev	Individual 95% CIs For Mean Based on Pooled StDev
New	47	3.483	5.196	(----------*----------)
Old	47	3.668	4.042	(----------*----------)
Pooled StDev =		4.655		2.40 3.20 4.00 4.80

One-way ANOVA: Gouge Angle versus Pressure

Analysis of Variance for Gouge An

Source	DF	SS	MS	F	P
Pressure	1	27.0	27.0	1.26	0.264
Error	92	1967.6	21.4		
Total	93	1994.5			

Level	N	Mean	StDev	Individual 95% CIs For Mean Based on Pooled StDev
High	46	3.028	4.953	(----------*----------)
Low	48	4.100	4.286	(----------*----------)
Pooled StDev =		4.625		2.4 3.6 4.8

One-way ANOVA: Gouge Angle versus Bit Speed

Analysis of Variance for Gouge An

Source	DF	SS	MS	F	P
Bit Spee	1	0.0	0.0	0.00	0.999
Error	92	1994.5	21.7		
Total	93	1994.5			

Level	N	Mean	StDev	Individual 95% CIs For Mean Based on Pooled StDev
Full	48	3.575	5.107	(----------*----------)
Stopped	46	3.576	4.134	(----------*----------)
Pooled StDev =		4.656		2.40 3.20 4.00 4.80

One-way ANOVA: Gouge Number versus Operator

Analysis of Variance for Gouge Nu

Source	DF	SS	MS	F	P
Operator	1	13.79	13.79	9.78	0.002
Error	92	129.70	1.41		
Total	93	143.49			

Level	N	Mean	StDev	Individual 95% CIs For Mean Based on Pooled StDev
A	47	1.872	1.361	(-------*-------)
B	47	1.106	0.983	(-------*-------)
Pooled StDev =		1.187		0.80 1.20 1.60 2.00

One-way ANOVA: Gouge Number versus Pilot Hole

Analysis of Variance for Gouge Nu

Source	DF	SS	MS	F	P
Pilot Ho	1	3.08	3.08	2.02	0.159
Error	92	140.41	1.53		
Total	93	143.49			

Level	N	Mean	StDev
No Pilot	46	1.304	1.030
Pilot Ho	48	1.667	1.404

Pooled StDev = 1.235

Individual 95% CIs For Mean Based on Pooled StDev

```
---------+---------+---------+-------
(-----------*------------)
             (-----------*----------)
---------+---------+---------+-------
      1.20      1.50      1.80
```

One-way ANOVA: Gouge Number versus Bit Length

Analysis of Variance for Gouge Nu

Source	DF	SS	MS	F	P
Bit Leng	1	0.68	0.68	0.44	0.509
Error	92	142.81	1.55		
Total	93	143.49			

Level	N	Mean	StDev
Long	47	1.404	1.077
Short	47	1.574	1.395

Pooled StDev = 1.246

Individual 95% CIs For Mean Based on Pooled StDev

```
---------+---------+---------+-------
 (-------------*-------------)
        (-------------*-------------)
---------+---------+---------+-------
      1.25      1.50      1.75
```

One-way ANOVA: Gouge Number versus Bit Condition

Analysis of Variance for Gouge Nu

Source	DF	SS	MS	F	P
Bit Cond	1	4.26	4.26	2.81	0.097
Error	92	139.23	1.51		
Total	93	143.49			

Level	N	Mean	StDev
New	47	1.277	1.057
Old	47	1.702	1.382

Pooled StDev = 1.230

Individual 95% CIs For Mean Based on Pooled StDev

```
----+---------+---------+---------+--
(---------*----------)
            (----------*---------)
----+---------+---------+---------+--
  1.05      1.40      1.75      2.10
```

One-way ANOVA: Gouge Number versus Pressure

Analysis of Variance for Gouge Nu

Source	DF	SS	MS	F	P
Pressure	1	0.27	0.27	0.17	0.679
Error	92	143.22	1.56		
Total	93	143.49			

Level	N	Mean	StDev
High	46	1.435	1.515
Low	48	1.542	0.922

Pooled StDev = 1.248

Individual 95% CIs For Mean Based on Pooled StDev

```
--------+---------+---------+--------
 (-------------*-------------)
     (-------------*-------------)
--------+---------+---------+--------
      1.25      1.50      1.75
```

One-way ANOVA: Gouge Number versus Bit Speed

Analysis of Variance for Gouge Nu

Source	DF	SS	MS	F	P
Bit Spee	1	0.09	0.09	0.06	0.806
Error	92	143.39	1.56		
Total	93	143.49			

Level	N	Mean	StDev
Full	48	1.458	1.352
Stopped	46	1.522	1.130

Pooled StDev = 1.248

Individual 95% CIs For Mean
Based on Pooled StDev

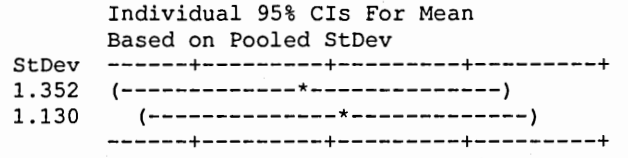

Machine Drilled Hole Quality

One-way ANOVA: Roughness versus Pilot

Analysis of Variance for Roughnes

Source	DF	SS	MS	F	P
Pilot	1	0.000043	0.000043	0.06	0.804
Error	22	0.014916	0.000678		
Total	23	0.014959			

Level	N	Mean	StDev
No Pilot	12	1.0736	0.0310
Pilot Ho	12	1.0763	0.0198

Pooled StDev = 0.0260

Individual 95% CIs For Mean
Based on Pooled StDev

```
--+---------+---------+---------+----
(---------------*--------------)
   (--------------*---------------)
--+---------+---------+---------+----
1.060     1.070     1.080     1.090
```

One-way ANOVA: Roughness versus Length

Analysis of Variance for Roughnes

Source	DF	SS	MS	F	P
Length	1	0.004782	0.004782	10.34	0.004
Error	22	0.010177	0.000463		
Total	23	0.014959			

Level	N	Mean	StDev
Long	12	1.0891	0.0263
Short	12	1.0608	0.0152

Pooled StDev = 0.0215

Individual 95% CIs For Mean
Based on Pooled StDev

```
--+---------+---------+---------+----
                  (--------*--------)
 (-------*--------)
--+---------+---------+---------+----
1.050     1.065     1.080     1.095
```

One-way ANOVA: Roughness versus Condition

Analysis of Variance for Roughnes

Source	DF	SS	MS	F	P
Conditio	1	0.000929	0.000929	1.46	0.240
Error	22	0.014030	0.000638		
Total	23	0.014959			

Level	N	Mean	StDev
New	12	1.0687	0.0134
Old	12	1.0812	0.0331

Pooled StDev = 0.0253

Individual 95% CIs For Mean
Based on Pooled StDev

```
--+---------+---------+---------+----
(------------*-----------)
          (------------*------------)
--+---------+---------+---------+----
1.056     1.068     1.080     1.092
```

One-way ANOVA: Roughness versus Feedrate

Analysis of Variance for Roughnes

Source	DF	SS	MS	F	P
Feedrate	1	0.000201	0.000201	0.30	0.589
Error	22	0.014758	0.000671		
Total	23	0.014959			

Level	N	Mean	StDev
High	12	1.0779	0.0284
Low	12	1.0721	0.0231

Pooled StDev = 0.0259

Individual 95% CIs For Mean Based on Pooled StDev

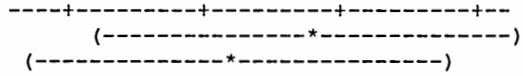

One-way ANOVA: Conicality versus Pilot

Analysis of Variance for Conicali

Source	DF	SS	MS	F	P
Pilot	1	62.40	62.40	14.92	0.001
Error	22	92.04	4.18		
Total	23	154.45			

Level	N	Mean	StDev
No Pilot	12	3.925	2.798
Pilot Ho	12	0.700	0.732

Pooled StDev = 2.045

Individual 95% CIs For Mean Based on Pooled StDev

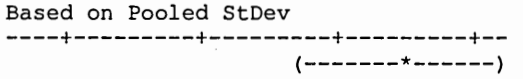

One-way ANOVA: Conicality versus Length

Analysis of Variance for Conicali

Source	DF	SS	MS	F	P
Length	1	17.51	17.51	2.81	0.108
Error	22	136.94	6.22		
Total	23	154.45			

Level	N	Mean	StDev
Long	12	3.167	3.355
Short	12	1.458	1.091

Pooled StDev = 2.495

Individual 95% CIs For Mean Based on Pooled StDev

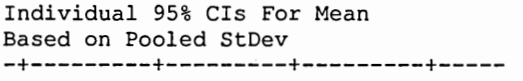

One-way ANOVA: Conicality versus Condition

Analysis of Variance for Conicali

Source	DF	SS	MS	F	P
Conditio	1	2.60	2.60	0.38	0.546
Error	22	151.85	6.90		
Total	23	154.45			

Level	N	Mean	StDev
New	12	2.642	3.320
Old	12	1.983	1.668

Pooled StDev = 2.627

Individual 95% CIs For Mean Based on Pooled StDev

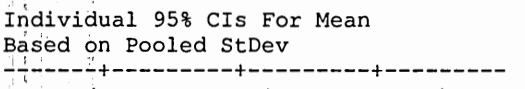

One-way ANOVA: Conicality versus Feedrate

Analysis of Variance for Conicali

Source	DF	SS	MS	F	P
Feedrate	1	10.80	10.80	1.65	0.212
Error	22	143.65	6.53		
Total	23	154.45			

Level	N	Mean	StDev
High	12	1.642	1.872
Low	12	2.983	3.091

Pooled StDev = 2.555

Individual 95% CIs For Mean
Based on Pooled StDev

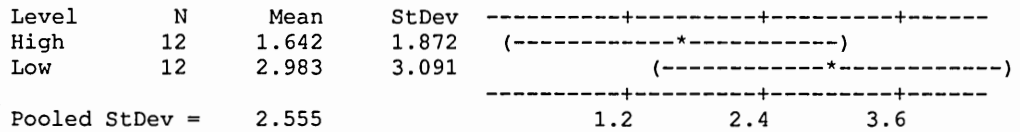

One-way ANOVA: Angle versus Pilot

Analysis of Variance for Angle

Source	DF	SS	MS	F	P
Pilot	1	49.6	49.6	1.61	0.218
Error	22	679.7	30.9		
Total	23	729.3			

Level	N	Mean	StDev
No Pilot	12	6.033	6.272
Pilot Ho	12	3.158	4.738

Pooled StDev = 5.558

Individual 95% CIs For Mean
Based on Pooled StDev

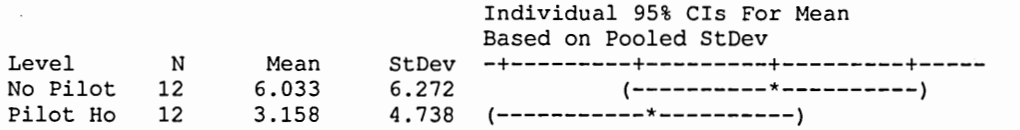

One-way ANOVA: Angle versus Length

Analysis of Variance for Angle

Source	DF	SS	MS	F	P
Length	1	84.0	84.0	2.86	0.105
Error	22	645.3	29.3		
Total	23	729.3			

Level	N	Mean	StDev
Long	12	6.467	6.270
Short	12	2.725	4.399

Pooled StDev = 5.416

Individual 95% CIs For Mean
Based on Pooled StDev

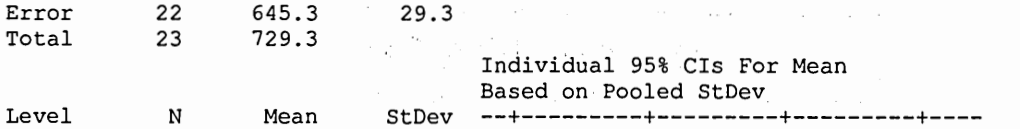

One-way ANOVA: Angle versus Condition

Analysis of Variance for Angle

Source	DF	SS	MS	F	P
Conditio	1	21.1	21.1	0.66	0.427
Error	22	708.2	32.2		
Total	23	729.3			

Level	N	Mean	StDev
New	12	5.533	6.489
Old	12	3.658	4.719

Pooled StDev = 5.674

Individual 95% CIs For Mean
Based on Pooled StDev

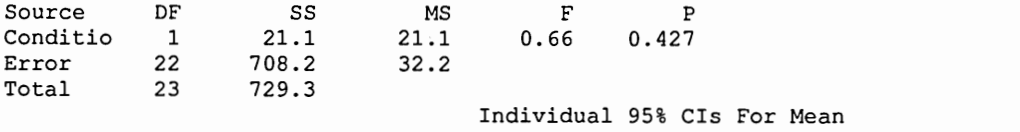

One-way ANOVA: Angle versus Feedrate

Analysis of Variance for Angle

Source	DF	SS	MS	F	P
Feedrate	1	0.4	0.4	0.01	0.913
Error	22	728.9	33.1		
Total	23	729.3			

Level	N	Mean	StDev	Individual 95% CIs For Mean Based on Pooled StDev
High	12	4.725	4.598	(----------*----------)
Low	12	4.467	6.717	(----------*----------)
Pooled StDev =		5.756		2.0 4.0 6.0 8.0

One-way ANOVA: Number versus Pilot

Analysis of Variance for Number

Source	DF	SS	MS	F	P
Pilot	1	8.17	8.17	3.65	0.069
Error	22	49.17	2.23		
Total	23	57.33			

Level	N	Mean	StDev	Individual 95% CIs For Mean Based on Pooled StDev
No Pilot	12	1.917	1.730	(----------*----------)
Pilot Ho	12	0.750	1.215	(----------*----------)
Pooled StDev =		1.495		0.00 0.80 1.60 2.40

One-way ANOVA: Number versus Length

Analysis of Variance for Number

Source	DF	SS	MS	F	P
Length	1	2.67	2.67	1.07	0.311
Error	22	54.67	2.48		
Total	23	57.33			

Level	N	Mean	StDev	Individual 95% CIs For Mean Based on Pooled StDev
Long	12	1.667	1.435	(----------*----------)
Short	12	1.000	1.706	(----------*----------)
Pooled StDev =		1.576		0.70 1.40 2.10

One-way ANOVA: Number versus Condition

Analysis of Variance for Number

Source	DF	SS	MS	F	P
Conditio	1	0.00	0.00	0.00	1.000
Error	22	57.33	2.61		
Total	23	57.33			

Level	N	Mean	StDev	Individual 95% CIs For Mean Based on Pooled StDev
New	12	1.333	1.670	(----------*----------)
Old	12	1.333	1.557	(----------*----------)
Pooled StDev =		1.614		0.60 1.20 1.80 2.40

One-way ANOVA: Number versus Feedrate

Analysis of Variance for Number

Source	DF	SS	MS	F	P
Feedrate	1	8.17	8.17	3.65	0.069
Error	22	49.17	2.23		
Total	23	57.33			

Level	N	Mean	StDev	Individual 95% CIs For Mean Based on Pooled StDev
High	12	1.917	1.730	(----------*----------)
Low	12	0.750	1.215	(----------*----------)
Pooled StDev =		1.495		0.00 0.80 1.60 2.40

Exit Burrs

Curling Burr

One-way ANOVA: C versus Operator

Analysis of Variance for C

Source	DF	SS	MS	F	P
Operator	2	13.078	6.539	19.08	0.000
Error	116	39.746	0.343		
Total	118	52.824			

Level	N	Mean	StDev
Experien	48	0.4792	0.7143
Machine	24	0.9583	0.7506
Novice	47	0.0638	0.2471

Pooled StDev = 0.5854

Individual 95% CIs For Mean Based on Pooled StDev

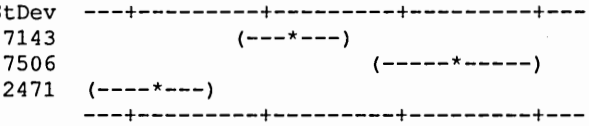

One-way ANOVA: C versus Pilot Hole

Analysis of Variance for C

Source	DF	SS	MS	F	P
Pilot Ho	1	1.996	1.996	4.59	0.034
Error	117	50.827	0.434		
Total	118	52.824			

Level	N	Mean	StDev
No Pilot	59	0.5424	0.6778
Pilot Ho	60	0.2833	0.6402

Pooled StDev = 0.6591

Individual 95% CIs For Mean Based on Pooled StDev

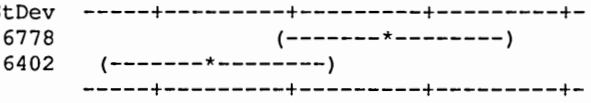

One-way ANOVA: C versus Bit Length

Analysis of Variance for C

Source	DF	SS	MS	F	P
Bit Leng	1	0.620	0.620	1.39	0.241
Error	117	52.204	0.446		
Total	118	52.824			

Level	N	Mean	StDev
Long	60	0.4833	0.7009
Short	59	0.3390	0.6327

Pooled StDev = 0.6680

Individual 95% CIs For Mean Based on Pooled StDev

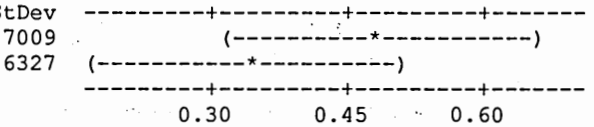

One-way ANOVA: C versus Bit Condition

Analysis of Variance for C

Source	DF	SS	MS	F	P
Bit Cond	1	0.003	0.003	0.01	0.936
Error	117	52.821	0.451		
Total	118	52.824			

Level	N	Mean	StDev	Individual 95% CIs For Mean Based on Pooled StDev
New	60	0.4167	0.6712	(----------*----------)
Old	59	0.4068	0.6726	(----------*----------)
Pooled StDev =		0.6719		0.30 0.40 0.50

One-way ANOVA: C versus Pressure

Analysis of Variance for C

Source	DF	SS	MS	F	P
Pressure	1	0.056	0.056	0.12	0.724
Error	117	52.767	0.451		
Total	118	52.824			

Level	N	Mean	StDev	Individual 95% CIs For Mean Based on Pooled StDev
High	59	0.3898	0.6952	(----------*----------)
Low	60	0.4333	0.6475	(----------*----------)
Pooled StDev =		0.6716		0.24 0.36 0.48 0.60

One-way ANOVA: C versus Bit Speed

Analysis of Variance for C

Source	DF	SS	MS	F	P
Bit Spee	1	1.008	1.008	2.28	0.134
Error	117	51.816	0.443		
Total	118	52.824			

Level	N	Mean	StDev	Individual 95% CIs For Mean Based on Pooled StDev
Full	72	0.4861	0.6919	(----------*----------)
Stopped	47	0.2979	0.6226	(----------*----------)
Pooled StDev =		0.6655		0.15 0.30 0.45 0.60

Triangular Burr

One-way ANOVA: T versus Operator

Analysis of Variance for T

Source	DF	SS	MS	F	P
Operator	2	1.982	0.991	1.73	0.182
Error	116	66.573	0.574		
Total	118	68.555			

Level	N	Mean	StDev
Experien	48	0.6250	0.7330
Machine	24	0.9167	0.7173
Novice	47	0.5745	0.8007
Pooled StDev =		0.7576	

Individual 95% CIs For Mean Based on Pooled StDev

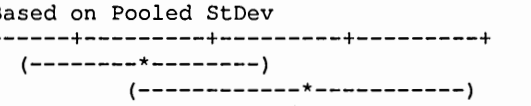

One-way ANOVA: T versus Pilot Hole

Analysis of Variance for T

Source	DF	SS	MS	F	P
Pilot Ho	1	17.524	17.524	40.18	0.000
Error	117	51.031	0.436		
Total	118	68.555			

Level	N	Mean	StDev
No Pilot	59	1.0508	0.7526
Pilot Ho	60	0.2833	0.5552
Pooled StDev =		0.6604	

Individual 95% CIs For Mean Based on Pooled StDev

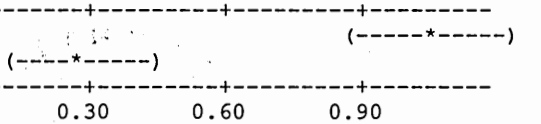

One-way ANOVA: T versus Bit Length

Analysis of Variance for T

Source	DF	SS	MS	F	P
Bit Leng	1	0.113	0.113	0.19	0.661
Error	117	68.442	0.585		
Total	118	68.555			

Level	N	Mean	StDev
Long	60	0.6333	0.7357
Short	59	0.6949	0.7934
Pooled StDev =		0.7648	

Individual 95% CIs For Mean Based on Pooled StDev

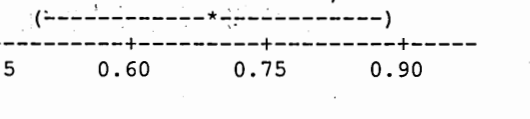

One-way ANOVA: T versus Bit Condition

Analysis of Variance for T

Source	DF	SS	MS	F	P
Bit Cond	1	0.001	0.001	0.00	0.968
Error	117	68.554	0.586		
Total	118	68.555			

Level	N	Mean	StDev
New	60	0.6667	0.7739
Old	59	0.6610	0.7568

Pooled StDev = 0.7655

Individual 95% CIs For Mean Based on Pooled StDev

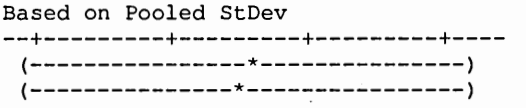

One-way ANOVA: T versus Pressure

Analysis of Variance for T

Source	DF	SS	MS	F	P
Pressure	1	0.584	0.584	1.01	0.318
Error	117	67.971	0.581		
Total	118	68.555			

Level	N	Mean	StDev
High	59	0.5932	0.7455
Low	60	0.7333	0.7782

Pooled StDev = 0.7622

Individual 95% CIs For Mean Based on Pooled StDev

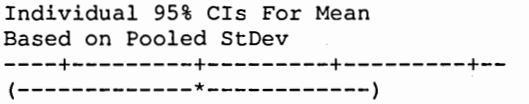

One-way ANOVA: T versus Bit Speed

Analysis of Variance for T

Source	DF	SS	MS	F	P
Bit Spee	1	0.051	0.051	0.09	0.769
Error	117	68.504	0.586		
Total	118	68.555			

Level	N	Mean	StDev
Full	72	0.6806	0.7659
Stopped	47	0.6383	0.7640

Pooled StDev = 0.7652

Individual 95% CIs For Mean Based on Pooled StDev

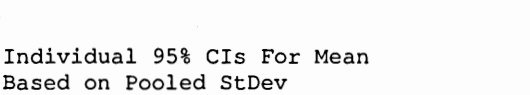

Bulge Burr

One-way ANOVA: B versus Operator

Analysis of Variance for B

Source	DF	SS	MS	F	P
Operator	2	3.674	1.837	4.02	0.020
Error	116	52.965	0.457		
Total	118	56.639			

Level	N	Mean	StDev
Experien	48	0.5625	0.7964
Machine	24	0.0833	0.2823
Novice	47	0.4043	0.6808
Pooled StDev =		0.6757	

Individual 95% CIs For Mean
Based on Pooled StDev

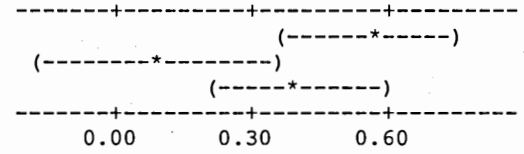

One-way ANOVA: B versus Pilot Hole

Analysis of Variance for B

Source	DF	SS	MS	F	P
Pilot Ho	1	6.400	6.400	14.91	0.000
Error	117	50.238	0.429		
Total	118	56.639			

Level	N	Mean	StDev
No Pilot	59	0.1695	0.3784
Pilot Ho	60	0.6333	0.8431
Pooled StDev =		0.6553	

Individual 95% CIs For Mean
Based on Pooled StDev

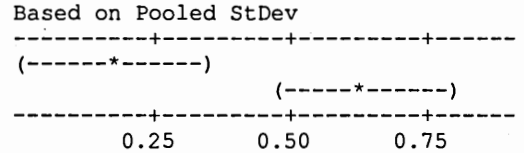

One-way ANOVA: B versus Bit Length

Analysis of Variance for B

Source	DF	SS	MS	F	P
Bit Leng	1	0.001	0.001	0.00	0.958
Error	117	56.637	0.484		
Total	118	56.639			

Level	N	Mean	StDev
Long	60	0.4000	0.6689
Short	59	0.4068	0.7220
Pooled StDev =		0.6958	

Individual 95% CIs For Mean
Based on Pooled StDev

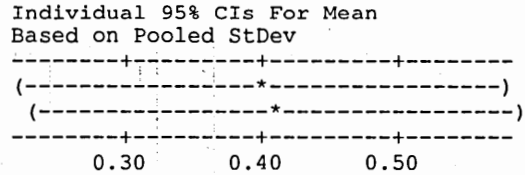

One-way ANOVA: B versus Bit Condition

Analysis of Variance for B

Source	DF	SS	MS	F	P
Bit Cond	1	0.109	0.109	0.23	0.636
Error	117	56.530	0.483		
Total	118	56.639			

Level	N	Mean	StDev	Individual 95% CIs For Mean Based on Pooled StDev
New	60	0.4333	0.6979	(----------*----------)
Old	59	0.3729	0.6923	(----------*----------)
Pooled StDev =		0.6951		0.24 0.36 0.48 0.60

One-way ANOVA: B versus Pressure

Analysis of Variance for B

Source	DF	SS	MS	F	P
Pressure	1	2.846	2.846	6.19	0.014
Error	117	53.792	0.460		
Total	118	56.639			

Level	N	Mean	StDev	Individual 95% CIs For Mean Based on Pooled StDev
High	59	0.5593	0.7938	(--------*--------)
Low	60	0.2500	0.5407	(--------*--------)
Pooled StDev =		0.6781		0.20 0.40 0.60

One-way ANOVA: B versus Bit Speed

Analysis of Variance for B

Source	DF	SS	MS	F	P
Bit Spee	1	1.284	1.284	2.71	0.102
Error	117	55.355	0.473		
Total	118	56.639			

Level	N	Mean	StDev	Individual 95% CIs For Mean Based on Pooled StDev
Full	72	0.3194	0.6241	(---------*---------)
Stopped	47	0.5319	0.7760	(-----------*-----------)
Pooled StDev =		0.6878		0.16 0.32 0.48 0.64

Fatigue Tests

Hand Drilling

One-way ANOVA: Nf versus Test Type

```
Analysis of Variance for Nf
Source     DF        SS        MS        F        P
Test Typ    1 2.401E+09 2.401E+09    15.18    0.001
Error      21 3.321E+09 158165691
Total      22 5.722E+09

                                  Individual 95% CIs For Mean
                                  Based on Pooled StDev
Level       N      Mean     StDev --+---------+---------+---------+----
Baseline    4     91438     28532                (--------*--------)
Hand Dri   19     64484      6989   (---*---)
                                  --+---------+---------+---------+----
Pooled StDev =    12576          60000     75000     90000    105000
```

One-way ANOVA: Ni1 versus Test Type

```
Analysis of Variance for Ni1
Source     DF        SS        MS        F        P
Test Typ    1 740644034 740644034     1.95    0.183
Error      15 5.688E+09 379225143
Total      16 6.429E+09

                                  Individual 95% CIs For Mean
                                  Based on Pooled StDev
Level       N      Mean     StDev -------+---------+---------+---------
Baseline    3     63500     44222     (---------------*---------------)
Hand Dri   14     46186     11692  (-------*------)
                                  -------+---------+---------+---------
Pooled StDev =    19474             45000     60000     75000
```

One-way ANOVA: Nf versus Bit Condition

```
Analysis of Variance for Nf
Source     DF        SS        MS        F        P
Bit Cond    1  63588142  63588142     1.33    0.266
Error      17 815605233  47976778
Total      18 879193374

                                  Individual 95% CIs For Mean
                                  Based on Pooled StDev
Level       N      Mean     StDev -----+---------+---------+---------+-
New        10     62748      5818  (-----------*----------)
Old         9     66412      7992            (-----------*-----------)
                                  -----+---------+---------+---------+-
Pooled StDev =     6927             60000     64000     68000     72000
```

One-way ANOVA: Nf versus Pilot Hole

Analysis of Variance for Nf

Source	DF	SS	MS	F	P
Pilot Ho	1	162865502	162865502	3.87	0.066
Error	17	716327872	42136934		
Total	18	879193374			

Level	N	Mean	StDev
No	10	61706	3384
Yes	9	67570	8755

Pooled StDev = 6491

Individual 95% CIs For Mean Based on Pooled StDev

```
-------+---------+---------+---------
(----------*----------)
               (----------*----------)
-------+---------+---------+---------
   60000     64000     68000
```

One-way ANOVA: Ni versus Bit Condition

Analysis of Variance for Ni

Source	DF	SS	MS	F	P
Bit Cond	1	769602857	769602857	9.17	0.011
Error	12	1.008E+09	83971190		
Total	13	1.777E+09			

Level	N	Mean	StDev
New	7	38771	8502
Old	7	53600	9780

Pooled StDev = 9164

Individual 95% CIs For Mean Based on Pooled StDev

```
---------+---------+---------+-------
(-------*------)
                (-------*------)
---------+---------+---------+-------
      40000     50000     60000
```

One-way ANOVA: Ni versus Pilot Hole

Analysis of Variance for Ni

Source	DF	SS	MS	F	P
Pilot Ho	1	105450060	105450060	0.76	0.401
Error	12	1.672E+09	139317257		
Total	13	1.777E+09			

Level	N	Mean	StDev
No	6	43017	9854
Yes	8	48563	13018

Pooled StDev = 11803

Individual 95% CIs For Mean Based on Pooled StDev

```
----+---------+---------+---------+--
(--------------*--------------)
          (------------*------------)
----+---------+---------+---------+--
35000     42000     49000     56000
```

One-way ANOVA: Ni/Nf versus Bit Condition

Analysis of Variance for Ni/Nf

Source	DF	SS	MS	F	P
Bit Cond	1	0.06750	0.06750	7.15	0.022
Error	11	0.10387	0.00944		
Total	12	0.17138			

Level	N	Mean	StDev
New	7	0.62627	0.11748
Old	6	0.77082	0.06491

Pooled StDev = 0.09718

Individual 95% CIs For Mean Based on Pooled StDev

```
------+---------+---------+---------+
 (-------*-------)
                (--------*--------)
------+---------+---------+---------+
    0.60      0.70      0.80      0.90
```

One-way ANOVA: Nf-Ni versus Bit Condition

Analysis of Variance for Nf-Ni

Source	DF	SS	MS	F	P
Bit Cond	1	190573883	190573883	5.40	0.040
Error	11	388187646	35289786		
Total	12	578761529			

Level	N	Mean	StDev
New	7	23021	7465
Old	6	15341	3282

Pooled StDev = 5941

Individual 95% CIs For Mean Based on Pooled StDev

```
---------+---------+---------+------
          (---------*---------)
(---------*---------)
---------+---------+---------+------
      15000     20000     25000
```

One-way ANOVA: Ni/Nf versus Pilot Hole

Analysis of Variance for Ni/Nf

Source	DF	SS	MS	F	P
Pilot Ho	1	0.0118	0.0118	0.82	0.385
Error	11	0.1595	0.0145		
Total	12	0.1714			

Level	N	Mean	StDev
No	5	0.6548	0.1029
Yes	8	0.7169	0.1294

Pooled StDev = 0.1204

Individual 95% CIs For Mean Based on Pooled StDev

```
---+---------+---------+---------+---
(--------------*--------------)
           (-----------*----------)
---+---------+---------+---------+---
  0.560     0.640     0.720     0.800
```

One-way ANOVA: Nf-Ni versus Pilot Hole

Analysis of Variance for Nf-Ni

Source	DF	SS	MS	F	P
Pilot Ho	1	17467024	17467024	0.34	0.570
Error	11	561294505	51026773		
Total	12	578761529			

Level	N	Mean	StDev
No	5	20943	5940
Yes	8	18560	7747

Pooled StDev = 7143

Individual 95% CIs For Mean Based on Pooled StDev

```
----+---------+---------+---------+--
  (-------------*-------------)
(----------*----------)
----+---------+---------+---------+--
15000     20000     25000     30000
```

One-way ANOVA: Ni2-Ni1 versus Bit Cond

Analysis of Variance for Ni2-Ni1

Source	DF	SS	MS	F	P
Bit Cond	1	101529167	101529167	2.40	0.153
Error	10	423540000	42354000		
Total	11	525069167			

Level	N	Mean	StDev
New	7	11900	7910
Old	5	6000	3468

Pooled StDev = 6508

Individual 95% CIs For Mean Based on Pooled StDev

```
-+---------+---------+---------+-----
                (----------*----------)
(------------*------------)
-+---------+---------+---------+-----
 0       5000     10000     15000
```

One-way ANOVA: Ni2-Ni1 versus Pilot Hole

Analysis of Variance for Ni2-Ni1

Source	DF	SS	MS	F	P
Pilot Ho	1	14006881	14006881	0.27	0.612
Error	10	511062286	51106229		
Total	11	525069167			

Level	N	Mean	StDev	Individual 95% CIs For Mean Based on Pooled StDev
No	5	10720	3685	(----------*----------)
Yes	7	8529	8725	(----------*----------)
Pooled StDev =		7149		5000 10000 15000 20000

One-way ANOVA: Ni2-Ni1/Nf versus Bit Cond

Analysis of Variance for Ni2-Ni1/

Source	DF	SS	MS	F	P
Bit Cond	1	0.0277	0.0277	2.71	0.131
Error	10	0.1024	0.0102		
Total	11	0.1301			

Level	N	Mean	StDev	Individual 95% CIs For Mean Based on Pooled StDev
New	7	0.1921	0.1210	(----------*----------)
Old	5	0.0946	0.0602	(----------*----------)
Pooled StDev =		0.1012		0.000 0.080 0.160 0.240

One-way ANOVA: Ni2-Ni1/Nf versus Pilot Hole

Analysis of Variance for Ni2-Ni1/

Source	DF	SS	MS	F	P
Pilot Ho	1	0.0055	0.0055	0.44	0.523
Error	10	0.1246	0.0125		
Total	11	0.1301			

Level	N	Mean	StDev	Individual 95% CIs For Mean Based on Pooled StDev
No	5	0.1767	0.0625	(----------*----------)
Yes	7	0.1335	0.1348	(----------*----------)
Pooled StDev =		0.1116		0.070 0.140 0.210 0.280

One-way ANOVA: Nf versus Description 2

Analysis of Variance for Nf

Source	DF	SS	MS	F	P
Descript	3	271261038	90420346	2.23	0.127
Error	15	607932336	40528822		
Total	18	879193374			

Level	N	Mean	StDev	Individual 95% CIs For Mean Based on Pooled StDev
NN	5	60947	4474	(--------*--------)
NY	5	64549	6931	(--------*--------)
ON	5	62465	2075	(--------*--------)
OY	4	71345	10303	(---------*---------)
Pooled StDev =		6366		56000 63000 70000 77000

One-way ANOVA: Ni versus Description 2

Analysis of Variance for Ni

Source	DF	SS	MS	F	P
Descript	3	921252976	307084325	3.59	0.054
Error	10	856004167	85600417		
Total	13	1.777E+09			

Level	N	Mean	StDev	Individual 95% CIs For Mean Based on Pooled StDev
NN	3	37700	8227	(---------*---------)
NY	4	39575	9871	(--------*--------)
ON	3	48333	9500	(---------*---------)
OY	4	57550	9088	(--------*--------)
Pooled StDev =		9252		36000 48000 60000

One-way ANOVA: Ni/Nf versus Description 2

Analysis of Variance for Ni/Nf

Source	DF	SS	MS	F	P
Descript	3	0.08223	0.02741	2.77	0.103
Error	9	0.08914	0.00990		
Total	12	0.17138			

Level	N	Mean	StDev	Individual 95% CIs For Mean Based on Pooled StDev
NN	3	0.62413	0.12489	(----------*----------)
NY	4	0.62787	0.13113	(--------*---------)
ON	2	0.70080	0.06435	(------------*-------------)
OY	4	0.80583	0.02721	(--------*---------)
Pooled StDev =		0.09952		0.60 0.72 0.84

One-way ANOVA: Nf-Ni versus Description 2

Analysis of Variance for Nf-Ni

Source	DF	SS	MS	F	P
Descript	3	220100139	73366713	1.84	0.210
Error	9	358661390	39851266		
Total	12	578761529			

Level	N	Mean	StDev	Individual 95% CIs For Mean Based on Pooled StDev
NN	3	22616	7494	(----------*----------)
NY	4	23325	8586	(---------*----------)
ON	2	18432	2794	(-------------*-------------)
OY	4	13795	2406	(---------*---------)
Pooled StDev =		6313		7000 14000 21000 28000

One-way ANOVA: Nf versus Factors

Analysis of Variance for Nf

Source	DF	SS	MS	F	P
Factors	4	2.672E+09	668009939	3.94	0.018
Error	18	3.050E+09	169456582		
Total	22	5.722E+09			

Level	N	Mean	StDev	Individual 95% CIs For Mean Based on Pooled StDev
BL	4	91438	28532	(-------*--------)
NN	5	60947	4474	(-------*-------)
NY	5	64549	6931	(------*-------)
ON	5	62465	2075	(-------*-------)
OY	4	71345	10303	(--------*-------)
Pooled StDev =		13018		64000 80000 96000

One-way ANOVA: Nf versus Test Type

Analysis of Variance for Nf

Source	DF	SS	MS	F	P
Test Typ	1	7.372E+12	7.372E+12	9.66	0.021
Error	6	4.581E+12	7.635E+11		
Total	7	1.195E+13			

Level	N	Mean	StDev	Individual 95% CIs For Mean Based on Pooled StDev
Overload	4	1972801	1235701	(-------*--------)
Underloa	4	52871	4130	(-------*--------)
Pooled StDev =		873777		0 1200000 2400000

One-way ANOVA: Nf versus Orientation

Analysis of Variance for Nf

Source	DF	SS	MS	F	P
Orientat	1	7.361E+11	7.361E+11	0.39	0.553
Error	6	1.122E+13	1.870E+12		
Total	7	1.195E+13			

Level	N	Mean	StDev
LT	4	709500	917576
TL	4	1316172	1702081

Pooled StDev = 1367301

Individual 95% CIs For Mean Based on Pooled StDev

```
---------+---------+---------+-------
 (-------------*-------------)
       (-------------*-------------)
---------+---------+---------+-------
         0   1200000   2400000
```

Results for: 17.5 ksi As-Drilled

One-way ANOVA: Nf versus Test Type

Analysis of Variance for Nf

Source	DF	SS	MS	F	P
Test Typ	1	7.979E+10	7.979E+10	4.75	0.061
Error	8	1.344E+11	1.679E+10		
Total	9	2.141E+11			

Level	N	Mean	StDev
Hand Dri	4	100795	8445
Machine	6	283135	163791

Pooled StDev = 129591

Individual 95% CIs For Mean Based on Pooled StDev

```
----+---------+---------+---------+--
 (---------*---------)
               (-------*-------)
----+---------+---------+---------+--
    0    150000    300000    450000
```

One-way ANOVA: Ni versus Test Type

Analysis of Variance for Ni

Source	DF	SS	MS	F	P
Test Typ	1	4.808E+10	4.808E+10	2.64	0.155
Error	6	1.092E+11	1.820E+10		
Total	7	1.573E+11			

Level	N	Mean	StDev
Hand Dri	2	59350	7000
Machine	6	238383	147753

Pooled StDev = 134910

Individual 95% CIs For Mean Based on Pooled StDev

```
--+---------+---------+---------+----
 (---------------*---------------)
                      (--------*--------)
--+---------+---------+---------+----
-150000         0    150000    300000
```

One-way ANOVA: Ni/Nf versus Test Type

Analysis of Variance for Ni/Nf

Source	DF	SS	MS	F	P
Test Typ	1	0.06942	0.06942	20.32	0.004
Error	6	0.02050	0.00342		
Total	7	0.08992			

Level	N	Mean	StDev
Hand Dri	2	0.62345	0.03444
Machine	6	0.83858	0.06214

Pooled StDev = 0.05845

Individual 95% CIs For Mean
Based on Pooled StDev

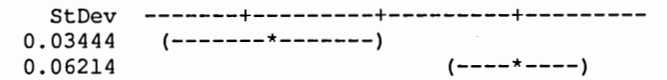

One-way ANOVA: Nf-Ni versus Test Type

Analysis of Variance for Nf-Ni

Source	DF	SS	MS	F	P
Test Typ	1	123515288	123515288	0.25	0.635
Error	6	2.971E+09	495186116		
Total	7	3.095E+09			

Level	N	Mean	StDev
Hand Dri	2	35677	1017
Machine	6	44751	24372

Pooled StDev = 22253

Individual 95% CIs For Mean
Based on Pooled StDev

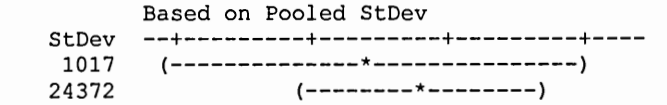

One-way ANOVA: Nf-Ni/Nf versus Test Type

Analysis of Variance for Nf-Ni/Nf

Source	DF	SS	MS	F	P
Test Typ	1	0.06940	0.06940	20.30	0.004
Error	6	0.02051	0.00342		
Total	7	0.08992			

Level	N	Mean	StDev
Hand Dri	2	0.37652	0.03441
Machine	6	0.16142	0.06218

Pooled StDev = 0.05847

Individual 95% CIs For Mean
Based on Pooled StDev

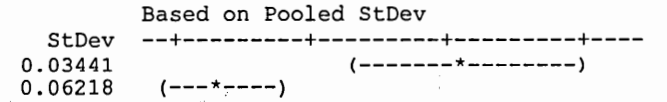

Results for: 17.5 ksi Machine Drilling

One-way ANOVA: Nf versus Params

Analysis of Variance for Nf

Source	DF	SS	MS	F	P
Params	1	5.123E+10	5.123E+10	2.47	0.191
Error	4	8.291E+10	2.073E+10		
Total	5	1.341E+11			

Level	N	Mean	StDev
NY	3	190734	52755
OY	3	375535	196652

Pooled StDev = 143971

Individual 95% CIs For Mean
Based on Pooled StDev

```
---+---------+---------+---------+---
 (-----------*----------)
           (-----------*----------)
---+---------+---------+---------+---
   0     200000    400000    600000
```

One-way ANOVA: Ni versus Params

Analysis of Variance for Ni

Source	DF	SS	MS	F	P
Params	1	3.341E+10	3.341E+10	1.76	0.255
Error	4	7.575E+10	1.894E+10		
Total	5	1.092E+11			

Level	N	Mean	StDev
NY	3	163767	39708
OY	3	313000	190520

Pooled StDev = 137613

Individual 95% CIs For Mean
Based on Pooled StDev

```
----+---------+---------+---------+--
(-------------*-------------)
          (-------------*-------------)
----+---------+---------+---------+--
    0     160000    320000    480000
```

One-way ANOVA: Nf-Ni versus Params

Analysis of Variance for Nf-Ni

Source	DF	SS	MS	F	P
Params	1	1.898E+09	1.898E+09	7.08	0.056
Error	4	1.072E+09	268114709		
Total	5	2.970E+09			

Level	N	Mean	StDev
NY	3	26967	14277
OY	3	62535	18232

Pooled StDev = 16374

Individual 95% CIs For Mean
Based on Pooled StDev

```
----------+---------+---------+------
(----------*---------)
               (---------*----------)
----------+---------+---------+------
      25000     50000     75000
```

One-way ANOVA: Ni/Nf versus Params

Analysis of Variance for Ni/Nf

Source	DF	SS	MS	F	P
Params	1	0.00377	0.00377	0.97	0.381
Error	4	0.01554	0.00389		
Total	5	0.01931			

Level	N	Mean	StDev	Individual 95% CIs For Mean Based on Pooled StDev
NY	3	0.86363	0.04089	(----------*----------)
OY	3	0.81353	0.07810	(----------*----------)

Pooled StDev = 0.06234

0.770 0.840 0.910

One-way ANOVA: Nf-Ni/Nf versus Params

Analysis of Variance for Nf-Ni/Nf

Source	DF	SS	MS	F	P
Params	1	0.00377	0.00377	0.97	0.381
Error	4	0.01556	0.00389		
Total	5	0.01933			

Level	N	Mean	StDev	Individual 95% CIs For Mean Based on Pooled StDev
NY	3	0.13635	0.04093	(----------*----------)
OY	3	0.18649	0.07813	(----------*----------)

Pooled StDev = 0.06237

0.070 0.140 0.210 0.280

One-way ANOVA: Ni2-Ni1 versus Params

Analysis of Variance for Ni2-Ni

Source	DF	SS	MS	F	P
Params	1	2.170E+09	2.170E+09	4.67	0.097
Error	4	1.857E+09	464151667		
Total	5	4.026E+09			

Level	N	Mean	StDev	Individual 95% CIs For Mean Based on Pooled StDev
NY	3	15100	20191	(----------*----------)
OY	3	53133	22817	(----------*----------)

Pooled StDev = 21544

0 30000 60000

One-way ANOVA: Ni2-Ni1/Nf-Ni1 versus Params

Analysis of Variance for Ni2-Ni/N

Source	DF	SS	MS	F	P
Params	1	0.252	0.252	2.44	0.194
Error	4	0.414	0.104		
Total	5	0.666			

Level	N	Mean	StDev	Individual 95% CIs For Mean Based on Pooled StDev
NY	3	0.4112	0.4264	(----------*----------)
OY	3	0.8212	0.1588	(----------*----------)

Pooled StDev = 0.3217

0.00 0.40 0.80 1.20

REFERENCES

1. DeGarmo, E. P., *Materials and Processes in Manufacturing*. Eighth ed. 1997, Upper Saddle River, NJ: Simon & Schuster.

2. Newman, J. C., Jr. and Edwards, P. R., *Short-Crack Growth Behavior In An Aluminum Alloy*. 1988, North Atlantic Treaty Organization, Advisory Group for Aerospace Research and Development.

3. Bannantine, J. A., Comer, J. J., and Handrock, J. L., *Fundamentals of Metal Fatigue Analysis*. 1990, Englewood Cliffs, New Jersey: Prentice Hall.

4. Lacarac, V., et al., *Fatigue crack growth from plain and cold expanded holes in aluminium alloys*. International Journal of Fatigue, 2000. **22**(3): p. 189-203.

5. Mahdi, M. and Zhang, L., *Applied mechanics in grinding. Part 7: residual stresses induced by the full coupling of mechanical deformation, thermal deformation and phase transformation.* International Journal of Machine Tools and Manufacture, 1999. **39**(8): p. 1285-1298.

6. Jang, D. Y., et al., *Surface residual stresses in machined austenitic stainless steel.* Wear, 1996. **194**(1-2): p. 168-173.

7. M'Saoubi, R., et al., *Residual stress analysis in orthogonal machining of standard and resulfurized AISI 316L steels.* Journal of Materials Processing Technology, 1999. **96**(1-3): p. 225-233.

8. Mahdi, M. and Zhang, L., *Applied mechanics in grinding--V. Thermal residual stresses.* International Journal of Machine Tools and Manufacture, 1997. **37**(5): p. 619-633.

9. Mahdi, M. and Zhang, L. C., *Residual stresses in ground components caused by coupled thermal and mechanical plastic deformation.* Journal of Materials Processing Technology, 1999. **95**(1-3): p. 238-245.

10. Papanikos, P. and Meguid, S. A., *Elasto-plastic finite-element analysis of the cold expansion of adjacent fastener holes.* Journal of Materials Processing Technology, 1999. **92-93**: p. 424-428.

11. Arola, D. and Ramulu, M., *Material removal in abrasive waterjet machining of metals. A residual stress analysis.* Wear, 1997. **211**(2): p. 302-310.

12. Lacarac, V. D., Smith, D. J., and Pavier, M. J., *The effect of cold expansion on fatigue crack growth from open holes at room and high temperature.* International Journal of Fatigue, 2001. **23**(1): p. 161-170.

13. Garcia-Granada, A. A., et al., *Creep relaxation of residual stresses around cold expanded holes.* Journal of Engineering Materials and Technology, Transactions of the ASME, 2001. **123**(1): p. 125-131.

14. Webster, G. A. *Propagation of fatigue cracks through residual stress fields.* in *Proceeding of the Fatigue and Stress of Engineering Materials and Components.* 1988. London: IITT-International.

15. Toparli, M., Aksoy, T., and Ozel, A., *Effect of the residual stresses on the fatigue crack growth behavior at fastener holes.* Materials Science and Engineering A, 1997. **225**(1-2): p. 196-203.

16. Pavier, M. J., Poussard, C. G. C., and Smith, D. J., *Effect of residual stress around cold worked holes on fracture under superimposed mechanical load.* Engineering Fracture Mechanics, 1999. **63**(6): p. 751-773.

17. Min, S., Kim, J., and Dornfeld, D. A., *Development of a drilling burr control chart for low alloy steel, AISI 4118.* Journal of Materials Processing Technology, 2001. **113**(1-3): p. 4-9.

18. Kim, J., Min, S., and Dornfeld, D. A., *Optimization and control of drilling burr formation of AISI 304L and AISI 4118 based on drilling burr control charts.* International Journal of Machine Tools and Manufacture, 2001. **41**(7): p. 923-936.

19. Ko, S.-L. and Lee, J.-K., *Analysis of burr formation in drilling with a new-concept drill.* Journal of Materials Processing Technology, 2001. **113**(1-3): p. 392-398.

20. Saunders, L. K. L., *A finite element model of exit burrs for drilling of metals.* Finite Elements in Analysis and Design, 2002.

21. Anderson, T. L., *Fracture Mechanics: Fundamentals and Applications*. 2nd ed. 1994, Boca Raton: CRC Press.

22. Starke, E. A. J. and Staley, J. T., *Application of modern aluminum alloys to aircraft.* Progress in Aerospace Sciences, 1996. **32**(2-3): p. 131-172.

23. Schaffer, J., Saxena, A., Antolovich, S., Sanders, T., Warner, S., *The Science and Design of Engineering Materials*. 2nd ed. 1999, Boston: McGraw-Hill.

24. Cullity, B. D., *Elements of X-Ray Diffraction*. 2nd ed. 1978, Reading, Massachusetts: Addison-Wesley Publishing Co., Inc.

25. Dowling, N. E., *Mechanical Behavior of Materials: Engineering Methods for Deformation, Fracture, and Fatigue*. 2nd ed. 1998, Upper Saddle River, NJ: Prentice Hall, Inc.